Universidad de Valladolid

Escuela de Doctorado Universidad de Valladolid

PROGRAMA DE DOCTORADO EN CONSERVACIÓN Y USO SOSTENIBLE DE SISTEMAS FORESTALES

TESIS DOCTORAL:

Predicción de cosechas de setas silvestres en bosques mediterráneos utilizando sensores remotos activos y pasivos

Presentada por Raquel Martínez Rodrigo
para optar al grado de
Doctora por la Universidad de Valladolid

Dirigida por:

Dra. Beatriz Águeda Hernández

Dra. Cristina Gómez Almaraz

Predicción de cosechas de setas silvestres en bosques mediterráneos utilizando sensores remotos activos y pasivos

Soria, 2023

La presente Tesis Doctoral ha sido cofinanciada por Ministerio de Ciencia e Innovación a través del Programa de Doctorado Industrial (ayuda DI-17-09626). Estas ayudas promueven la formación de doctoras y doctores en empresas y están integradas dentro del Programa Estatal de Promoción del Talento y su Empleabilidad, Subprograma Estatal de Formación, en el marco del Plan Estatal de Investigación Científica y Técnica y de Innovación 2017-2020 (convocatoria del año 2017, BOE 18-10-2017).

La doctoranda es trabajadora de föra forest technologies SLL, empresa que le ha proporcionado los medios técnicos necesarios (*hardware* y *software*), apoyo científico a través de su personal y ha cofinanciado los trabajos desarrollados durante la realización de esta tesis.

La doctoranda es alumna del Programa de Doctorado en Conservación y Uso Sostenible de Sistemas Forestales, vinculado al Instituto Universitario de Investigación de Gestión Forestal Sostenible (iuFOR), de la Escuela de Doctorado de la Universidad de Valladolid. Las directoras de la tesis forman parte de la plantilla docente de la Escuela Universitaria de la Ingeniería Forestal, Agronómica y de la Bioenergía (EIFAB) del Campus Duques de Soria de la Universidad de Valladolid.

La doctoranda ha recibido una ayuda a la investigación desarrollada en el curso 2022-2023 de la Cátedra CeI Caja Rural de Soria de la Universidad de Valladolid.

Índice de contenido

Índice de figuras

Introducción:

Capítulo 1:

Capítulo 2:

Capítulo 3:

Índice de tablas

Introducción:

Capítulo 1:

Capítulo 2:

Capítulo 3:

Resumen

Los bosques proporcionan recursos beneficiosos para la sociedad. Su gestión sostenible hace que se maximice la producción de los recursos que ofrecen, realizándose a un ritmo que permita mantener su biodiversidad, su productividad y su capacidad de regeneración. Entre los recursos forestales se encuentran los productos forestales no madereros (PFNM), entre los que se encuentran las setas silvestres. Además de los servicios ecosistémicos directos de abastecimiento y culturales que ofrecen, los hongos también brindan servicios de soporte y regulatorios. Actualmente, la recolección de setas silvestres comestibles ha aumentado notablemente, pero sus cosechas están afectadas directamente por los procesos de cambio global. La gestión sostenible de este PFNM puede apoyarse en las nuevas herramientas que ofrecen las tecnologías de la información, entre las que se encuentra la teledetección, que proporciona multitud de datos *in situ*, a bajo coste y con alta resolución espacial y temporal.

La hipótesis de partida de que los datos obtenidos mediante sensores remotos pueden ser utilizados para predecir las cosechas de setas silvestres en los bosques mediterráneos constituye el innovador planteamiento de partida de esta Tesis Doctoral. El principal objetivo es predecir y estimar la producción de setas con datos obtenidos a partir de sensores remotos activos y pasivos. Para ello, se han desarrollado tres metodologías en las que se combinan datos meteo-climáticos con datos procedentes de la teledetección: imágenes ópticas multiespectrales, datos obtenidos con LiDAR terrestre (TLS) y datos SAR para estimar las cosechas de setas.

El primer capítulo se centra en comprobar si los datos de teledetección permiten predecir los rendimientos de setas silvestres a partir del NDVI, la humedad del suelo e imágenes ópticas multiespectrales. La combinación de datos procedentes de sensores remotos y datos meteo-climáticos predice mejor las cosechas de setas silvestres que los datos de teledetección solamente. Este capítulo ha sido publicado en el artículo "*Primary productivity and climate control mushroom yields in Mediterranean pine forests*" en la revista Agricultural and Forest Meteorology (2020), incluida en el JCI.

El segundo capítulo, "*Stand Structural Characteristics Derived from Combined TLS and Landsat Data Support Predictions of Mushroom Yields in Mediterranean Forest*", publicado en la revista incluida en el JCI Remote Sensing (2022), parte de la hipótesis de que el uso combinado de diferentes tipos de datos de teledetección tiene un gran potencial para la estimación de cosechas de setas silvestres. La interacción entre los datos Landsat y TLS tienen capacidad de predicción de las cosechas de setas silvestres en los bosques mediterráneos.

El tercer capítulo de esta tesis se centra en el análisis de series temporales de datos SAR. Existen muy buenas correlaciones entre la coherencia interferométrica y la producción de setas silvestres micorrícicas. Este capítulo se encuentra actualmente en revisión para su publicación en una revista del JCI: "*Towards prediction of forest wild mushrooms yields with time series of Sentinel-1 interferometric coherence data*".

Todos estos trabajos suponen una nueva perspectiva para el estudio de las setas silvestres utilizando la teledetección, pudiendo mejorar así la resolución temporal y espacial de las predicciones de sus cosechas y contribuyendo a desvelar los factores que desencadenan la fructificación de los hongos silvestres.

Abstract

Forests provide valuable resources for society. Their sustainable management maximises the production of the products they provide, at a rate that maintains their biodiversity, productivity, and regenerative capacity. Forest resources include non-wood forest products (NWFP), including wild mushrooms. In addition to the direct provisioning and cultural ecosystem services they provide, mushrooms also offer supporting and regulatory services. Currently, the harvesting of edible wild mushrooms has increased dramatically, but their yields are directly affected by global change processes. Sustainable management of this NWFP can be supported by new tools offered by information technologies, including remote sensing, which provides a multitude of *in situ* data, at low cost and with high spatial and temporal resolution.

The starting hypothesis that remotely sensed data can be used to predict wild mushroom yields in Mediterranean forests is the innovative approach of this PhD Thesis. The main objective is to predict and to estimate mushroom production with data obtained from active and passive remote sensors. For this purpose, three methodologies have been developed combining meteo-climatic data with remotely sensed data: multispectral optical imagery, terrestrial LiDAR (TLS) data and SAR data to estimate mushroom yields.

The first chapter focuses on testing whether remote sensing data can predict wild mushroom yields from NDVI, soil moisture and multispectral optical images. The combination of remotely sensed data and meteo-climatic data predicts wild mushrooms yields better than remote sensing data alone. This chapter has been published in the article "*Primary productivity and climate control mushroom yields in Mediterranean pine forests*" in the JCI journal Agricultural and Forest Meteorology (2020).

The second chapter, "*Stand Structural Characteristics Derived from Combined TLS and Landsat Data Support Predictions of Mushroom Yields in Mediterranean Forest*", published in the JCI journal Remote Sensing (2022), hypothesises that the combined use of different types of remotely sensed data has great potential for wild mushrooms yield estimation. The interaction between Landsat and TLS data has the potential to predict wild mushrooms yields in Mediterranean forests.

The third chapter of this PhD Thesis focuses on the time series analysis of SAR data. There are very good correlations between interferometric coherence and mycorrhizal wild mushrooms yields. This chapter is currently under review for publication in a JCI journal: "*Towards prediction of forest wild mushrooms yields with time series of Sentinel-1 interferometric coherence data*".

All this research provides a new perspective for the study of wild mushrooms using remote sensing, improving the temporal and spatial resolution of mushroom yield predictions, and contributing to unveiling the factors that trigger the fruiting of wild mushrooms.

Introducción

Introducción

RECURSOS FORESTALES

El 31% de la superficie terrestre, 4.060 millones de ha, está ocupada por bosques (FAO, 2022),. La región mediterránea constituye el 6,5% de la superficie terrestre (FAO y Plan Bleu, 2018), estando el 10% de esta cubierto actualmente por bosques (Peñuelas y Sardans, 2021). El ritmo de pérdida neta de bosques disminuyó notablemente durante el período 1990-2020 debido a una reducción de la deforestación en algunos países, además de un aumento de la superficie forestal en otros a través de la forestación y la expansión natural de los bosques (FAO, 2021). Los procesos de cambio global están afectando de forma directa a la evolución de esta superficie. La expansión de las tierras de cultivo, la deforestación, el abandono del pastoreo y otras perturbaciones como los incendios forestales, las enfermedades y fenómenos meteorológicos graves afectan a su capacidad de proporcionar una amplia gama de bienes y servicios ecosistémicos (FAO, 2021; M'Hirit, 1999).

En España, los ecosistemas forestales ocupan algo más de 26 millones de hectáreas (26.280.281 ha), de las cuales casi 15 millones (14.717.898 ha) están arboladas y unos 12 millones (11.562.382 ha) desarboladas, que suponen respectivamente el 29% y el 23% del territorio nacional (MITECO, 2023). Gracias al Inventario Forestal Nacional (IFN), existen estadísticas actualizadas, casi en tiempo real, sobre la evolución de los montes en las zonas ya inventariadas, detectándose un notable aumento de la superficie de monte arbolado a costa de una disminución de la del desarbolado y cultivo. De hecho, la biomasa arbórea existente en los montes españoles es ahora mayor que la que mostraba el IFN2 (MITECO-IFN, 2023). Es reseñable que los valores de las cortas obtenidos por comparación del IFN3 con el IFN2 son superiores a los mostrados en las estadísticas oficiales elaboradas por el MAPA. Una fracción importante de estas cortas queda en los montes para el beneficio de los bosques, aumentando la protección de la biodiversidad y la retención del carbono y, también, el peligro de incendios y el de ataque de plagas y enfermedades.

Los bosques mediterráneos forman buena parte de los montes españoles, son ecosistemas muy heterogéneos y están modelados de forma directa por la influencia antrópica, de tal forma que el aprovechamiento de sus recursos es el aliciente que los sostiene (Montero y Cañellas, 1999). Su conformación está condicionada por las sequías y las altas temperaturas del verano, por lo que las principales consecuencias del cambio climático en estos bosques se deben a los cambios en la disponibilidad de agua y al aumento de las temperaturas (Sabaté et al., 2002).

Todos los bosques, incluidos los mediterráneos, son estructuras esenciales para la salud y el bienestar de toda la sociedad y juegan un papel importante en la economía (Unión Europea, 2021). El 75% de la población rural vive cerca de los bosques, que les facilita su desarrollo, especialmente en las zonas más desfavorecidas (FAO, 2022). Los bosques proporcionan multitud de beneficios para la sociedad (e.g. recreo, producción) y su gestión sostenible hace que estos beneficios aumenten, potenciando la prestación de servicios sociales, incrementándose la conservación de la biodiversidad, y maximizándose la producción de recursos forestales, la protección del suelo y del agua

(FAO, 2021). Dada la importancia de los bosques para el planeta, la gestión forestal sostenible es esencial para garantizar que las demandas de la sociedad no comprometan los recursos futuros. La gestión forestal sostenible ofrece un enfoque holístico para garantizar que las actividades forestales aporten beneficios sociales, ambientales y económicos, y así mejoren las funciones de los bosques en la actualidad y en el futuro.

Los servicios ecosistémicos son aquellos beneficios que un ecosistema aporta a la sociedad y que mejoran la salud, la economía y la calidad de vida de las personas. Los servicios ecosistémicos resultan del propio funcionamiento de los ecosistemas como la producción de agua limpia, la formación de suelo, la regulación del clima por parte de los bosques, la polinización, etc (CREAF, 2016). Es imprescindible conservar los servicios ecosistémicos porque sustentan la salud, la economía y la calidad de vida. Cuando no se es capaz de conservarlos, su degradación conduce a perjuicios significativos en el bienestar humano (Valladares, 2020).

Tal y como se explica en la Evaluación de los Ecosistemas del Milenio de España (Montes et al., 2012), el término servicios de los ecosistemas tiene origen en el ámbito científico a finales de los años 1970 con un enfoque utilitarista. Sin embargo, se utiliza como hito la obra de Ehrlich y Ehrlich, (1981) donde incluye varios capítulos bajo el epígrafe de servicios de ecosistemas, aunque es Daily, (1997) quien ofrece una primera formalización del concepto. A la vez, Costanza et al., (1997) ofrecen la valoración económica total de los servicios de 16 grandes ecosistemas del planeta, popularizando el término entre conservacionistas y medios de comunicación. Su aproximación es económica, todavía utilitarista, y el mensaje que lanza es claro: el PIB mundial es muy inferior al valor de los servicios generados por los ecosistemas. El debate se centra sobre la valoración económica de los servicios y los ecosistemas pasan a ser considerados como un *stock* de capital natural.

Desde entonces, el término 'servicios de los ecosistemas' ha ido ganando en importancia y ha desplazado en diferentes ámbitos a la expresión desarrollo sostenible. En este momento, se está convirtiendo en una referencia integradora de las políticas de conservación, tanto a escala global como de la Unión Europea y estatal, así como en un enfoque básico para orientar estrategias y normativas relacionadas con la conservación de la naturaleza en España. Así, por ejemplo, la meta 5 de la Estrategia de Biodiversidad 2030 de la Unión Europea, refiere a la evaluación del estado de los ecosistemas terrestres y sus servicios, y el Objetivo 15 de la Agenda 2030, habla específicamente de la conservación y uso sostenible de los ecosistemas para asegurar sus servicios y se utilizan como indicadores de la calidad del entorno (CREAF, 2016).

Los servicios ecosistémicos (Tab. 1) se dividen en cuatro categorías: aprovisionamiento, regulación, culturales, y de soporte (Devkota et al., 2023).

Tab. 1. Clasificación y ejemplos de los servicios ecosistémicos. Fuente: Alcamo et al., (2003).

Clasificación	¿Qué son?	Ejemplos
Servicios de suministro o aprovisionamiento	Son aquellos referidos a la cantidad de bienes o materias primas que un ecosistema ofrece.	Madera Agua Alimentos
Servicios de regulación	Son aquellos que derivan de las funciones clave de los ecosistemas, que ayudan a reducir ciertos impactos locales y globales.	Polinización Purificación del agua Regulación del clima Control de la erosión del suelo
Servicios culturales	Son aquellos que están relacionados con el tiempo libre, el ocio o aspectos más generales de la cultura.	Recreación y turismo Educacionales De inspiración
Servicios de soporte o apoyo	Son los servicios necesarios para garantizar buena parte de los demás servicios.	Biodiversidad Fotosíntesis Ciclo del agua Ciclo de los nutrientes

Tanto los servicios de abastecimiento como los culturales dependen en última instancia de los de regulación y los de soporte, que son los menos visibles, y, a la postre, los más importantes. El enfoque de la gestión territorial a partir de los servicios ecosistémicos combina la conservación del medio natural a la vez que se hace un uso sostenible de los ecosistemas.

La planificación y gestión sostenible de los recursos forestales, servicios ecosistémicos de aprovisionamiento, se centra en los productos maderables (madera y biomasa) y no maderables (resina, frutos y bayas silvestres, setas silvestres y trufas, corcho, plantas aromáticas y medicinales, etc.). La madera y los productos maderables han tenido un papel muy importante desde el principio de la existencia del ser humano por su aprovechamiento energético y como material de construcción, entre otros aspectos, lo que les hace ser parte esencial de la economía hasta la actualidad. En muchas regiones del mundo, los productos forestales no maderables (PFNM) contribuyen al bienestar de la sociedad de muchas formas diferentes. Suponen un ingreso adicional para las familias, especialmente en los hogares con ingresos bajos; contribuyen a su seguridad alimentaria; son una importante fuente de remedios medicinales y forman parte de su patrimonio cultural y de su vida espiritual (Martínez de Arano et al., 2021).

Se consideran PFNM a los *bienes de origen biológico distintos de la madera, procedentes de los bosques, de otros terrenos arbolados y de árboles situados fuera de los bosques* (FAO, 1999). Dentro de estos productos se encuentran el corcho, la resina, las bayas, las setas y las trufas, la miel y el polen, las plantas aromáticas y decorativas, la caza, etc. La Unión Europea (2021) estimó que en 2018 el valor de todos los productos no madereros aprovechados de Europa era de 19.500 millones de € al año y que el 86% de los PFNM aprovechados se destinaban al consumo personal. En 28 países de Europa (parte europea de Rusia, Serbia y Turquía y los Estados miembros excepto Chipre, Malta y Luxemburgo e incluido Reino Unido), alrededor del 90% de los hogares consumen PFNM, siendo los frutos frescos o secos los más consumidos, seguidos de las bayas, y, además, más del 25% de los hogares recolectan PFNM de forma habitual (Lovrić et al., 2021). En España la producción de algunos PFNM ha disminuido drásticamente en los últimos años, como la del esparto y la de resina por el bajo coste de la importación, pero hay otros PFNM cuya importancia económica ha ascendido, como la de las plantas aromáticas y medicinales y la de otros productos como la castaña, el corcho, la miel y el piñón, que han mantenido su importancia a lo largo del tiempo (Sánchez-González et al., 2020). La recolección de setas silvestres comestibles es una actividad cada vez con mayor auge. Las setas son productos que, aunque se han recolectado a lo largo de toda la historia para la alimentación, actualmente son clave para la economía y el turismo, entre otros sectores de interés (Martínez de Arano et al., 2021).

SETAS SILVESTRES

Los hongos son organismos clave en el funcionamiento de los ecosistemas. Además de los servicios ecosistémicos de abastecimiento y culturales que prestan de forma directa, su interacción con la fauna y la flora es esencial en los procesos de mineralización y humificación en los suelos y suponen importantes servicios ecosistémicos tanto regulatorios como de soporte (Devkota et al., 2023; Niego et al., 2023).

En la actualidad, la recolección de setas comestibles es una actividad en auge entre la población de toda Europa, ya sea por su importancia gastronómica o social. La población local recolecta cada temporada setas para su consumo o para generar rentas complementarias, bien por su venta directa, bien por su explotación turística (Boa, 2004). Es conocido que los antepasados ya consumían este recurso, y, con el tiempo, ha ido en auge la comercialización y recolección de diferentes especies comestibles, como *Boletus edulis* Bull. y *Lactarius deliciosus* (L.) Gray (Sánchez-González et al., 2020).

La cadena de valor de las setas silvestres comestibles es muy compleja. El proyecto INCREDIBLE financiado por la Comisión Europea ha avanzado en su concreción, identificando a todos los actores implicados en su aprovechamiento y los problemas y oportunidades que se generan en Europa (Fig. 1). Las setas silvestres son un producto alimenticio que se recolecta con fines económicos y/o recreativos. Los recolectores de setas no suelen ser los propietarios de los bosques y la legislación sobre la propiedad varía de un país a otro. Las actividades derivadas de la cadena de valor de las setas silvestres comestibles dependen de diferentes legislaciones gubernamentales, como la forestal, la medioambiental, la fiscal, la alimentaria y la sanitaria. Esto presenta un escenario complejo en el que diferentes administraciones tienen competencias legislativas sobre la cadena de valor de las setas silvestres. El micoturismo está muy desarrollado en determinadas zonas, mientras que es muy reciente o inexistente en otras zonas productivas. Así, la legislación que afecta a toda la cadena de valor es muy compleja (Brenko et al., 2018).

El gran interés social por este PFNM se ha visto también reflejado en el desarrollo de numerosas herramientas de modelización y predicción de las cosechas de setas silvestres, tanto a nivel científico como de gestión territorial y de información directa a los recolectores, muchas de ellas para los bosques mediterráneos, cuyo desarrollo está marcado por la extrema complejidad que caracteriza los ciclos de vida de los hongos (Sánchez-González et al., 2020).

Los hongos son organismos muy diversos, todos ellos eucarióticos, heterótrofos, y cuya alimentación es por absorción. Abundantes en todo el mundo, la mayoría pasan desapercibidos por el pequeño tamaño de sus estructuras y su estilo de vida críptico, en el suelo o sobre materia orgánica muerta. Los hongos pueden ser simbiontes de plantas, animales u otros hongos, y también parásitos. Habitualmente, se hacen visibles cuando fructifican, ya sea en forma de setas o mohos. Los hongos desempeñan un papel esencial en la descomposición de la materia orgánica y tienen funciones fundamentales en el ciclo y el intercambio de nutrientes en el medio ambiente. El reino Fungi abarca una enorme diversidad de taxones con variadas ecologías, estrategias de ciclo vital y morfologías que van desde los unicelulares hasta los hongos superiores. Sin embargo, poco se sabe de la verdadera biodiversidad del

reino fúngico, que se ha estimado entre 2,2 y 3,8 millones de especies (Hawksworth y Lücking, 2017), de las que sólo se han descrito unas 148.000 (Cheek et al., 2020), con más de 8.000 especies conocidas por ser perjudiciales para las plantas y al menos 300 que pueden ser patógenas para el ser humano ("Correction," 2017).

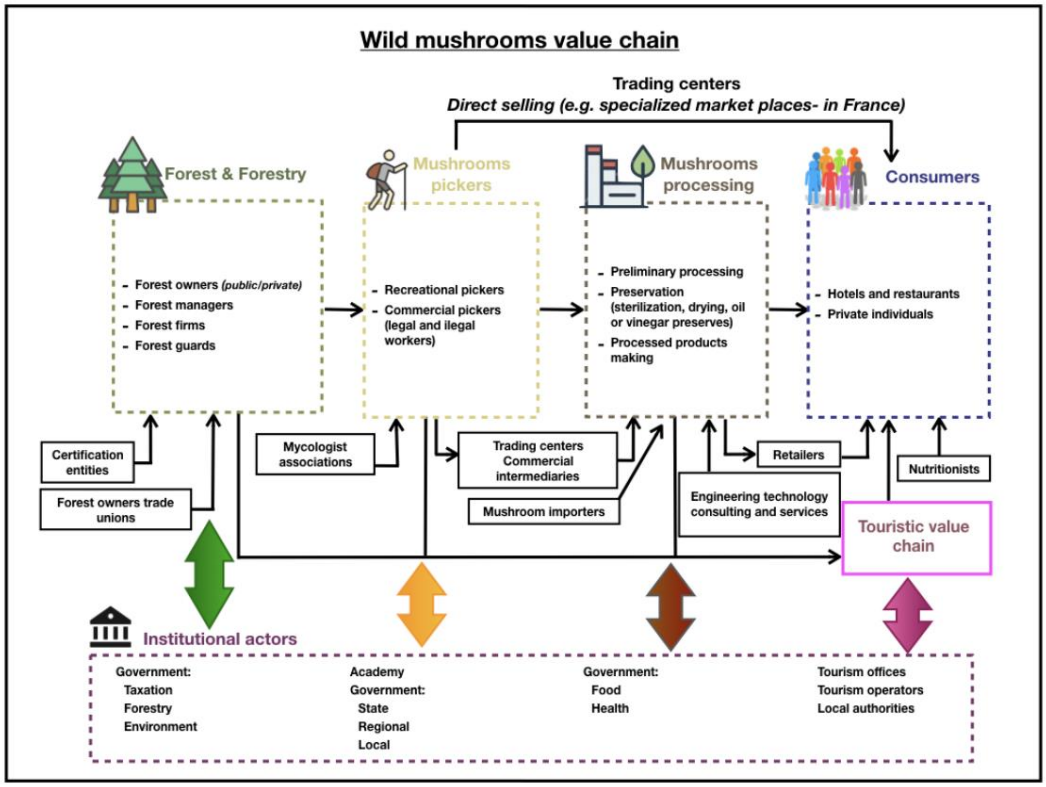

Fig. 1. Mapa de la cadena de valor de las setas silvestres comestibles desarrollado en el proyecto INCREDIBLE. Fuente: Brenko et al., (2018).

Dependiendo de su estrategia de alimentación, los hongos se clasifican en tres grupos tróficos: parásitos, saprófitos y simbiontes (Allen, 1991). Los hongos parásitos se alimentan de sus huéspedes, que pueden ser plantas, animales u otros hongos, pudiéndoles causar deterioro e incluso la muerte. Los hongos saprófitos son los mayores descomponedores de los bosques, segregan enzimas para la descomposición de la materia orgánica muerta, liberando nutrientes y mejorando así la fertilidad del suelo (Niego et al., 2023). En el grupo trófico de los hongos simbiontes aparecen los hongos liquenizados y los micorrícicos. La liquenización requiere la asociación íntima de un hongo con un alga o una cianobacteria. Los líquenes están presentes en la mayoría de los ecosistemas terrestres, lo que indica que es un proceso muy eficiente que ha permitido a muchas especies de hongos y algas colonizar ambientes que les estaban vedados de forma independiente. En la actualidad se conocen unas 17.000 especies de hongos liquenizados. Los hongos micorrícicos obtienen carbono y otras sustancias orgánicas esenciales a través de su asociación con las raíces de las plantas vasculares (Zhang et al., 2022). Independientemente de su forma de vida, más de 2.000 especies de hongos producen fructificaciones comestibles: setas y trufas (Boa, 2004).

En los trabajos compilados en esta tesis se ha trabajado con setas silvestres, teniendo en cuenta los tres grupos tróficos en los que se agrupan los hongos, y se hace referencia especial a dos especies comestibles con gran importancia culinaria, social y económica en los bosques mediterráneos: *Lactarius deliciosus* (Fig. 2a) y *Boletus edulis* (Fig. 2b).

Fig. 2. Setas silvestres comestibles. a) *Lactarius deliciosus*. b) *Boletus edulis*.

Los hongos basidiomicetos del género *Lactarius* Pers., de la familia Russulaceae, constituyen uno de los grupos de especies más diversos de entre los hongos ectomicorrícicos. Crecen tanto en suelos ácidos como calcáreos y, generalmente, se asocian en simbiosis con plantas huéspedes de la familia Pinaceae (Hutchison, 1999). La especie más representativa de entre las que se recogen en los pinares mediterráneos es el níscalo, *Lactarius deliciosus*, una seta comestible que se produce durante el otoño. Los pinares más productivos de níscalos, en los años de máxima producción, son capaces de producir más de 300 kg/ha en una sola temporada, aunque los valores medios se encuentran alrededor de 50 kg/ha y año (Sánchez-González et al., 2020). El precio pagado al recolector es más bajo en comparación con otras especies de setas silvestres, 10 €/kg en la Lonja de Soria del Mercado Municipal a 19 de noviembre de 2022. Este precio desciende según va aumentando su fructificación y ronda 1 €/kg en la época de máxima producción (Martínez-Peña et al., 2011).

Los hongos basidiomicetos del género *Boletus* L., de la familia Boletaceae, agrupan unas 300 especies de hongos ectomicorrícicos. *Boletus edulis* es una de las especies de setas silvestres comestibles más apreciadas a nivel mundial (Alonso Ponce et al., 2011; Águeda et al., 2006). Sus hospedantes son muy diversos, se asocia en simbiosis con especies de los géneros *Pinus* L., *Quercus* L., *Castanea* Mill. e incluso *Cistus* L. (Águeda et al., 2006; Mediavilla et al., 2016). *Boletus edulis* tiene una producción media de 50 kg/ha y año en pinares de *Pinus sylvestris* L., que, dependiendo de las condiciones meteo-climáticas, puede variar entre 5 y 350 kg/ha y año (Martínez-Peña et al., 2011). Su precio es mayor que el de *Lactarius deliciosus*, 39 €/kg en la Lonja de Soria del Mercado Municipal a 19 de noviembre de 2022.

El aprovechamiento de las setas silvestres comestibles se ve limitado por la gran variabilidad intra e interanual de sus cosechas, a lo que se suma de forma directa el efecto del cambio global, que provoca que la fructificación de los hongos sea cada vez más escasa en los ambientes mediterráneos (Ágreda et al., 2015; Morera et al., 2022). Los hongos en las latitudes templadas generalmente fructifican después de que las condiciones meteorológicas sean cálidas y húmedas. De hecho, cuando las temperaturas primaverales y las precipitaciones de finales de verano del año de fructificación son las adecuadas, en los bosques mediterráneos se producen setas en abundancia (Ágreda et al., 2016; Alday et al., 2017a). Además de por los factores abióticos climáticos, la producción de setas se ve afectada de forma directa por otros factores bióticos y abióticos de los ecosistemas, como la fisiografía (Bonet et al., 2008), las propiedades físicas y químicas del suelo (Hagenbo et al., 2022) y las variables estructurales del bosque (Hagenbo et al., 2022; Tomao et al., 2017), entre otras.

El estado de la vegetación y, por lo tanto, sus cambios a diferentes escalas espaciales y temporales, afectan de forma directa al desarrollo de los hongos, debido a su íntima relación con las plantas, sobre todo en el caso de los hongos micorrícicos (Lauber et al., 2008). De hecho, la productividad primaria de la masa forestal es un parámetro relevante para la estimación de las cosechas de setas silvestres (Olano et al., 2020). Además, también ha demostrado ser relevante tanto la edad del hospedante (Ágreda et al., 2013; Martínez-Peña et al., 2012) como la densidad del rodal (Martínez-Rodrigo et al., 2022). La eliminación de los árboles, fuente de energía y materia orgánica para la producción de las setas, provoca la disminución de los hongos ectomicorrícicos a corto plazo (Küçüker y Baskent, 2014; Tomao et al., 2017). Así, la adecuada gestión selvícola, especialmente en los bosques mediterráneos, tiene relación directa con la producción de setas silvestres (Oria de Rueda et al., 2008).

Teniendo en cuenta todas estas premisas, la elaboración de modelos de distribución de especies y de predicción de cosechas de setas silvestres se ha basado principalmente en variables edafo-climáticas y de masa. Respecto a los modelos de distribución de especies, la revisión de Hao et al., (2020) pone de manifiesto que su desarrollo está en crecimiento en todo el mundo gracias a la ciencia ciudadana y a la alta disponibilidad de datos ambientales, que, junto con la mejora en las técnicas de computación, permite el desarrollo de herramientas que permitan evaluar el impacto del cambio global y de la invasión de especies exóticas, por ejemplo. Los modelos de predicción de cosechas de setas silvestres, muy abundantes para los bosques mediterráneos, permiten disponer de estimaciones precisas de la producción, no sólo para que los gestores puedan integrarlas en la planificación de la gestión forestal o para que el sector industrial establezca estrategias de negocio (Sánchez-González et al., 2019), sino también para cumplir con los requisitos internacionales de información de Forest Europe (Forest Europe, 2015) y la FAO (Forest Resource Assessment-FRA) (MacDicken, 2015). Los modelos empíricos contribuyen directamente proporcionando tanto una comprensión cualitativa como predicciones cuantitativas del impacto de las diversas prácticas de gestión y los escenarios climáticos sobre el comportamiento de los ecosistemas forestales en diferentes escalas espacio-temporales, permitiendo integrar la producción de los diferentes productos en los sistemas de planificación de gestión ya existentes, como los simuladores de rodales y las herramientas de Sistemas

de Apoyo a la Toma de Decisiones (DSS) (Küçüker and Başkent, 2017a, 2017b; Sánchez-González et al., 2015).

Los trabajos previos han demostrado que los factores meteo-climáticos son claves para controlar el rendimiento de los hongos (Ágreda et al., 2016; Alday et al., 2017b; Karavani et al., 2018; Kauserud et al., 2008). Los otoños húmedos y cálidos parecen favorecer las cosechas de los hongos ectomicorrícicos en los pinares españoles (Alday et al., 2017a; Martínez-Peña et al., 2012; Taye et al., 2016). Sin embargo, los factores climáticos por sí solos no explican completamente la aparición de las setas silvestres: factores topográficos, como la pendiente, la orientación o la altitud (Egli, 2011), las características del suelo (pH, textura, etc.) (Martínez-Peña et al., 2012) y las variables de estructura de la masa (Tahvanainen et al., 2016) parecen tener también influencia en la fructificación de los hongos (Tomao et al., 2017). Entre este último grupo de variables, el área basal de la masa forestal se ha correlacionado de forma directa con la producción de setas en numerosas ocasiones (Bonet et al., 2010, 2008; de-Miguel et al., 2014; Martínez-Peña et al., 2012; Tahvanainen, 2014).

La planificación forestal sostenible del aprovechamiento micológico y la información a los recolectores de setas se apoya en las herramientas de seguimiento ambiental que ofrecen las tecnologías de la información. Por ejemplo, el servidor MICODATA (Martínez-Peña et al., 2011) gestiona la cartografía de producción de setas silvestres para cuya elaboración se utilizan capas cartográficas derivadas como el Mapa Forestal de España, ortofotos e información meteo-climática para predecir las cosechas de setas en Castilla y León. Además, dentro del Grupo Operativo del Ministerio de Agricultura Pesca y Alimentación MIKOGEST, se ha desarrollado la aplicación móvil *smartbasket*, abierta para todos los usuarios y cuya https://smartbasket.mikogest.net/función principal es la transferencia de datos micológicos entre el recolector y el gestor del aprovechamiento. *Smartbasket* es una herramienta que contribuye a la gestión sostenible del recurso mediante la identificación y localización de setales, integrando las tecnologías de la información (Altelarrea et al., 2022).

En los últimos años, variables obtenidas a partir de información territorial generada mediante teledetección ha permitido refinar estos modelos, mejorándolos cuantitativa y cualitativamente. Ejemplos de esta integración son el uso de información procedente de sensores activos LiDAR (*Light Detection and Ranging*) para identificar áreas de fructificación de setas (Peura et al., 2016; Thers et al., 2017) y para el desarrollo de modelos selvícolas que permitan optimizar la producción de este recurso no maderable (Pascual y de-Miguel, 2022), y los trabajos de uso de información TLS (*Terrestrial Laser Scanning*), SAR y multiespectral presentados en esta tesis. Toda esta información aporta datos a una escala espacial más que adecuada para la gestión forestal y con alta resolución temporal, lo que permite que la información esté realmente actualizada. La combinación de datos climáticos con datos procedentes de sensores mejora notablemente la predicción y, por lo tanto, la estimación de las cosechas de setas silvestres (Olano et al., 2020), lo que abre las puertas a un nuevo campo de aplicación directa de esta tecnología para la cuantificación de los servicios ecosistémicos que aportan los hongos y las setas silvestres.

TELEDETECCIÓN

La teledetección, junto a las técnicas de almacenamiento y procesado de datos geográficos, permite disponer de una cantidad ingente de datos territoriales, algunos de ellos accesibles en tiempo real (Chuvieco, 2010), por lo que constituye una herramienta esencial para adquirir información con múltiples aplicaciones ambientales.

La teledetección aérea se remonta a 1858 cuando se toma la primera fotografía aérea desde un globo aerostático (Blaschke et al., 2011). En 1909, se obtiene la primera fotografía aérea desde un avión, abriendo camino a una larga historia de observación desde plataformas remotas (Campbell y Wynne, 2011). A finales de los años 1950, se lanza el primer satélite artificial, Sputnik, y el primer satélite para la observación de la Tierra, TIROS-1. En 1972 se lanza Landsat-1, desencadenando el inicio de numerosos estudios y proyectos espaciales (Chuvieco, 2010). Posteriormente, varios satélites meteorológicos y de observación, como AVHRR, Landsat y SPOT, han proporcionado mediciones globales de diversas variables para todo tipo de fines, como la investigación de los procesos de cambio global, la agricultura, la exploración de los recursos de la Tierra o el seguimiento de las actividades humanas (Wong et al., 2021). Ya en 2014, se lanza el primer satélite de la misión Copernicus de la Agencia Espacial Europea (ESA), con el objetivo de observar el medio ambiente para su comprensión y protección y contribuir así a mejorar tanto la salud como la seguridad de los ciudadanos (MITECO-Copernicus, 2023).

Imágenes multiespectrales

La obtención de imágenes ópticas multiespectrales se realiza utilizando sensores pasivos, que registran la respuesta de los objetos a la radiación del sol. Estos sensores obtienen la información de la superficie terrestre a través de la energía que refleja, definida en función de su longitud de onda, y se organiza en las bandas correspondientes al espectro electromagnético. Por esta razón, las imágenes de los sensores pasivos se denominan multiespectrales. Los sensores pasivos tienen la capacidad de convertir los datos registrados en radiancias y permiten transmitir los datos de grandes superficies en tiempo real, además, esta información permite su tratamiento a través de distintas técnicas de computación. El principal inconveniente de estos sensores es su dependencia de las condiciones externas, como la disponibilidad de luz solar o la presencia de nubes, para que en sus imágenes se obtenga toda la información de la superficie terrestre.

Las longitudes de onda que con mayor frecuencia se utilizan en sensores de observación de la tierra (*Earth Observation*, EO por sus siglas en inglés) son las comprendidas entre 0.4 y 0.7 µm, que corresponden a la región del espectro visible (Chuvieco, 2010), la única radiación apreciable por el ser humano, y, por esta razón, estas imágenes son también denominadas ópticas, ya que se pueden apreciar igual que por el ojo humano. Además, otras longitudes de onda utilizadas en sensores EO proporcionan información que no es apreciable por el ojo humano, como la región del infrarrojo cercano (IRC) y la del infrarrojo medio (SWIR), con longitudes de onda comprendidas entre 0.7 y 1.2 µm para el IRC, y 1.2 y 2.5 µm para el SWIR. Las bandas espectrales que tiene un sensor determinan su resolución espectral. Otros datos para tener en cuenta a la hora de elegir el sensor son: su resolución espacial, refiriéndose al

tamaño del pixel captado; su resolución radiométrica, que es la sensibilidad del sensor para detectar las variaciones de la radiancia espectral; y su resolución temporal, que es la frecuencia con la que podemos obtener información del sensor y generar series temporales de datos (Campbell y Wynne, 2011).

Así, los sensores orbitales multiespectrales de alta resolución espacial y espectral permiten acceder a información detallada sobre la cobertura del suelo, indicando cómo se comporta cada objeto frente a la reflectancia de la radiación electromagnética (Haneda et al., 2023). Analizando la respuesta de reflectividad de una superficie en cada longitud de onda, se obtiene su firma espectral o signatura. Con esta firma se puede reconocer cualquier superficie de interés, ya que cada superficie de comporta de una manera diferente.

Una de las signaturas más características es la de la vegetación, con su baja reflectividad en el rango del visible, su alta reflectividad en el IRC y su decadencia en el SWIR. La absorción en la parte del espectro visible por los pigmentos clorofílicos hace que tengan una menor reflectividad, de hecho, la clorofila se manifiesta de color verde porque absorbe más radiación en el rojo y en el azul (Gates et al., (1965). En condiciones de vigor de la planta, la clorofila se comporta como el pigmento fundamental y dominante. Esto permite que se pueda diferenciar la vegetación sana de la vegetación enferma, ya que, a mayor cantidad de clorofila, mejor es su estado y, por lo tanto, menor reflectancia tiene en el espectro visible. En cambio, la vegetación enferma muestra mayor reflectancia en el espectro visible, ya que cuanto menor es la cantidad de clorofila, aumenta la reflexión en las zonas donde actúa, el azul y el rojo. En el IRC la vegetación tiene una alta reflectividad que se mantiene durante todo el rango, por esta razón se suele instalar solamente un sensor en el infrarrojo cercano en cada satélite. La reflectancia en el SWIR indica el contenido en agua; cuanto mayor humedad, la planta absorberá más energía y reflejará menos, así que, por tanto, un vegetal enfermo con poco contenido de agua en sus células reflejará más (Fig. 3).

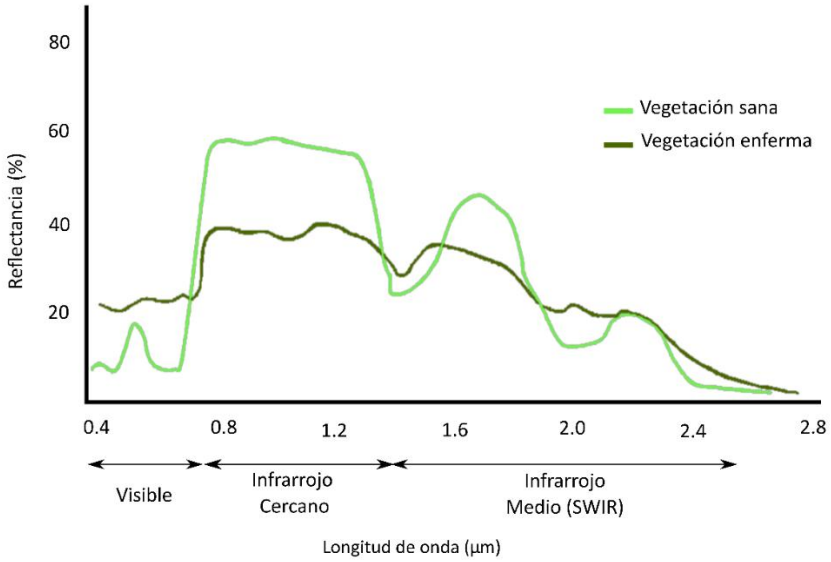

Fig. 3. Firmas espectrales de la vegetación sana y vegetación enferma. Fuente: Elaboración propia a partir de Chuvieco, (2010).

Desde la perspectiva de la teledetección, los procesos pueden caracterizarse mediante índices de vegetación derivados o series temporales de valores espectrales (Liang et al., 2016).

Los índices de vegetación se basan en la diversa respuesta de las cubiertas vegetales de la superficie en diferentes zonas del espectro de radiación. Los índices son valores adimensionales, basados en mediciones de radiación indicadoras de la actividad y abundancia relativa del verde (Jensen, 2005). El índice de vegetación más utilizado es el NDVI (índice de Diferencia Normalizada) desarrollado por Rouse et al., (1973), y que se define como:

$$NDVI = \frac{IRC - RED}{IRC + RED}$$

Donde RED son los valores de reflectividad en la banda del rojo e IRC los de la banda del infrarrojo cercano. Los valores del NDVI en la vegetación están comprendidos entre 0 y 1, y están relacionados de forma directa con la productividad primaria neta de los ecosistemas y con el vigor de la vegetación a estudiar (Birky, 2001; Rouse et al., 1973; Wang et al., 2004b). El NDVI se utiliza principalmente para discriminar la vegetación y ver sus cambios estacionales o anuales (Fig. 4). En esta tesis, los valores de NDVI son calculados a partir de los datos tomados por los satélites del programa Landsat, obteniendo una serie de datos continua desde 1993 hasta 2021.

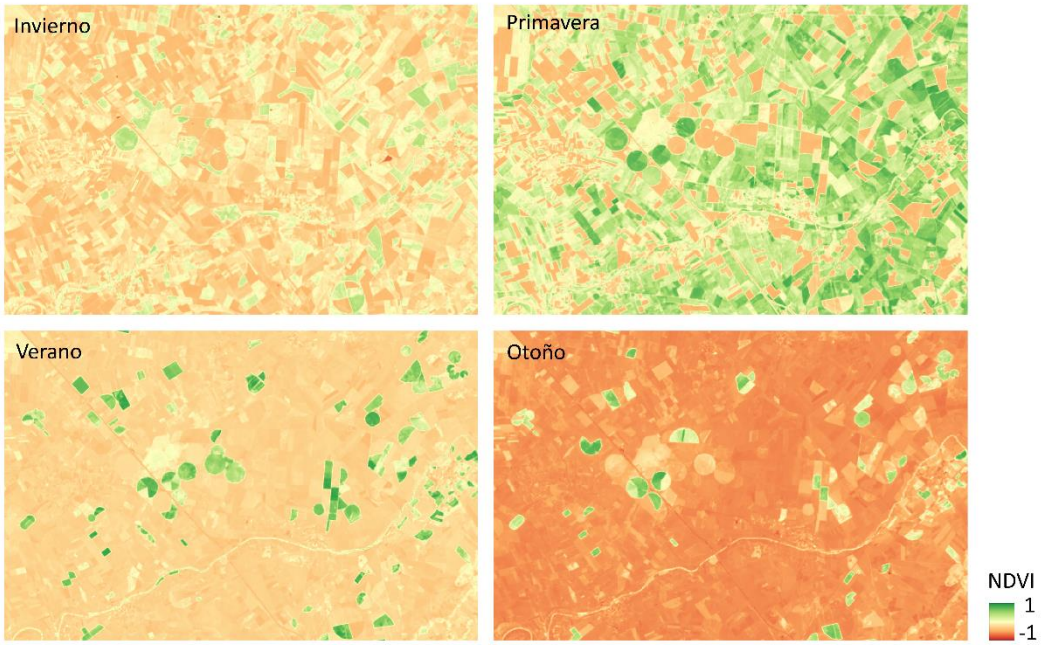

Fig. 4. Cambio anual en la vegetación de campos de cultivo en diferentes estaciones. Fuente: Elaboración propia a partir de datos de Landsat-8 y Landsat-9.

El NDVI es el índice espectral más utilizado para la evaluación de la vegetación (Huang et al., 2020). Es un índice ampliamente utilizado en la agricultura, desde para el seguimiento de los cultivos (Seo et al., 2019), hasta para la predicción de su rendimiento (Ji et al., 2021). El seguimiento de la vegetación y, por lo tanto, del estado ecológico de

los bosques es una de las aplicaciones directas de uso del NDVI más habituales en el ámbito ambiental y forestal (Prăvălie et al., 2022), aunque también ha demostrado tener utilidad para la cuantificación del carbono orgánico del suelo en pastizales (Li et al., 2023), la estimación de la humedad del suelo (Wang et al., 2004a), la estimación de biomasa (Zhu y Liu, 2015), o incluso para realizar el seguimiento de la cubierta vegetal de líquenes (Erlandsson et al (2023). No se puede olvidar que el NDVI ha demostrado ser en todos los casos un buen estimador de la productividad primaria (Vicente-Serrano et al., 2016), lo que le ha hecho ser el índice de más amplio uso desde los inicios de la teledetección.

La disponibilidad de grandes volúmenes de imágenes, de acceso libre y gratuito, junto con los avances de procesamiento y la capacidad computacional han estimulado asimismo el uso habitual de las series temporales (Banskota et al., 2014). Una serie temporal de imágenes de sensores remotos permite identificar una gran variedad de procesos ecosistémicos, así como caracterizar patrones temporales en su variación (Gómez et al., 2011). Su uso es cada vez más común para la detección de cambios en los bosques, ya que proporcionan información precisa sobre el momento en que estos se producen (Woodcock et al., 2020) y su magnitud.

Las series temporales de datos ópticos de resolución espacial media han demostrado tener una gran capacidad para la caracterización de fenómenos ambientales (Gómez et al., 2016). Se han utilizado series temporales de datos ópticos para la detección de cambios en la cobertura del suelo (Zhu et al., 2020), el monitoreo forestal (Banskota et al., 2014; Masek et al., 2013) y la estimación de biomasa con series temporales de NDVI (Zhu y Liu, 2015), entre otros usos. También se han utilizado con datos procedentes de otros sensores, como Sentinel-1 para la detección de cambios en los bosques (Tanase et al., 2019), como la combinación de datos Sentinel-1 y Sentinel-2 para detectar eventos de siega en pastos (Komisarenco et al., 2022) y para la estimación de biomasa en bosques tropicales a partir de datos SAR (Cartus y Santoro, 2019). El tercer capítulo de esta tesis es un ejemplo de aplicación de las series temporales al estudio de las cosechas de setas silvestres.

Sensores SAR

El SAR (*Synthetic Aperture Radar*) es una tecnología de teledetección por microondas concebida a principios de los años 1950 (Tsokas et al., 2022). Los sensores SAR son activos, emiten energía cuya respuesta captan después de interaccionar con el objeto alcanzado. Los sensores SAR son capaces de penetrar en la atmósfera en casi cualquier situación (nubes, humo, lluvia fina, etc.) (Ulaby, et al., 2014), lo que hace que sus datos sean de gran utilidad en los procesos de EO.

Los sistemas SAR son capaces de registrar la intensidad de la señal de retorno (radiación retrodispersada) y el retardo de tiempo entre la transmisión y la recepción de cada pulso de energía, el cual se relaciona con la distancia a los objetos o superficies observados. La magnitud física medida directamente por el sensor es la intensidad de la radiación retrodispersada, la cual depende del coeficiente de retrodispersión o *backscattering* de cada superficie. Este coeficiente relaciona la energía retrodispersada con la recibida por unidad de área en la dirección del alcance terrestre (Marchionni y Cavayas, 2014). El coeficiente de retrodispersión es sensible a las características de la

superficie de la Tierra, incluida la constante dieléctrica y la rugosidad superficial del suelo, además de a las propiedades geométricas de la vegetación (contenido de agua de la vegetación, forma, orientación, etc.), y a la frecuencia y a la polarización de la onda emitida (Bhagat, 2017).

La constante dieléctrica influye en la capacidad de los materiales para absorber, reflejar y transmitir la energía de las microondas (Marchionni y Cavayas, 2014) y determina qué parte de la radiación entrante se dispersa sobre la superficie, cuánta señal penetra en el medio y qué parte de la energía se pierde por absorción (Flores-Anderson et al., 2019). En la Fig. 6 se muestra la capacidad de penetración de la señal SAR en función de su longitud de onda. Las longitudes de onda más cortas (banda X, con una longitud de onda de entre 2.40 y 3.75 cm) reflejan desde las superficies superiores del dosel de la vegetación, mientras que las longitudes de onda más largas (banda L, longitud de onda comprendida entre 15 y 30 cm) penetran a través del dosel y se reflejan desde la superficie del suelo (Barrett et al., 2009).

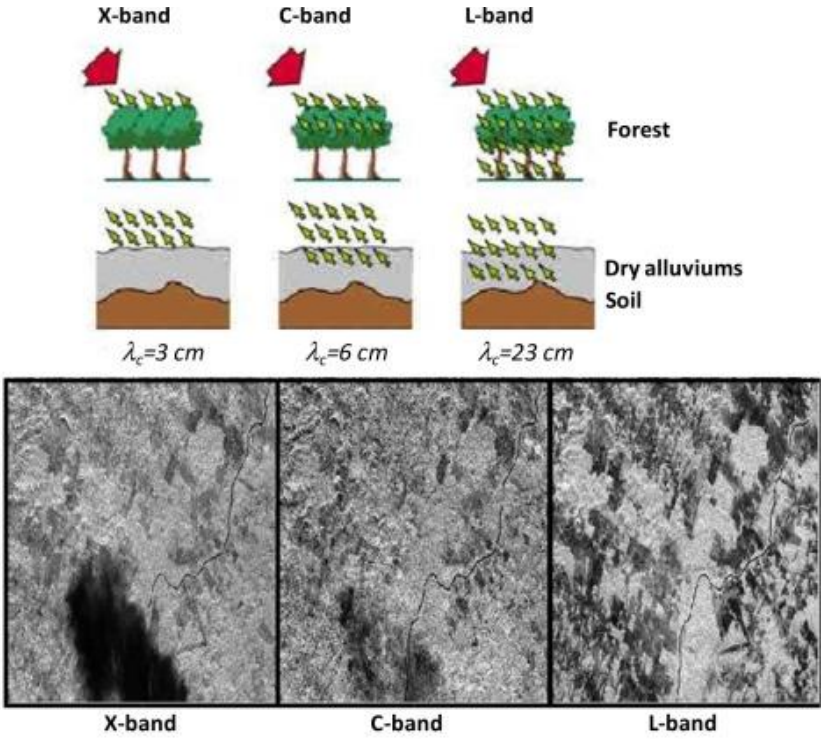

Fig. 5. Penetración de la intensidad de retrodispersión en el dosel vegetal y suelo dependiendo de la banda. Fuente: Ferro-Famil y Pottier, (2016).

En esta tesis se trabaja con los datos SAR obtenidos por la misión Sentinel-1 del programa Copernicus, que está compuesta por dos satélites gemelos, Sentinel-1A, lanzado en abril de 2014, y Sentinel-1B, lanzado en abril de 2016. Cada uno de ellos está equipado con un sensor SAR de banda C (longitud de onda entre 3.75 y 7.50 cm) y están diseñados para facilitar la observación de la Tierra a través imágenes RADAR. Su resolución espacial es de 5 x 20 m (*single look*) en el modo de adquisición *Interferometric Wide swath* (IW), con un ancho de la escena de 250 km y una resolución temporal de 12 días, si se considera una sola órbita de un solo satélite, seis días considerando ambos

satélites. Al paso por la Península Ibérica estos sensores tienen polarización dual VV+VH (ESA-SENTINEL-1, 2023). La polarización describe la orientación del plano de oscilación de la señal que propaga el sensor SAR. La mayoría de los sensores SAR son linealmente polarizados y transmiten las ondas de forma horizontal (H) y vertical (V) (Flores-Anderson et al., 2019). El que Sentinel-1 sea de polarización dual, significa que emite una señal vertical y la recibe verticalmente (VV) y emite otra señal vertical y la recibe horizontalmente (VH).

Además, con las imágenes SAR se pueden trabajar las técnicas de interferometría (InSAR). El InSAR permite analizar las variaciones en la superficie terrestre a partir de la diferencia entre las señales de fase de dos adquisiciones cercanas en el tiempo (Flores-Anderson et al., 2019). Como resultado de las técnicas InSAR, se obtiene la correlación entre dos imágenes adquiridas, la coherencia interferométrica (Borlaf-Mena et al., 2021). La coherencia tiene valores comprendidos entre 0 y 1, siendo 0 cuando menos coherencia hay y, por lo tanto, más cambio, y 1 cuando la coherencia es mayor y en la comparativa de imágenes no hay cambios. Tanto la fase interferométrica como la coherencia están relacionadas con la elevación de los objetos dispersos y la densidad de la vegetación (Abdel-Hamid et al., 2021). Gracias a la dualidad de la misión Sentinel-1 se puede calcular la interferometría de la misión Sentinel-1 cada seis días.

En las últimas décadas se han desarrollado una gran variedad de técnicas con multitud de aplicaciones en diversos campos (Tsokas et al., 2022), por lo que se clasifican los usos y aplicaciones de los datos SAR en tres categorías en función de su objetivo final: (i) mapeo y clasificación de terrenos: identifican y clasifican el tipo de superficie (Dostálová et al., 2018; Nikaein et al., 2021), el monitoreo forestal (Pulella et al., 2020a; Ygorra et al., 2021) y los derrames de petróleo (Dasari et al., 2022), por ejemplo; (ii) recuperación de parámetros: como la estimación de humedad (Barrett et al., 2009; Dorigo et al., 2017; Paloscia et al., 2013), el cálculo de la biomasa aérea (Cartus et al., 2022; Cartus y Santoro, 2019; Ghosh y Behera, 2021) o la estructura del dosel vegetal (Li et al., 2022; Pinto et al., 2013); y (iii) detección de objetos: para localizarlos e identificarlos en las imágenes, como el petróleo en el mar (Chaudhary y Kumar, 2020).

Sensor LiDAR terrestre

La tecnología LiDAR (*Light Detection and Ranging*) se aplica utilizando sensores remotos activos. Estos instrumentos miden el tiempo de ida y vuelta que tarda un pulso de energía láser en viajar entre el sensor y un objeto, lo que proporciona una distancia o rango desde el instrumento hasta él. El LiDAR forma una nube de puntos tridimensionales que son adecuados para estimar los atributos tanto de las superficies como de los objetos (Dubayah y Drake, 2000). A principios de los años 1980, el Servicio Forestal Canadiense demostró que los sensores LiDAR aerotransportados (ALS de sus siglas en inglés, *Airborne Laser Scanning*) proporcionaban estimaciones muy precisas de la altura, la cobertura, la estructura y la función del dosel arbóreo (Lim et al., 2003). A finales de los 1990 y la primera década del siglo XXI aparecieron los primeros instrumentos *Terrestrial Laser Scanner* (TLS) (Newnham et al., 2015), que ofrecen datos de resolución subcentimétrica de superficies topográficas y de otro tipo, incluidas

imágenes tridimensionales de topografía, afloramientos rocosos o de hielo, cuevas, árboles y vegetación, y edificaciones.

En esta tesis se utiliza el TLS, un sistema de detección LiDAR capaz de adquirir información estructural 3D de alta resolución con un nivel de detalle considerablemente superior al del ALS, que capta principalmente la capa superior del dosel, registrando los elementos del dosel inferior con menos detalle (Li et al., 2014). El TLS es capaz de registrar los elementos del dosel inferior de la vegetación con gran detalle.

Además, el TLS ofrece la oportunidad de realizar mediciones rápidas, no destructivas, precisas y exhaustivas de un gran número de árboles en poco tiempo, permitiendo investigar el desarrollo espacial de las copas en detalle (Li et al., 2014). El TLS ha demostrado tener gran potencial para estimar la biomasa aérea (AGB) (Disney et al., 2019), identificar los tallos y estimar sus diámetros (Cabo et al., 2018).

Aparte de la estructura física de la vegetación (Pascu et al., 2019), con el TLS y en combinación con algoritmos de aprendizaje automático (*machine learning*) se pueden llegar a cuantificar las perturbaciones de los bosques (Ghizoni Santos et al., 2022), a clasificar especies en el inventario forestal (Othmani et al., 2013), a estimar el índice de área foliar (Huang y Pretzsch, 2010), a detectar el estrés por deficiencia hídrica en los árboles (Jacobs et al., 2021) y a utilizar sus datos como indicador de defoliación de plagas (Jacobs et al., 2022), entre otras muchas aplicaciones directas al ámbito forestal.

Programa Landsat

En julio de 1972 la NASA (Administración Nacional de Aeronáutica y el Espacio de EE. UU.) y el Servicio Geológico de EE. UU. (USGS) lanzan el primer satélite ERTS (*Earth Resources Technology Satellite*), más tarde llamado Landsat-1, lo que marca el primer hito del programa Landsat, completado posteriormente con el lanzamiento de otros ocho satélites más (Loveland et al., 2022) para la obtención de imágenes ópticas multiespectrales, y gestionando así el registro espacial continuo más largo que existe en la actualidad (USGS, 2023). En la figura (Fig. 6) se observa la cronología de las misiones Landsat.

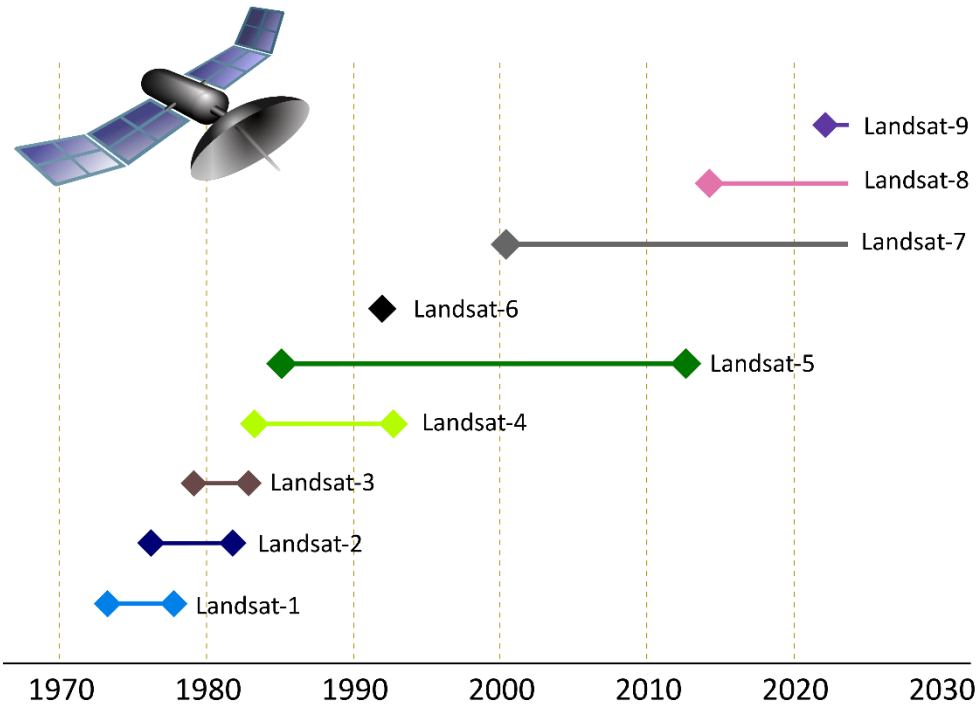

Fig. 6. Misiones Landsat desde 1972 hasta la actualidad. Fuente: Elaboración propia a partir de datos de la NASA.

Las imágenes de la serie Landsat han proporcionado recursos únicos para la EO en todo el mundo, para investigar el cambio global y desarrollar aplicaciones para la agricultura, la cartografía, la geología, la silvicultura, la planificación regional, la vigilancia y la educación (Wong et al., 2021). En octubre de 2008, el USGS puso en marcha una política para proporcionar los contenidos de Landsat de forma libre, sin coste alguno a cualquier persona a través de Internet (Wulder et al., 2022). El repositorio de datos Landsat completo es accesible a través de la aplicación EarthExplorer del USGS.

La combinación de datos de las ocho misiones Landsat proporciona la principal línea de base medioambiental global (Wulder et al., 2022). Las misiones Landsat han ido mejorando sus sensores para la obtención de datos EO. En la Tab. 2 se resumen las características de los sensores de toda la serie de satélites Landsat.

Tab. 2. Resumen de las características de los satélites Landsat. Fuente: Elaboración propia a partir de datos del USGS, (2023).

Satélite Landsat	Fechas	Sensor Multiespectral	Resolución espectral	Resolución espacial	Resolución temporal	Datos y mejoras
1	1972-1978	MSS (Multispectral Scanner)	2 visible 2 IRC	57 x 79 m	18 días	Solo investigadores principales podían usar sus datos
2	1975-1982 (1983 oficialmente)	MSS	2 visible 2 IRC	57 x 79 m	18 días	Con este satélite apareció un experimento cooperativo de inventario agrícola que comenzó a monitorear cultivos en todo el mundo.
3	1978-1983	MSS	2 visible 2 IRC	57 x 79 m	18 días	El sensor MSS del Landsat 3 originalmente tenía cinco bandas espectrales, pero una falló poco después del lanzamiento.
4	1982-1993 (2001 se dio de baja el satélite)	MSS	2 visible 2 IRC	57 x 79 m	16 días	Se añade el sensor TM, con una resolución espectral y espacial mejorada
		TM (Thematic Mapper)	3 visible	30 m		
			1 IRC			
			Térmica	120 m		
			2 SWIR	30 m		
5	1984-2013	MSS	2 visible	57 x 79 m	16 días	Es el satélite que más datos ha proporcionado por su larga durabilidad.
		TM	3 visible	30 m		
			1 IRC			
			Térmica	120 m		
			2 SWIR	30 m		
6	1993 (No llegó a alcanzar la órbita)	ETM (Enhanced Thematic Mapper)	3 visible	30 m	-	Llevaba un TM mejorado
			1 IRC			
			Térmica	120 m		
			2 SWIR	30 m		
			Pancromática	15 m		

Satélite Landsat	Fechas	Sensor Multiespectral	Resolución espectral	Resolución espacial	Resolución temporal	Datos y mejoras
7	1999-actualmente	ETM + (Enhanced Thematic Mapper Plus)	3 visible	30 m	16 días	Mejora de TM. Desde 2003 las imágenes tienen un problema, llamado bandeado, son brechas sin datos en las imágenes.
			1 IRC			
			Térmica	60 m		
			2 SWIR	30 m		
			Pancromática	15 m		
8	2013-actualmente	OLI (Operational Land Imager)	Aerosol	30 m	16 días	Incluye sensores OLI y TIRS.
			3 visible			
			IRC			
			2 SWIR			
			Pancromática	15 m		
			Cirros	30 m		
		TIRS (Sensor Infrarrojo Térmico)	2 TIRS	100 m		
9	2021-actualmente	OLI-2	Aerosol	30 m	16 días	Los sensores de este satélite son replicas mejoradas de Landsat-8. Permite una corrección atmosférica mejorada y mediciones de temperatura superficial más precisas.
			3 visible			
			IRC			
			2 SWIR			
			Pancromática	15 m		
			Cirros	30 m		
		TIRS-2	2 TIRS	100 m		

Actualmente, el satélite Landsat-7 sigue en funcionamiento, aunque en una órbita inferior a la habitual, y sus datos son útiles, aunque sin el nivel de calidad necesario para trabajos de seguimiento de ecosistemas. Landsat-8 y Landsat-9 están operativos, dando cobertura global cada ocho días (Wu et al., 2019). El programa Landsat, en continua evolución, prevé el lanzamiento de la nueva misión Landsat Next para 2030. Landsat Next proporcionará resoluciones espaciales, temporales y espectrales (26 bandas) mejoradas (NASA, 2021).

En los dos primeros capítulos de esta tesis se utilizan datos procedentes de las misiones Landsat, de los satélites Landsat-5, Landsat-7 y Landsat-8, a través del índice NDVI.

Programa Copernicus

La Agencia Espacial Europea (ESA) en colaboración con la Comisión Europea ha desarrollado el programa Copernicus, cuyo objetivo es proporcionar información precisa, actualizada y accesible para mejorar la gestión del medio ambiente, comprender y mitigar los efectos del cambio climático y garantizar la seguridad ciudadana (ESA, 2023). El programa Copernicus está formado por seis familias de misiones Sentinel, contando Sentinel-5 y Sentinel-5P como una independiente:

- Misión Sentinel-1 (ESA-SENTINEL-1, 2023): comprende una constelación de dos satélites gemelos, que operan con un sensor SAR. Tienen la capacidad de operar de día y de noche y en cualquier circunstancia climatológica, obteniendo información actualizada cada seis días entre los dos satélites. Sentinel-1A fue lanzado en 2014 y Sentinel-1B en 2017. En diciembre de 2021 empezó a fallar el sistema de sensores del satélite Sentinel-1B y en julio de 2022 se declaró el final de su misión. Esto ha hecho que se apresure la construcción para el lanzamiento de Sentinel-1C y poder así complementar a Sentinel-1A.
- Misión Sentinel-2 (ESA-SENTINEL-2, 2023): formada por dos satélites colocados en la misma orbita, en fase de 180º entre sí. Su principal objetivo es monitorear la superficie terrestre proporcionando imágenes ópticas multiespectrales de alta resolución espectral (13 bandas espectrales), espacial (10 m) y temporal (cinco días entre los dos satélites). En junio de 2015 se lanzó Sentinel-2A y en marzo de 2017 Sentinel-2B.
- Misión Sentinel-3 (ESA-SENTINEL-3, 2023): al igual que las anteriores consta de dos satélites, que fueron lanzados en el mismo año, 2018, y proporcionan una revisita de 27 días. Los datos de Sentinel-3 son utilizados para el monitoreo del océano, ambiental y del clima. Estos satélites llevan cuatro instrumentos: uno para medir el color del océano, otro para medir la temperatura marina y terrestre, un altímetro de radar SAR y un radiómetro de microondas.
- Misiones Sentinel-4 (ESA-SENTINEL-4, 2023), Sentinel-5 (ESA-SENTINEL-5, 2023) y Sentinel-5P (ESA-SENTINEL-5P, 2023). Estas misiones ofrecen datos para el seguimiento de la composición de la atmósfera desde órbitas polares y geoestacionarias. La principal misión de Sentinel-4 es monitorear los gases traza y los aerosoles clave de la calidad del aire en Europa con una alta resolución espacial y temporal. La misión de Sentinel-5 es un sistema de espectrómetro de alta resolución con siete bandas espectrales diferentes entre el ultravioleta y el infrarrojo de onda corta. Sentinel-5P reduce las brechas en la disponibilidad de datos de las dos misiones anteriores, además de las de los datos atmosféricos existentes. En 2017 se lanzó con éxito Sentinel-5P y se prevé el lanzamiento de Sentinel-4 para 2024.
- Misión Sentinel-6 (ESA-SENTINEL-6, 2023): el satélite Sentinel-6 Michael Freilich fue lanzado en 2020. Es una misión de referencia de altimetría por radar para obtener la altura global de la superficie del mar.

El programa Copernicus aboga por un acceso a sus datos y servicios abierto y gratuito. Actualmente, los datos se pueden descargar en el portal *Copernicus Data Hub*. Está previsto que, a partir de Julio de 2023, se actualice este portal y se pueda acceder a la información desde la nueva plataforma *Copernicus Data Space Ecosystem*.

En el tercer capítulo de esta tesis se han utilizado datos SAR procedentes de la misión de Sentinel-1.

ESTIMACIÓN DE RECURSOS FORESTALES CON TELEDETECCIÓN

Las técnicas avanzadas de procesamiento digital de imágenes tienen un gran potencial para ser utilizadas para el seguimiento y gestión de los ecosistemas terrestres y, *por ende*, de las masas forestales. Tal y como se ha detallado, la tecnología de teledetección proporciona una fuente excepcional de datos adquiridos con perspectiva general, así como potentes herramientas para el seguimiento de la dinámica forestal y sus factores de cambio. La teledetección proporciona datos con una gran variedad de resoluciones espectrales, espaciales y temporales que permiten modelizar el estado y el cambio de los bosques en diferentes escenarios (Gómez et al., 2019).

Desde principios de la década de 1970, cuando los primeros datos de observación de la Tierra estuvieron disponibles, las aplicaciones forestales se han beneficiado de los datos de teledetección (Cohen y Goward, 2004). Poco a poco, las aplicaciones se han vuelto más detalladas y específicas gracias a la mejora de la calidad de los datos, la capacidad de almacenamiento y las técnicas de análisis, y, también, como resultado de las necesidades de información impuestas por la sociedad, pasando de la simple caracterización a la medición y modelización complejas (Gómez et al., 2019).

Para obtener información que tenga valor para la gestión de los bosques, sus recursos y los servicios ecosistémicos, los datos obtenidos por teledetección se combinan sinérgicamente con los Sistemas de Información Geográfica (SIG) y técnicas estadísticas para el análisis y modelización de datos espaciales (Fig. 7). Muchas de estas técnicas se han utilizado y se utilizan en la actualidad para el seguimiento de los bosques mediterráneos y para la cuantificación de servicios ecosistémicos.

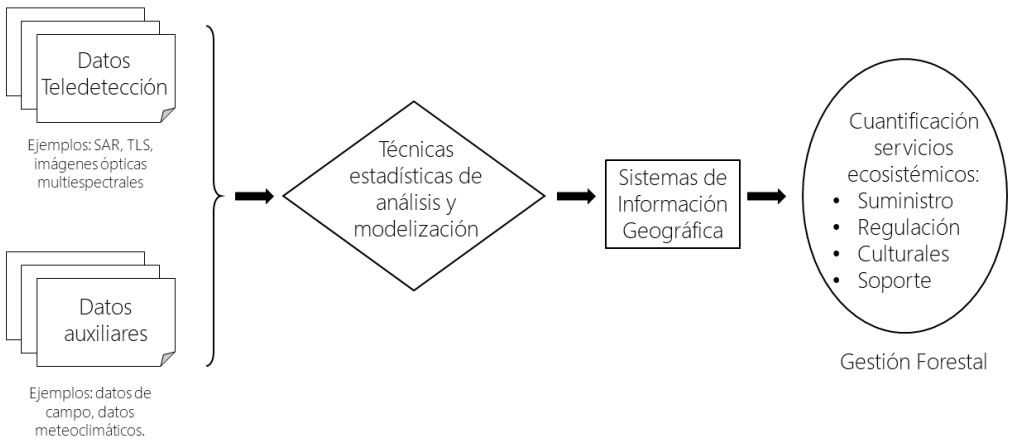

Fig. 7. Ejemplo de diagrama de flujo para la cuantificación de servicios ecosistémicos. Elaboración propia a partir de (Gómez et al., 2019).

La cobertura del suelo, su uso y sus cambios a lo largo del tiempo son información fundamental para muchas aplicaciones medioambientales, incluyendo la evaluación del almacén de carbono y la diversidad y la caracterización de la estructura y la dinámica forestal. La teledetección ofrece datos espacialmente explícitos y exhaustivos para obtener información valiosa sobre la cubierta y el uso del suelo a diferentes escalas (Gómez et al., 2019). El seguimiento global de los paisajes españoles

se apoya actualmente en tres proyectos que emplean alguna forma de teledetección: el Mapa Forestal Español (MFE), el Sistema de Información de Ocupación del Suelo en España (SIOSE) y CORINE Land Cover.

Otros ejemplos de uso habitual de datos remotos para conservación de los ecosistemas forestales son la cartografía de hábitat para el cumplimiento de los compromisos europeos de conservación de la red Natura 2000 en Castilla y León (Bengoa et al., 2017) y en Cantabria (Álvarez-Martínez et al., 2017), que se realiza combinando datos ópticos, LiDAR y auxiliares para clasificar y cartografiar los tipos de vegetación con técnicas de aprendizaje automático. En cuanto a conservación de especies emblemáticas, Cisneros-Araujo et al., (2021) compararon el rendimiento de mapas de coberturas de suelo creados a partir de Sentinel-2 y Sentinel-1, PNOA LiDAR, datos MFE y datos CORINE para evaluar la idoneidad del hábitat forestal para el oso pardo en la Cordillera Cantábrica empleando variables de cubierta de copas. Regos et al., (2022) proporciona un flujo de trabajo que conecta diferentes componentes del funcionamiento de un ecosistema derivados de series temporales de productos de teledetección, y Pace et al., (2022) y Assal et al., (2021) tienen el objetivo de evaluar la capacidad de las métricas de teledetección para detectar impactos en los elementos de las zonas de ribera y en el monitoreo de los ríos.

Con los avances en la teledetección los resultados de la precisión de clasificación de imágenes para la detección de cultivos, tipos de usos o la cobertura ha mejorado notablemente (Mazzia et al., 2019). Por ejemplo, Pulella et al., (2020b), utilizaron técnicas de clasificación del uso del suelo a partir de las texturas de las imágenes SAR en la Amazonia. Mestre-Quereda et al., (2020) clasificaron cultivos agrícolas con Sentinel-1, a partir de la coherencia y el coeficiente de retrodispersión, aunque también hay otros ejemplos de clasificaciones utilizando solamente imágenes ópticas multiespectrales (Bouslihim et al., 2022) o incluso imágenes SAR con apoyo de imágenes ópticas (Nasiri et al., 2022).

La amplia gama de capacidades que ofrecen las tecnologías de la teledetección hacen que sea una excelente opción para evaluar el estado de los bosques (Torres et al., 2021) y la cuantificación de sus recursos maderables. La tecnología LiDAR es clave para la estimación de datos relacionados con la estructura de la masa (Lefsky et al., 2002; Lim et al., 2003). Domingo et al., (2019) midieron la biomasa residual en bosques de *Pinus halepensis* Mill. con datos procedentes de ALS, mientras que Montealegre et al., (2016) estimaron variables estructurales con ALS de baja densidad a nivel de rodal. Esteban et al., (2021) han sido capaces de detectar los cambios asociados a los tratamientos selvícolas de distinta intensidad en los montes mediterráneos utilizando datos procedentes del PNOA-ALS de baja densidad de puntos y series temporales de datos Landsat.

Además, la teledetección ha demostrado ser una herramienta eficaz para comprender cómo responden los ecosistemas mediterráneos a perturbaciones de gran importancia, como el fuego, permitiendo evaluar la recuperación de la vegetación tras un incendio (Pérez-Cabello et al., 2021) y, de forma más práctica, para la planificación de áreas cortafuegos en el interfaz urbano-forestal, minimizando los riesgos directos sobre la población (Rodríguez-Puerta et al., 2020).

La monitorización de grandes superficies utilizando datos remotos supone un avance importante en la planificación de la gestión de la salud de los bosques, especialmente en lo referente a plagas y enfermedades, y autores como Guillen-Climent et al., (2020) proponen soluciones basadas en datos remotos e inteligencia artificial (IA) para su detección precoz. Las técnicas de teledetección utilizando datos de resolución espacial media permiten identificar defoliaciones y evaluar su grado de intensidad (Jönsson y Eklundh, 2004). Además, los archivos históricos de datos, entre los cuales destaca el de Landsat por su continuidad y coherencia durante más de cuatro décadas (Wulder et al., 2019), permiten modelizar y cartografiar eventos y procesos de cambio de forma retrospectiva (Gómez et al., 2011). Una serie anual de mapas de afección por procesionaria con datos de teledetección puede, por ejemplo, contribuir a mejorar el conocimiento detallado de los patrones de ocurrencia de la procesionaria del pino (Gómez et al., 2022) y, a partir de índices de vegetación, poder evaluar sus daños Sangüesa-Barreda et al., (2014).

La cuantificación y predicción de la dinámica de los PFNM puede ser también realizada utilizando datos remotos, aunque los ejemplos son más escasos. Además de los ejemplos ya citados para las setas silvestres, cuyas producciones se están empezando a predecir y cuantificar utilizando datos remotos (Martínez-Rodrigo et al., 2022; Olano et al., 2020; Pascual y de-Miguel, 2022; Peura et al., 2016; Thers et al., 2017), otros autores han trabajado en la predicción y monitoreo de otros PFMN. Por ejemplo, Blázquez-Casado et al., (2019) distinguieron entre *Pinus pinaster* y *Pinus pinea* L. a nivel de árbol individual utilizando datos LiDAR e imágenes ópticas multiespectrales con diferentes resoluciones espaciales para poder aplicar modelos de producción de resina y piña en pinares mediterráneos mixtos. En el caso de las bayas silvestres, Kositsyn, (1999) propone el uso de imágenes para identificar zonas de producción de moras, dando rangos de producción. Aubard et al., (2019) cuantifican las áreas con tendencias crecientes y decrecientes de productividad de corcho y bellotas utilizando el NDVI de las imágenes Landsat y Soares et al., (2022) evalúan los parámetros biofísicos de los alcornocales utilizando series temporales de índices de vegetación. Para las trufas, González-Zamora et al., (2022) utilizan series de datos de humedad del suelo inferidas con teledetección para determinar los periodos críticos de este parámetro en relación con su fructificación. Los ejemplos son más abundantes respecto a las plantas aromáticas y medicinales silvestres. Los datos remotos se han utilizado para determinar sus áreas de distribución (Fadeev et al., 2019; Sahel et al., 2022) y para evaluar el efecto de la sequía en sus cambios morfológicos (Al-hamed et al., 2022). Incluso es posible predecir las mejores ubicaciones para las colonias de abejas melíferas con teledetección (Abou-Shaara y Eid, 2019).

Tal y como se ha expuesto, la amplia gama de capacidades que ofrecen las tecnologías ligadas a la teledetección las hace una excelente opción para evaluar el estado de los bosques y sus servicios ecosistémicos tanto espacial como temporalmente a bajo coste (Torres et al, 2021), abriendo una oportunidad para desarrollar herramientas que faciliten la gestión, planificación y optimización del manejo de los PFNM. El principal limitante en el uso de los datos procedentes de sensores pasivos para la caracterización de las masas y los hábitats forestales es la escasa información que proporcionan sobre la estructura de la vegetación (Graf et al., 2009), mientras que los sensores activos atraviesan las copas, caracterizan la estructura y la posición de los

objetos detectados (Leutner et al., 2012). Por esta razón, en esta Tesis Doctoral se combina la información procedente de sensores activos y pasivos, para estimar la influencia de la estructura y la composición de las masas forestales en la producción de setas silvestres, utilizando los datos provenientes de sensores pasivos (Landsat-8) e información obtenida mediante sensores activos LiDAR (TLS) y datos SAR (Sentinel-1).

OBJETIVOS Y CONTENIDOS DE LA TESIS

La hipótesis de partida de esta Tesis Doctoral es que los datos obtenidos mediante sensores remotos pueden ser utilizados como predictores de las cosechas de setas silvestres en los bosques mediterráneos.

El objetivo principal de esta tesis es predecir y estimar la producción de setas silvestres a partir de datos obtenidos mediante sensores remotos activos y pasivos. Para ello se utilizan mediciones *in situ*, datos climáticos y datos procedentes de sensores remotos activos (SAR y TLS) y pasivos (multiespectral) y datos de producción de setas silvestres.

Esta Tesis Doctoral consta de tres capítulos, cada uno de ellos contiene una investigación publicada o en revisión en revistas indexadas SCI. En cada capítulo se desarrolla una metodología diferente basada en la utilización de datos remotos para la estimación de cosechas de setas silvestres en pinares mediterráneos (Tab. 3). La predicción y estimación de la producción de setas silvestres a partir de datos obtenidos mediante sensores remotos activos y pasivos se hace a partir de datos de partida procedentes de cuatro sensores y distintos métodos estadísticos de análisis (Tab. 3, Fig. 8). De forma específica, cada capítulo tiene los siguientes objetivos:

1. Estudiar el efecto de la productividad primaria neta de los ecosistemas, estimada utilizando el NDVI, y la humedad del suelo, estimada a partir de la combinación de datos SAR y multiespectrales, en las cosechas de setas silvestres. Considerar las diferencias de este efecto entre bosques mediterráneos secos y húmedos y entre grupos tróficos de setas y especies. (Capítulo 1).
2. Evaluar la capacidad de las variables procedentes de sensores multiespectrales y de TLS para predecir la producción de setas silvestres en bosques mediterráneos. Demostrar si la capacidad productiva forestal y el volumen de biomasa aérea total del bosque determinan la capacidad de producción de setas silvestres, especialmente de *Lactarius deliciosus*. (Capítulo 2).
3. Estudiar el potencial de los datos procedentes de los sensores SAR para caracterizar la producción de setas silvestres a nivel de parcela. Construir series temporales de datos, caracterizarlas y explorar la relación de éstas con las producciones semanales de setas silvestres saprofitas y micorrícicas. (Capítulo 3).

Tab. 3. Resumen general de las metodologías y datos utilizados en los capítulos de esta tesis.

Capítulo	Datos procedentes de sensores	Datos *in situ*	Análisis	Objetivo principal
Capítulo 1: Primary productivity and climate control mushroom yields in Mediterranean pine forests. (Olano et al., 2020)	• NDVI • Humedad del suelo (ESA CCI)	• Producción de setas • Meteo-climáticos	Análisis de correlación	Comprobar si los datos de teledetección permiten predecir el rendimiento de las cosechas de setas
Capítulo 2: Stand Structural Characteristics Derived from Combined TLS and Landsat Data Support Predictions of Mushroom Yields in Mediterranean Forest. (Martínez-Rodrigo et al., 2022)	• Volumen de biomasa • Porcentaje de cobertura • NDVI	• Producción de setas • Medición de árboles. • Meteo-climáticos	GAMMs	Evaluar la capacidad de las variables multiespectrales y TLS para la predicción de cosechas de setas
Capítulo 3: Towards prediction of forest wild mushrooms yields with time series of Sentinel-1 interferometric coherence data.	• Coeficiente de retrodispersión • Coherencia interferométrica • Volumen de biomasa	• Producción de setas • Medición de árboles. • Climáticos	Análisis de correlación. Correlación cruzada para las series temporales.	Explorar la capacidad de las series temporales de datos SAR en banda C procedentes de Sentinel-1 para caracterizar la producción de setas a nivel de parcela

Fig. 8. Diagrama conceptual seguido en esta tesis, que detalla los sensores utilizados y las variables obtenidas de ellos. Elaboración propia.

Capítulo 1: Primary productivity and climate control mushroom yields in Mediterranean pine forests

Olano, J.M., Martínez-Rodrigo, R., Altelarrea, J.M., Ágreda, T., Fernández-Toirán, M., García-Cervigón, A.I., Rodríguez-Puerta, F., Águeda, B., (2020). *Agricultural and Forest Meteorology*.

Capítulo 1: Primary productivity and climate control mushroom yields in Mediterranean pine forests

José Miguel Olano [a,*], Raquel Martínez-Rodrigo [a,b], José Miguel Altelarrea [c], Teresa Ágreda [d], Marina Fernández-Toirán [a], Ana I. García-Cervigón [e], Francisco Rodríguez-Puerta [a,b], Beatriz Águeda [a,b]

[a] EIFAB – iuFOR. Universidad de Valladolid, Campus Duques de Soria, E-42004 Soria, Spain
[b] föra forest technologies, Campus Duques de Soria, E-42004 Soria, Spain
[c] Fundación Cesefor, Calle C, E-42005 Soria, Spain
[d] Fundación Parque Científico de la Universidad de Valladolid, Campus Duques de Soria, E-42004 Soria, Spain e Department of Biology and Geology, Rey Juan Carlos University. C/ Tulipán s/n, E-28933 Móstoles (Madrid), Spain

ABSTRACT

Mushrooms play a provisioning ecosystem service as wild food. The abundance of this resource shows high annual and interannual variability, particularly in Mediterranean ecosystems. Climate conditions have been considered the main factor promoting mushroom production variability, but several evidences suggest that forest composition, age and growth play also a role.

Long-term mushroom production datasets are critical to understand the factors behind mushroom productivity. We used 22 and 24 year-long time series of mushroom production in *Pinus pinaster* and *Pinus sylvestris* forests in Central Spain to evaluate the effect of climate and forest productivity on mushroom yield. We combined climatic data (precipitation and temperature) and remote sensing data (soil moisture and the Normalized Difference Vegetation Index, NDVI, a surrogate of primary productivity) to model mushroom yields for each forest and for the main edible species of economic interest (*Boletus edulis* and *Lactarius deliciosus*).

We hypothesized that mushroom yield would be related to (i) forest primary productivity inferred from NDVI affects mushroom yields, that (ii) soil moisture inferred from remote sensors will equal the predictive power precipitation data, and that (iii) combining climatic and remote sensing will improve mushroom yield models. We found that (i) previous year NDVI correlated (r = 0.41–0.6) with mushroom yields; (ii) soil moisture from remote sensors rivaled the predictive power of precipitation (r = 0.63–0.72); and (iii) primary production and climate variances were independent, thus the combination of climatic and remote sensing data improved models with mean R^2_{adj} as high as 0.629.

On the light of these results, we propose as a working hypothesis that mushroom production might be modelled as a twostep process. Previous year primary productivity would favour resource accumulation at tree level, potentially increasing resources for mycelia growth, climatic conditions during the fruiting season control the ability of mycelia to transform available resources into fruiting bodies.

INTRODUCTION

Fungi play key functions in forest ecosystems. Fungi contribute to soil nutrient balance by decomposing organic matter and turning it into inorganic components that are accessible to tree roots. Mycorrhizal fungi also form symbiotic associations that increase trees rhizosphere, eventually improving water and nutrient availability, enhancing tree growth and survival and providing defense against pathogen (Allen, 1991). In addition, mushrooms play a provisioning ecosystem service as wild food that has been acknowledged for a long time across multiple cultures (Boa, 2004). The growing consideration of mushrooms as a delicatessen, with their consequent commercialization, is triggering a transformation on the alimentary sector (Zambonelli and Bonito, 2012). Mushroom supplies are mostly collected in the wild and, as a result, mushroom picking has become a popular leisure activity for urban people. In fact, the development of a mycological touristic sector is having high impact in low-populated, rural areas, contributing to diversify its economy and to expand the touristic season into the mushroom fruiting season (Ágreda et al., 2014; Boa, 2004).

Mycological tourism is compromised by the existence of high uncertainty in wild mushroom yields, which impedes a stable touristic offer (Zambonelli and Bonito, 2012). This phenomenon is particularly acute in environments where climatic conditions show extreme variability among consecutive years, such as Mediterranean ones, since mushroom yields reflect inter-annual climate variations, both in terms of total production and timing of the yield season (Ágreda et al., 2015; Collado et al., 2019). Although forest management can enhance wild mushroom production by promoting tree vigor (Tomao et al., 2017), it does not diminish inter-annual variability driven by weather conditions (Ágreda et al., 2016). As a result, climate change might affect wild mushroom yields, since more intense drought events and higher evapotranspiration may play deleterious effects. However, later mushroom seasons and, particularly, more abundant spring yields due to changes in climate might provide novel windows of opportunity (Büntgen et al., 2012; Sato et al., 2012).

Developing reliable predictive models for mushroom yields is therefore a must for the expansion of this economic sector (Tomao et al., 2017). Indeed, modeling factors that determine wild mushroom yields has become an expanding area of research that benefits from the ever-growing availability of long-term data sets of mushroom yields (Alday et al., 2017; Egli et al., 2006; Fernández-Toirán et al., 2006; Herrero et al., 2019; Martínez-Peña et al., 2012). Weather conditions have been the main environmental factor considered in modelling mushroom yields, temperature being key in temperate forests (Sato et al., 2012) and precipitation in drought-limited Mediterranean environments (Ágreda et al., 2015, 2016; Alday et al., 2017; Herrero et al., 2019). Minimum temperatures can also affect mushroom yields through their effect on fruiting season length (Ágreda et al., 2015). More refined models include forest structure and tree growth rates (Bonet et al., 2008; Herrero et al., 2019), with some attempts to link mushroom yields with series of tree secondary growth (Collado et al., 2019; Primicia et al., 2016). The predictive power of these models is, however, limited and highly dependent on data collected at a local scale.

Remote sensing data have disrupted forest management by being able to monitor forest dynamics at multiple spatio-temporal scales (Barrett et al., 2016), and

LiDAR techniques have been proven successful to evaluate mushrooms diversity and production (Moeslund et al., 2019; Peura et al., 2016). Soil moisture content, a critical factor for fungal growth and mushroom production (Karavani et al., 2018), can be inferred from RADAR sensors (Dorigo et al., 2017; Moran et al., 2000; Paloscia et al., 2013) with time series that are available since 1978 (Dorigo et al., 2017). In the same way, remote sensors give information about the Normalized Difference Vegetation Index (NDVI), which is a good estimator of primary productivity (Birky, 2001; Rouse et al., 1973; Wang et al., 2004b) whose interannual variations have been correlated to tree secondary growth at different spatial and temporal scales (Vicente-Serrano et al., 2016). Although preliminary attempts to correlate fungal fruiting phenology and fungal diversity to annual NDVI have been recently undertaken (Andrew et al., 2018, 2019), the relation between NDVI and fungal production has not yet been explored to the best of our knowledge, in spite of the existing well-known positive relationship between forest primary productivity and fungal yields (Ágreda et al., 2014; Alday et al., 2017; Collado et al., 2019; Herrero et al., 2019). Remote sensing data are not independent from climate, since soil moisture responds to precipitation, evapotranspiration and soil characteristics (Entekhabi et al., 1996) and climate is one of the main drivers of primary productivity in terrestrial ecosystems. Therefore, incorporating remote sensors to mushroom yields' models is a first step towards the future development of detailed predictive models, which will help to boost the mycological touristic sector at different parts of the world. At the same time, this is also an opportunity to explore more in depth the ecological role of environmental drivers on mushroom production, as well as their potential consequences on ecosystem function.

In this study, we benefited from two of the longest time series of fungal production (22 and 24 years), both collected in central Spain. We used climatic (precipitation and temperature) and remote sensing (soil moisture and NDVI) data to model total mushroom yields in wet and dry pine forests, as well as to model the production of the main species of economic interest at each forest type –*Boletus edulis* Bull. (King bolete) in wet forests and *Lactarius deliciosus* (L.) Gray (saffron milk cap) in dry forests–. Our main aim was to check whether and which of remote sensing data will allow to predict mushroom yields. Specifically, we hypothesized that (i) forest primary productivity (estimated by NDVI) will have a positive effect on mushroom yields, albeit this effect will vary depending on the trophic guild (saprophytic vs. mycorrhizal), (ii) soil moisture inferred from RADAR sensors will equal the predictive power of traditionally-used precipitation data, and (iii) the combination of climatic and remote sensing data will increase the predictive power of models for mushroom yields.

MATERIAL AND METHODS

Sampling design and mushroom data

Mushroom data used in this research were collected in central Spain, in the province of Soria (Castilla y León region). Elevation ranges from 1000 m to 1200 m a.s.l. and climate is Mediterranean continental, with cold winters and a summer drought period from July to August. In this area, two pine forests dominated by *Pinus pinaster* Ait. and *Pinus sylvestris* L. were selected (Fig. 9). *Pinus pinaster* forest (dry forest, hereafter) grows over sandy soils with high permeability and low nutrient content. *Pinus sylvestris* forest (wet forest, hereafter) grows in more humid environments, over acidic soils as well but with higher nutrient content. Eighteen permanent plots were established in each forest, in 1995 for the wet forest and in 1997 for the dry forest. Plots had 150 m^2 surface and were fenced to prevent harvesting and trampling. Sporocarps (fungi fruiting bodies) were sampled on a weekly basis during the main fruiting period (September to December) until 2018. All sporocarps within the plots were collected, fresh-weighed, identified to the species level and classified according to fungal guild (see Ágreda et al., 2015 for details). Dry forest plots were selected using a stratified design to represent all forest structures, whereas wet forest plots were located in bottom areas, thus increasing the difference in water availability among forest types.

For each forest, we obtained time series of annual mushroom yield. We also obtained annual time series of each of the main trophic guilds (saprophytic and mycorrhizal) as well as production of the main commercial species per site, i.e., saffron milk cap (*Lactarius deliciosus*) for the dry forest and king bolete (*Boletus edulis*) for the wet forest.

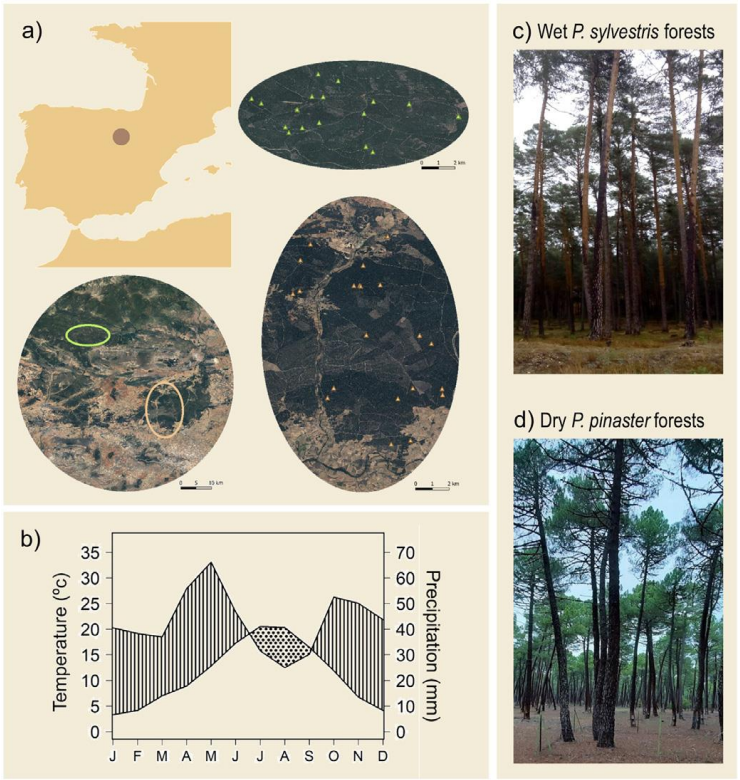

Fig. 9. Geographical location of study area and sampling plot design (a), climatogram of Soria city (b) and images of dry (Pinus pinaster) and wet (Pinus sylvestris) forests (c-d).

Climate and remote sensing data

Records of monthly temperature and total monthly precipitation were obtained from the Soria meteorological station (41°46'30'' N, 02°28' 59'' W; 1082 m a.s.l., ≈35 km away from sampling sites, AEMET, Spanish Government) for the 1995–2018 period. Annual mean temperature was 11.1 °C, the coldest month being January (with mean daily minimum temperature of -1.2 °C) and the warmest month being July (with mean daily maximum temperature of 28.6 °C). Average annual rainfall was 517 mm, with a summer drought period typically occurring from mid-July to August (Fig. S1).

Soil moisture data were obtained from the ESA CCI combined Soil Moisture dataset with a spatial resolution of 0.25 × 0.25° (Dorigo et al., 2017; Gruber et al., 2017, 2019). These data are produced by merging both passive and active soil moisture datasets (Liu et al., 2012) and were available from 11/1978 to 12/2018 on a global scale. These include ASCAT scatterometer-based soil moisture data (ERS 1/2 and MetOp A/B satellites) and radiometer-based soil moisture data (SMMR, SSM/I, TMI, AMSR-E, WindSat, AMSR2, and SMOS). The merging between active and passive soil moisture products is done based on a weighted average method with the weights being proportional to Signal to Noise Ratio, estimated using triple collocation analysis of each product (Dorigo et al., 2013; Gruber et al., 2017). All these different datasets are scaled to a common model of soil moisture climatology, provided by the Global Land Data Assimilation System (GLDAS) Noah Land Surface Model (Rodell et al., 2004). More details about the theoretical and algorithmic base of this product and detailed analysis about the uncertainties of the soil moisture datasets can be found in Dorigo et al. (2017), Gruber et al. (2019, 2017) and Liu et al. (2012). Information about the daily CCI volumetric (m^3/m^3) soil moisture product can be retrieved at http://www.esa-soilmoisturecci.org. For our study, monthly values of soil moisture were calculated as the average of available daily values.

We used the difference between summer NDVI and winter NDVI as an estimate of yearly primary productivity, since we considered this was the period that better explains tree performance in Mediterranean continental climates (Arzac et al., 2018b). NDVI data were extracted from LS-5, LS-7, and LS-8 NASA missions. NDVI values for all the 30-m side pixels that included each of the plots were obtained for every winter and summer season from the study period. We chose February 14th for winter and August 15th for summer. Since images for selected data were sometimes not available due to clouds interference, we searched for the closest date with a clear image available. We averaged NDVI values over the 18 plots per forest type, year and season.

Statistical analyses

Model parameters selection

As a first step, we selected climatic and remote sensing variables to be included in the definition of predictive models. To do this, we obtained Pearson's correlations between mushroom yields and monthly climate parameters (precipitation and minimum temperature) from June to December, according to the mushroom fruiting season. For each climatic parameter, we selected the month and the accumulated period with the highest correlation to be included in predictive models. This resulted in four climate parameters (two for precipitation, two for minimum temperature) per mushroom series

(i.e., mushroom yields in wet forests, in dry forests, and production of the two main commercial species).

We followed the same procedure for selecting parameters about soil moisture data. Then, we obtained Pearson's correlations between mushroom series and NDVI data for the fruiting year. Since previous years' primary productivity may have a delayed positive effect on mushroom yields through the accumulation of photo-assimilates and/or organic matter that can be later used by fungi, we also correlated mushroom series with NDVI data from the previous year and from two years before (i.e., one and two-years lag). From these three temporal lags, we selected the one with the highest correlation to be included in predictive models. Since NDVI and primary productivity have a nonlinear relationship, we also included a quadratic term of NDVI in the models (Wang et al. 2004b).

Model definition

We used the selected parameters to fit three different sets of linear models for each mushroom time series: (i) *Climate models*, using the four climate parameters previously selected, (ii) *Remote sensing models*, using two parameters for soil moisture and the best NDVI lag and its quadratic term, and (iii) *Combined models*, using climate and remote sensing parameters. Residuals of full models were analysed for normality using Shapiro-Wilk Normality test, if residuals for any of the three models of a times series were not normal, time series was square root-transformed for all three models to make results comparable. Residuals normality was achieved in all cases after transformation. For each set of models, we compared all additive combinations of explanatory variables using *dredge()* function from *MuMin* package (Barton, 2009) in R environment (R Core Team, 2019) and selected the most informative model following the Bayesian information criterion (BIC), which yields more conservative models than the Akaike information criterion (Aho et al., 2014). Variance Inflation Factors (VIF) were checked for the most informative models to search for multicollinearity. Since remote sensing data were not available for some periods, model comparison for remote sensing and combined models was based on a reduced dataset including solely years with complete datasets. Selected models were readjusted using all years available, thus penalizing estimated models.

Trophic guilds response to NDVI

Since fungi belonging to different trophic guilds show different feeding strategies, we assessed whether the main fungal trophic guilds showed distinct responses to primary productivity. In order to do this, we correlated mycorrhizal and saprophytic yields in both forest types with NDVI values at the fruiting year and with one and two-years lag.

RESULTS

Mushroom yields data

We collected 1325 kg of mushrooms: 519.1 kg in dry forests (from which 71.4 kg were saffron milk cap, 13.8%) and 806.3 kg in wet forests (from which 182.5 kg were king bolete, 23.3%). Mycorrhizal fungi dominated both communities, with saprophytic comprising around 10% of the total fresh weight. Production per ha ranged from 87.3 kg in dry forests to 124.4 kg in wet forests, but with high interannual variability: coefficient of variation was 93.8% for wet and 81.7% for dry forests, being even larger for individual species (141.7% for milk saffron cap; 92.8% for king bolete). The relative contribution of these two species to the total yields also showed extreme variability, ranging from 0% to 23% for milk saffron cap and to 57% for king bolete.

Selected predictors

Climate parameters

The best climate predictors (Fig. 10) for mushroom yields in dry forests (n = 22) were November (r = 0.53, P = 0.011) and summer-autumn (June to November) accumulated precipitation (r = 0.59, P = 0.004), as well as November (r = 0.46, P = 0.032) and autumn (September to November) (r = 0.55, P = 0.009) average minimum temperature. Climate predictors in wet forests (n = 24) peaked a bit earlier, in September (r = 0.64, P < 0.001) and summer-autumn (June to November; r = 0.69, P < 0.001) for precipitation, and in September (r = 0.54, P = 0.007) and early autumn (September to October; r = 0.57, P = 0.003) for average minimum temperature. Saffron milk cap showed marginally significant responses to November (r = 0.38, P = 0.082) and September to November precipitation (r = 0.37, P = 0.088), whereas its response to minimum temperature was marginal in September (r = 0.39, P = 0.069) and significant in September-October (r = 0.46, P = 0.033). The best predictors for king bolete production occurred in the same months as in wet forests, i.e., September (r = 0.41, P = 0.034) and June to November precipitation (r = 0.42, P = 0.040), and September (r = 0.41, P = 0.049) and September to October minimum temperatures (r = 0.38, P = 0.067).

Soil moisture data

Soil moisture in summer-autumn was highly correlated with mushroom yields, both in dry (July to December; r = 0.63, P = 0.002, n = 18) and wet (July to November; r = 0.66, P = 0.001, n = 20) forests (Fig. 10). The best monthly correlation occurred later in dry forests (October; r = 0.45, P = 0.063, n = 18) than in wet forests (September; r = 0.63, P = 0.001, n = 23). Saffron milk cap shared its accumulated signal period (July-December) with dry forests (r = 0.49, P = 0.037, n = 18), but the highest single-month signal occurred in December (r = 0.48, P = 0.082, n = 18), instead of October. King bolete shared the soil moisture signal with wet forests, peaking from July to November (r = 0.72, P < 0.001, n = 20) and in September (r = 0.48, P = 0.019, n = 20).

NDVI effect on yields

Both forest types and single species responded positively to NDVI in the previous year (Fig. 11a), although this response was marginal in wet forests (r = 0.40, P = 0.053, n = 24). Mushroom yields were neither significantly related to NDVI in the fruiting year, nor two years before, suggesting that fungal production depends on primary productivity in the previous year, instead of in the fruiting year.

Mycorrhizal mushroom production increased with higher NDVI increment in the previous year in both forest types (r = 0.601, P = 0.003, n = 22 for dry forests; r = 0.410, P = 0.047, n = 24 for wet forests), but did not respond to NDVI increment in the current year, or two years before (Fig. 11b). Saprophytic mushrooms showed disparate results depending on the forest type. In dry forests, the saprophytic guild showed strong correlation with primary productivity at one- and two-year lags (r = 0.60, P = 0.004, n = 22 for one-year lag; r = 0.55, P = 0.008, n = 22 for two-year lag) and, in fact, a linear model including NDVI increments with one and two-year lags explained a large fraction of the variance (R^2_{adj} = 0.536, P < 0.001, n = 22). In contrast, we observed no relationship with NDVI increments at any lag for saprophytic mushrooms in wet forests (Fig. 11b).

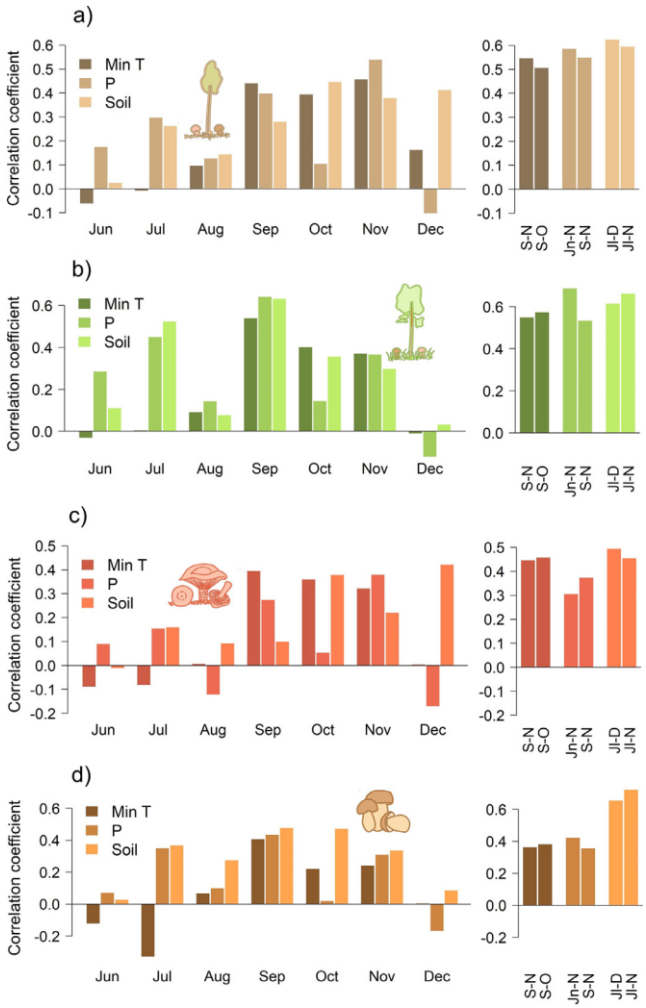

Fig. 10. Correlation between yearly mushroom biomass and minimum temperature (Min T), precipitation (P) and soil moisture (Soil) at monthly (left) and aggregated (right) periods for dry (a) and wet (b) pine forests, as well as for milk saffron cap *Lactarius deliciosus* (c) and king bolete *Boletus edulis* (d).

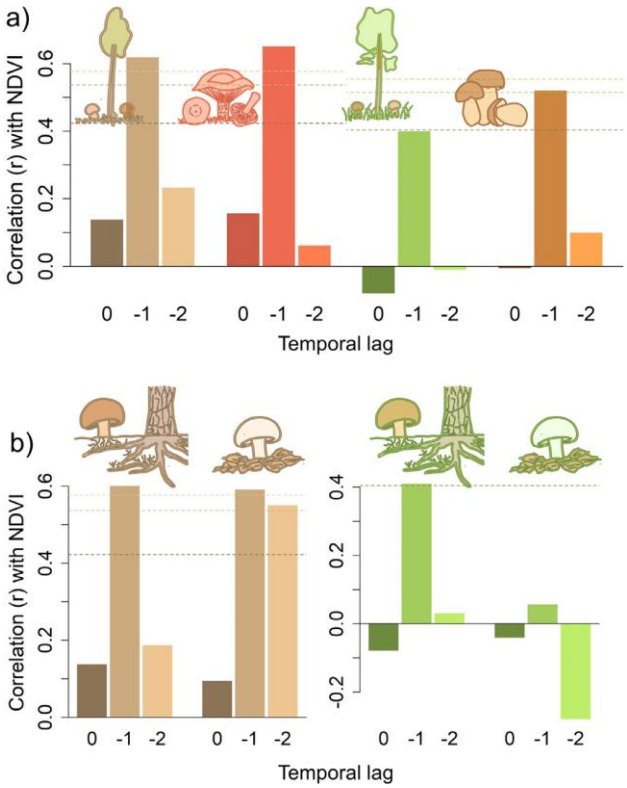

Fig. 11. Correlation between mushroom yields and NDVI (Normalized Difference Vegetation Index) in the fruiting year (lag = 0) and one and two years before (lag = –1 and –2, respectively). a) Correlation coefficients for each forest type and for the two main commercial species. From left to right: dry forests, saffron milk cap, wet forests and king bolete. b) Correlation coefficients for mycorrhizal and saprophytic guilds in dry forests (left plot) and in wet forests (right plot). Lighter bar colors are used for increasing temporal lags. NDVI increment was obtained as the difference of summer minus winter NDVI. Dashed lines with decreasing width indicate P values of 0.05 (the thickest), 0.01 and 0.001 (the thinnest).

Models

Climate models

Models for dry forests and single species were root transformed. Accumulated precipitation from June to November (Fig. 12, Tab. 4) was the only parameter included in the most informative model for explaining mushroom yields in dry forests (R^2_{adj} = 0.399, P = 0.001, n = 22). In wet forests, maximum yields occurred when wet June-to November periods were combined with humid Septembers (R^2_{adj} = 0.563, P < 0.001, n = 24; Tab. 4). The most informative model for saffron milk cap yields only included accumulated September-October precipitation (R^2_{adj} = 0.122, P = 0.063, n = 22), whereas king bolete yields were higher in years with humid Septembers (R^2_{adj} = 0.220, P = 0.012, n = 24).

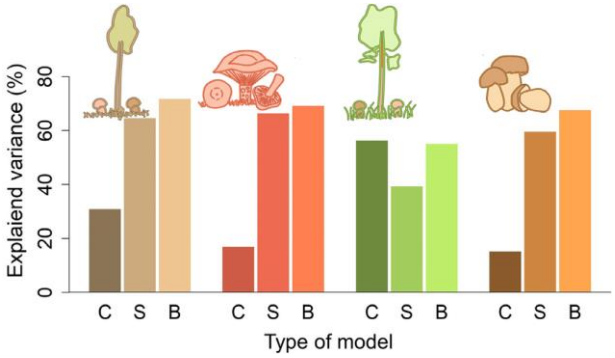

Fig. 12. Percentage of adjusted variance explained by climate (C), remote sensing (S) and combined (B) models. Selection of the most informative model was based on BIC. From left to right, results for mushroom yields in dry forests, milk saffron cap production, mushroom yields in wet forests and king bolete production.

Remote sensing models

Average soil moisture from June to December and previous year and NDVI variation (Fig. 12, Table S1) explained a large part of mushroom yields in dry forests (R^2_{adj} = 0.547, P = 0.001, n = 18). In wet forests, previous year NDVI and soil moisture in September built the most informative model (R^2_{adj} = 0.393, P = 0.003, n = 22). Saffron milk cap yields responded to previous year July to December mean soil moisture and NDVI (R^2_{adj} j = 0.551, P = 0.001, n = 18), whereas king bolete yields were maximal when high soil moisture from July to November occurred after a year with high NDVI (R^2_{adj} = 0.750, P < 0.001, n = 20).

Combined models

Mushroom yields in dry forests (Fig. 12, Tab. 4) increased when rainy conditions from June to November occurred after a previous year with high NDVI variation (R^2_{adj} = 0.682, P < 0.001, n = 22). Conditions for high mushroom yields were very similar in wet forests, with a positive effect of NDVI, June to November precipitation and high minimum September-October temperatures (R^2_{adj} = 0.550, P < 0.001, n = 24). The effect of NDVI increment in the previous year was significant for saffron milk cap and king bolete. The most informative model for saffron milk cap included accumulated precipitation from September to October and NDVI (R^2_{adj} = 0.484, P < 0.001, n = 22), whereas the model for king bolete included NDVI as well as the effects of high soil moisture from July to September (R^2_{adj} = 0.750, P < 0.001, n = 20). VIF < 2 in all cases, indicating no multicollinearity.

Tab. 4. Parameters (Par) included in the most informative models explaining mushroom yields in (a) dry forests and (b) wet forests, as well as for the species (c) Lactarius deliciosus and (d) Boletus edulis. Climatic parameters include precipitation (P) and minimum temperature (Tmin). Remote sensing parameters include soil moisture (soil) and the Normalized Difference Vegetation Index (NDVI), obtained as the difference of summer minus winter NDVI in the previous year (prev). Colored cells indicate that the corresponding predictor variable (in rows) was included for that month (in columns) or period (several consecutive months) in the most informative model. Dark blue in September in wet forests indicates the additive effect of September precipitation and the accumulated precipitation from June to November. All factors had positive effects on mushroom yield.

a) Dry forests

Model	Par	prev	J	J	A	S	O	N	D
Climate	P								
	T_{min}								
Remote sensing	soil								
	NDVI								
Combined	P								
	T_{min}								
	soil								
	NDVI								

b) Wet forests

Model	Par	prev	J	J	A	S	O	N	D
Climate	P								
	T_{min}								
Remote sensing	soil								
	NDVI								
Combined	P								
	T_{min}								
	soil								
	NDVI								

c) *Lactarius deliciosus*

Model	Par	prev	J	J	A	S	O	N	D
Climate	P								
	T_{min}								
Remote sensing	soil								
	NDVI								
Combined	P								
	T_{min}								
	soil								
	NDVI								

d) *Boletus edulis*

Model	Par	prev	J	J	A	S	O	N	D
Climate	P								
	T_{min}								
Remote sensing	soil								
	NDVI								
Combined	P								
	T_{min}								
	soil								
	NDVI								

Combined models provide better adjustment

Combined models included more parameters and explained a higher proportion of variance than climate and remote sensing models on their own (Fig. 12, Tab. 4). Globally, combined models provided the best fit to the data (mean R^2_{adj} = 0.629), followed by remote sensing models (mean R^2_{adj} = 0.561). Climate models provided the worst fit (mean R^2_{adj} = 0.326) with the only exception of wet forests, for which climate models had the best fit (Fig. 12). Note that in remote sensing and combined models, the most informative model was selected excluding years with missing data on soil moisture and then R^2_{adj} was recalculated using all available data for the selected parameters, which yielded lower R^2_{adj} values.

DISCUSSION

According to our first hypothesis, previous year primary productivity (inferred from NDVI) had a positive correlation with fungal yield. When exploring this signal at guild level, we found differences across forests: the signal was similar for mycorrhizal fungi in dry and wet forests but differed for the saprotrophic guild. The effect was strong at one and two-year lags in dry forests but disappeared in more productive wet forests. Data also supported our second hypothesis, since soil moisture inferred from RADAR sensors rivaled the predictive power of precipitation data. Finally, models including remote sensing and climate data improved models based solely on climate data, thus confirming our third hypothesis.

Soil moisture data based on remote sensors provided similar results than precipitation in predicting mushroom yields. Soil moisture values can be partially attributed to rain, but other parameters like temperature, insolation as well as other soil variables have also strong influence on daily and seasonal variations in soil moisture (Robock, 2014). In fact, long-term predictions for mushroom yields differ when evapotranspiration, instead of precipitation, is included in the models (Collado et al., 2019). Considering soil moisture values instead of climate parameters in predictive models therefore circumvents this limitation. Moreover, soil moisture along the fruiting season was linked with mushroom yields in a more stable way than precipitation, which suggests that the biological process was reflected in a more realistic fashion.

Considering the predictive power of NDVI as a surrogate of forest primary productivity also showed promising results. Growth of forest fungal mycelia is supported by trees either directly –through photoassimilates transference (mycorrhizal fungi)– or indirectly –through the effect of higher biomass production on substrate availability for decomposers (saprophytic fungi)–. Different attempts have tried to link temporal series of tree growth with fungal production (Collado et al., 2019; Primicia et al., 2016) due to the existing relationship between tree growth and photo-assimilate levels (von Arx et al., 2017). Tree growth has shown promising results in Mediterranean pine forests, but this relationship might respond to common climatic control on tree growth and fungal production (Ágreda et al., 2015; Arzac et al., 2018a). In this sense, remote sensing NDVI data have the potential to link primary productivity with fungal growth, since NDVI is a more robust estimate of primary productivity than ring width (Schloss et al., 1999). But in addition, the consistent correlation we found between previous year NDVI and mushroom yields in all models that combined remote sensing with climatic data suggested a clear time domain separation between primary productivity and mushroom production, thus reducing potentially confounding effects due to a common climate forcing (Collado et al., 2019).

Our study suggests that trees' resource accumulation in a given year might promote fungal production in the next fruiting season. Since different fungal guilds use different resources, contrasting responses were expected between saprophytic and mycorrhizal fungi and, in fact, we found some support for this expectation. Mycorrhizal fungi were correlated to primary production in the previous year. Since mycorrhizal fungal biomass depends on carbon transfer by the host (Allen, 1991), this correlation with NDVI in the previous year might be attributed to a direct benefit from higher tree resource availability. The effect on saprophytic fungi, on the contrary, was indirect and

depended on site productivity. Saprophytic fungi in less productive dry forests showed strong positive responses to primary productivity with one and two-year lags. In this managed forest with low availability of dead wood, litterfall provides the main substrata for saprophytic fungi. Higher primary productivity has been shown to have a direct effect on litterfall (Schlesinger 1997; Wang et al., 2004c), albeit with some lag for perennial species. Thus, in our pine forest, it could be expected a one to two years lagged effect of primary productivity on litterfall, posing a plausible explanation for the lagged correlation between NDVI and saprophytic fungal development. In contrast, the saprophytic fraction from more productive wet forests did not respond to primary productivity at any temporal scale, probably due to the existence of higher biomass accumulation, but also to the topography of sampling plots, which were located in bottom areas, being subsidized with organic matter from surrounding areas. With plenty of organic matter, mushroom production control would only depend on weather conditions at annual scale.

Based on these results, we propose as working hypothesis that mushroom production may respond to a two-step process: resource accumulation during the previous year would determine the energy available to support mycelial growth, acting as a predisposing factor, whereas weather conditions during the fruiting season would regulate the ability of mycelia to transform this energy into fruiting bodies, acting as a triggering factor (Fig. 13). This hypothesis might help to understand how environment control mushroom production, but we are aware that our current results only suggest limited evidence to support it. Therefore, future studies should test and validate (or falsify) this hypothesis with experimental work along forests with different productivity and fungal communities.

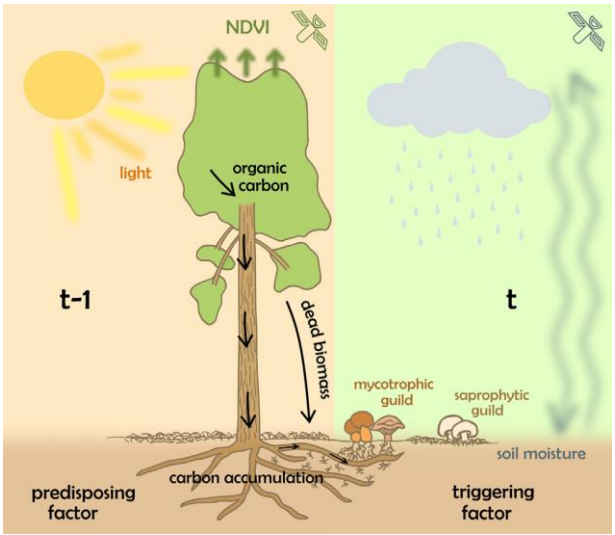

Fig. 13. Schematic view of the working hypothesis proposed to study environmental factors that control mushroom production. Primary productivity (NDVI) in a given year (t-1) controls carbon gain, leading to carbon accumulation in roots. Higher carbon accumulation would favor the development of mycorrhizal fungi, enhancing mushroom yields of mycorrhizal species in the following year (t) and thus acting as a predisposing factor. In the case of saprophytic fungi, the accumulation of dead biomass under tree canopies would also promote mushroom production in the following year or even two years later. In any case, final mushroom production would depend on the existence of favorable weather conditions (humidity, temperature…) during the fruiting season (triggering factor).

CONCLUSIONS

The combination of remote sensing sources with climatic data improved our ability to model mushroom production in two Mediterranean pine forests with contrasting humidity levels. Our soil moisture dataset was based on coarse-grained data, but novel remote sensing products for soil moisture already allow the estimation of soil humidity at higher spatial (decametres) and temporal (days) resolution (ESA – Copernicus, 2014). Moreover, fine-grained daily temperature values are also available with remote sensing methods in a daily fashion (Wang et al., 2004b), and remote sensing data on primary productivity are at a very mature stage, multiple satellite-based data being freely available. Altogether, our results open a path to use remote sensing data at high spatio-temporal resolution to face the challenge of predicting intra-seasonal mushroom yields over space and time.

FUNDING

This work was supported by Junta de Castilla y León [project VA026P17]; and the Spanish Ministry of Science, Innovation and Universities [grant numbers DI-17-09626, PTQ-16-08411 and IJCI- 2017-34052 to RMR, BÁ, and AIGC, respectively].

DECLARATION OF COMPETING INTEREST

The authors declare that they have no known competing financial interests or personal relationships that could have appeared to influence the work reported in this paper.

ACKNOWLEDGMENTS

We thank Consejería de Medio Ambiente from Castilla y León Regional Government for funding the permanent plots and granting access to mushroom yields time series, and to Centro Forestal de Valonsadero, Cesefor Fundation and all people involved in plot monitoring.

SUPPLEMENTARY MATERIALS

Supplementary material associated with this article can be found, in the online version, at doi:10.1016/j.agrformet.2020.108015

Capítulo 2: Stand Structural Characteristics Derived from Combined TLS and Landsat Data Support Predictions of Mushroom Yields in Mediterranean Forest

Martínez-Rodrigo, R., Gómez, C., Toraño-Caicoya, A., Bohnhorst, L., Uhl, E., Águeda, B., (2022).
Remote Sensing 14, 5025.

Capítulo 2: Stand Structural Characteristics Derived from Combined TLS and Landsat Data Support Predictions of Mushroom Yields in Mediterranean Forest

Raquel Martínez-Rodrigo [1,2,*], Cristina Gómez [2,3], Astor Toraño-Caicoya [4], Luke Bohnhorst [4], Enno Uhl [4,5] and Beatriz Águeda [1,2]

[1] föra Forest Technologies, Campus Duques de Soria, E-42004 Soria, Spain
[2] iuFOR-EiFAB, Campus Duques de Soria, Universidad de Valladolid, E-42004 Soria, Spain
[3] Department of Geography and Environment, School of Geoscience, University of Aberdeen, Aberdeen AB24 3UE, UK
[4] Chair of Forest Growth and Yield Science, TUM School of Live Sciences Weihenstephan, Technical University of Munich, Hans-Carl-von-Carlowitz-Platz 2, 85354 Freising, Germany
[5] Bavarian State Institute of Forestry, Hans-Carl-von-Carlowitz-Platz 1, 85354 Freising, Germany

ABSTRACT

Forest fungi provide recreational and economic services, as well as ecosystem biodiversity. Wild mushroom yields are difficult to estimate; climatic conditions are known to trigger temporally localised yields, and forest structure also affects productivity. In this work, we analyse the capacity of remotely sensed variables to estimate wild mushroom biomass production in Mediterranean *Pinus pinaster* forests in Soria (Spain) using generalised additive mixed models (GAMMs). In addition to climate variables, multitemporal NDVI derived from Landsat data, as well as structural variables measured with mobile Terrestrial Laser Scanner (TLS), are considered. Models are built for all mushroom species as a single pool and for *Lactarius deliciosus* individually. Our results show that, in addition to autumn precipitation, the interaction of multitemporal NDVI and vegetation biomass are most explanatory of mushroom productivity in the models. When analysing the productivity models of *Lactarius deliciosus*, in addition to the interaction between canopy cover and autumn minimum temperature, basal area (BA) becomes relevant, indicating an optimal BA range for the development of this species. These findings contribute to the improvement of knowledge about wild mushroom productivity, helping to meet Goal 15 of the 2030 UN Agenda.

INTRODUCTION

Remote sensing is an exceptional technology for applications in forest ecosystems (Lechner et al., 2020), particularly for assessment of resources (White et al., 2016). Remote sensing provides data with overall perspective (Li and Roy, 2017) as well as powerful tools for monitoring forest dynamics (Hansen et al., 2013) and the drivers of change (Kennedy et al., 2014). Applications have become more detailed and specific with the improvement of data quality, storage capacity, and analysis techniques (Wulder et al., 2018), and as a result of the information needs imposed by society, going from simple characterization to complex measure and modelling (Gómez et al., 2019).

In the last decade, mushroom-related attributes such as presence, occurrence, and productivity have been modelled with a range of approaches, highlighting a growing interest in the prediction of these non-wood forest products (Herrero et al., 2019; Sánchez-González et al., 2019; Küçüker and Başkent, 2014), as they provide a wide range of ecosystem services. Moreover, fungi contribute to maintaining and augmenting the biodiversity of other taxa (Cockle et al., 2012; Müller and Bütler, 2010) and are considered for provisioning of economic and sociocultural services, as they are among the most appreciated edible non-wood forest products, particularly in Mediterranean areas (Croitoru, 2007), and they generate recreation and economic returns (Boa, 2004). Therefore, predicting fungal yields may help the sustainable management of forest ecosystems and contribute to the achievement of the Sustainable Development Goal 15 of the 2030 UN Agenda for Sustainable Development (United Nations, 2022a).

The interaction among factors triggering mushroom production is complex and nonlinear (Alday et al., 2017). Climatic and environmental parameters are paramount drivers of the naturally irregular productivity of mushrooms (Ágreda et al., 2015). Climate parameters, particularly accumulated precipitation, have a strong influence on the fruiting time and total productivity (Olano et al., 2020). Furthermore, the inter- and intra-annual irregularity of mushroom production related to precipitation events is being augmented by the climate change effects which, in Mediterranean environments, cause the fruiting of mushrooms to be increasingly scarce (Morera et al., 2022; Olano et al., 2020; Ágreda et al., 2015). In addition to climate, site-specific characteristics such as soil (Rühling and Tyler, 1990; Straatsma et al., 2001) and topography drive mushroom specificity (Hagenbo et al., 2022). Habitat spatial and temporal fragmentation also play a role in maintaining diversity in communities of ectomycorrhizal fungi (Koide et al., 2011).

An additional important factor in mushroom development is the forest structure (Tomao et al., 2017). Here, stand density was found as a key driver by Bonet et al. (2008, 2010) when modelling total mushroom production in pines of northern Spain, and Ágreda et al. (2013) pointed out stand age as a particularly relevant factor in Mediterranean forests. At the landscape scale, the structure and composition of forest stands have been found to be important for the distribution of mushroom yields (Küçüker and Başkent, 2014; de-Miguel et al., 2014). Therefore, forest management practices such as thinning, clearcutting, or planting, as well as natural disturbances, influence mushroom yields distribution and quantity (Tomao et al., 2017; Küçüker and Başkent, 2017; Bonet et al., 2012).

Overall, the climatic and structural parameters driving mushroom productivity can currently be measured or estimated at medium to large scale with high precision and spatial detail employing remote sensing technologies. Remotely sensed data have capacity for estimation of forest structural parameters and for assessment of forest vigour and condition at different spatial scales. Light Detection and Range (LiDAR) is the preferred technology for characterization of structure due to the high precision its data provide, the lower cost, and wide coverage relative to field data (Lefsky et al., 2002). LiDAR is being increasingly employed in all its variants (aerial, terrestrial, and mobile) for multiple applications (Beland et al., 2019). In particular, Terrestrial Laser Scanning (TLS) provides enormous detail about interior canopy features and is a natural choice for studies of stem allometry and biomass, simulation of light environments, testing of photosynthesis, and production models (Åkerblom and Kaitaniemi, 2021). Optical sensors acquiring frequent data from satellite platforms, like those from the Landsat Programme, provide comparative reflectance values through the year that respond to the vigour and phenology state of forest stands. Individually, and better still in combination, remote sensing active and passive technologies may facilitate, through the approximation of forest structural parameters and the estimation of primary productivity, the assessment of mushroom yields.

Despite the advantages of using remote sensing, there have been yet few attempts to employ this kind of data to explain fungal dynamics. Recently, some efforts have incorporated remotely sensed measures in the modelling of mushroom traits. For example, Thers et al. (2017) found airborne LiDAR-based structural variables more explicative than botanical and environmental variables when modelling fungi species richness and composition in Denmark. Peura et al. (2016) demonstrated that LiDAR structural variables are more explanatory than field-measured variables when modelling the occurrence of forest fungi in temperate forests of Germany. Similarly, Olano et al. (2020) demonstrated that mushroom yields are linked to forest primary productivity and to soil moisture-inferred from Landsat NDVI values and the ESA CCI combined Soil Moisture dataset respectively-in Mediterranean ecosystems.

All this information leads to hypothesise that the combined use of different types of remote sensing data has a strong potential for estimating mushroom yields. The specific objectives of this work are: (i) to evaluate the capacity of multitemporal optical variables (primary productivity, vigour, and condition) and TLS-derived variables (structure) to predict mushroom production in Mediterranean forests; (ii) to demonstrate whether the forest productive capacity, and the volume of total aboveground biomass in particular, determine mushroom production, and (iii) to assess whether the variables that determine total mushroom production in Mediterranean ecosystems are the same as for a specific mushroom species.

MATERIALS AND METHODS

Study Area and Experimental Design

Mushroom data were collected from forests dominated by *Pinus pinaster* Ait. in the province of Soria (autonomous region of Castilla y León), in Central Spain (Fig. 14). The area (~17.000 ha) is relatively flat, with an elevation ranging from 1000 m to 1200 m a.s.l. Climate is Mediterranean continental, with cold winters and a summer drought period from July to August. Total annual precipitation is, on average, 511 mm, and rain events occur mainly in spring and autumn. *Pinus pinaster* forests grow over sandy soils with high permeability and low nutrient content.

Pinus pinaster is a widely distributed species in the Mediterranean basin, employed in protective and productive reforestations due to its frugality and productivity of wood, resin, and fungi (Oria-de-Rueda et al., 2010). Several edible mushroom species such as *Hygrophorus latitabundus* Britz, *Lactarius deliciosus* (L.) S.F. Gray, *Macrolepiota excoriata* (Schaeff.) M.M. Moser, *Macrolepiota konradii* (Huijsm.), *Macrolepiota mastoidea* (Fr.) Singer, *Macrolepiota procera* (Scop.) Sing, *Suillus luteus* (L.) Roussel, *Tricholoma portentosum* (Fr.) Quél, and *Tricholoma terreum* (Sch.) Kumm can be found in these forests (Vásquez et al., 2015).

Seventeen permanent plots of 150 m^2 (5 × 30 m) have been established in this forest since 1997, with an external fence to prevent harvesting and trampling. Plots were located applying a stratified design to represent all forest structures. Sporocarps, the fungi fruiting bodies, were sampled on a weekly basis during the main fruiting period, which is September to December. All sporocarps within the plots were collected, fresh-weighted, and identified to the species level (see Ágreda et al., 2015 for details).

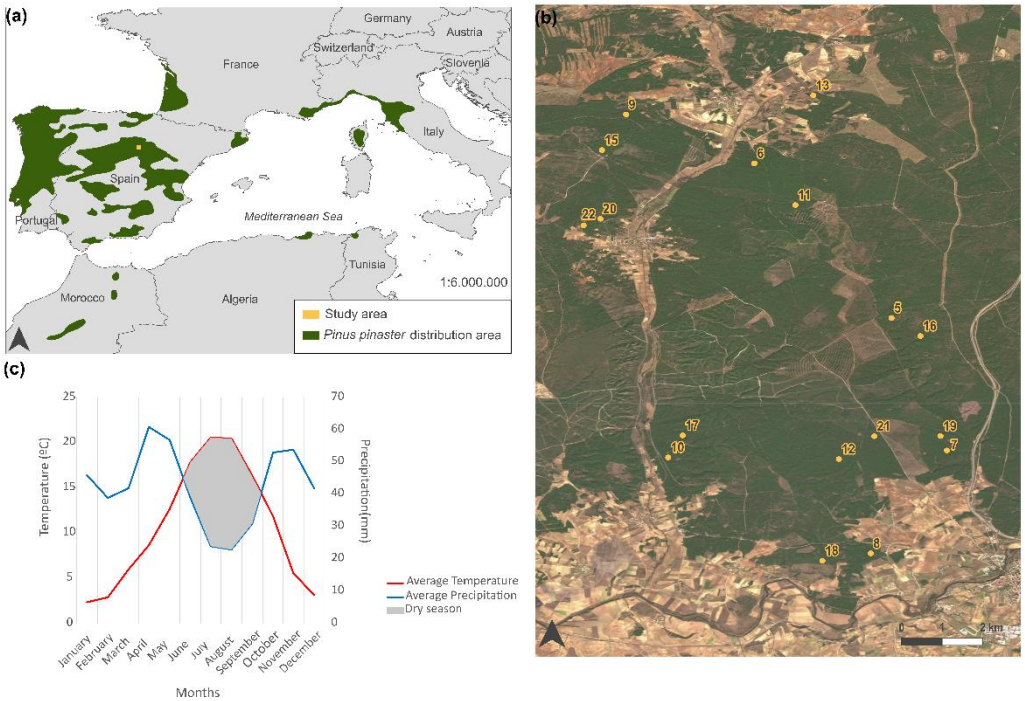

Fig. 14. Chacterization of the study area: (a) overall location in the Mediterranean basin *Pinus pinaster* distributes (source: Caudullo et al., 2017); (b) location and distribution network of plots (numbered yellow dots); and (c) climograph (source: AEMET).

Mushroom Yield Data

A database with values of the annual mushroom production at the plot level records the inside-plot yields, indicating species, number of individuals, and biomass per species as collected every week. Since these forests are slow-growing and there were no silvicultural treatments in the last decade, we considered that for this period the forest structure remained stable. We worked with the last 10 years of the database (2012–2021), a period in which the forest structure can be characterised and considered stable.

Annual values of total biomass (g) were calculated with all mushroom species in a single pool. Additionally, total biomass of the main commercial species, i.e., saffron milk cap (*Lactarius deliciosus*), was also evaluated. Therefore, we built a ten-year time series (2012–2021) of annual mushroom yields for all species in a pool, and of saffron milk cap individually (Fig. 15). In total, 295.15 kg of mushrooms were collected, of which 53.6 kg (18.16%) were *Lactarius deliciosus*, the most appreciated edible mushroom species in the area (Fig. 15).

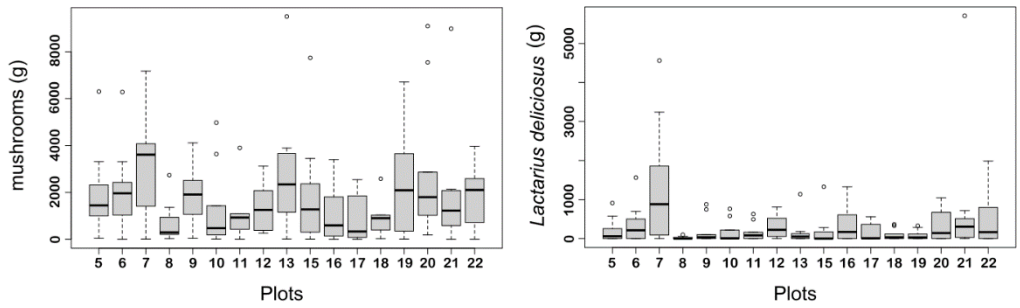

Fig. 15. Statistical characterization of annual mushroom yield (g) in the experimental network of plots during the period 2012–2021. (left): total mushroom biomass and (right): *Lactarius deliciosus* biomass.

Climatic Data

Ten years (2012–2021) of precipitation and temperature time series were retrieved from the AEMET (Spanish Meteorological Agency) meteorological station in Soria. From the original daily database, we calculated the accumulated precipitation of the autumn season (September, October, and November) and the average monthly minimum temperature in this season. These parameters are known to be the most relevant climatic variables for estimation of Lactarius deliciosus productivity in the study area, which is the most relevant species in these forest (Olano et al., 2020).

Forest Structural Measurements

To characterise forest structure at the plot level and to estimate overall vegetation volume of biomass, Terrestrial Laser Scanner (TLS) measurements were acquired in February 2022. A GeoSLAM mobile TLS with six sensors was thoroughly walked through each plot, retrieving very dense point clouds (300,000 points per second, a range of 100 m, and a relative accuracy up to 6 mm depending on the environment). The original point clouds were clipped to each plot area with proprietary

software (Fig. 16a). The resulting point clouds were used for estimation of overll vegetation volume employing the VoxR package in R (Lecigne et al., 2018), voxelizing the point cloud with a voxel size of 10 cm (Fig. 16b). The stand volume is the sum of the voxels multiplied by their size.

From the TLs point cloud, we also derived the percentage of canopy cover. To calculate the percentage of canopy cover, we considered the crowns of trees shading any part of the plot, including those which stand outside the plot fence. We removed the lowest 3 m from the point cloud to ensure isolation of the trees' canopy. The value of 3 m is an arbitrary threshold as, in our experience, this is enough to ensure that the ground vegetation is not included. Afterwards, we voxelized the point cloud with a voxel size of 5 cm using the VoxR package and calculated the canopy cover for each plot as the ratio of the area occupied by tree crowns to the plot area (Fig. 17).

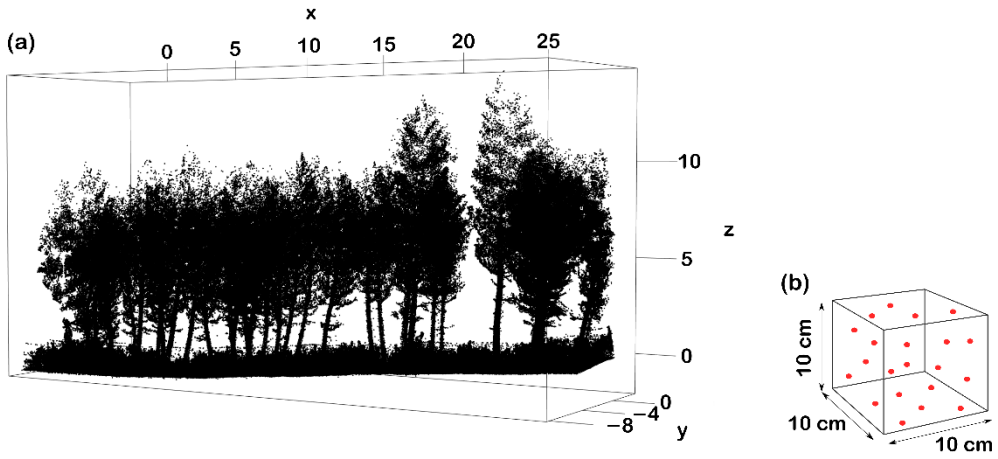

Fig. 16. Point cloud acquired with GeosLAM. (a) Example of a clipped plot point cloud corresponding to plot 22. (b) Schematic example of voxelization.

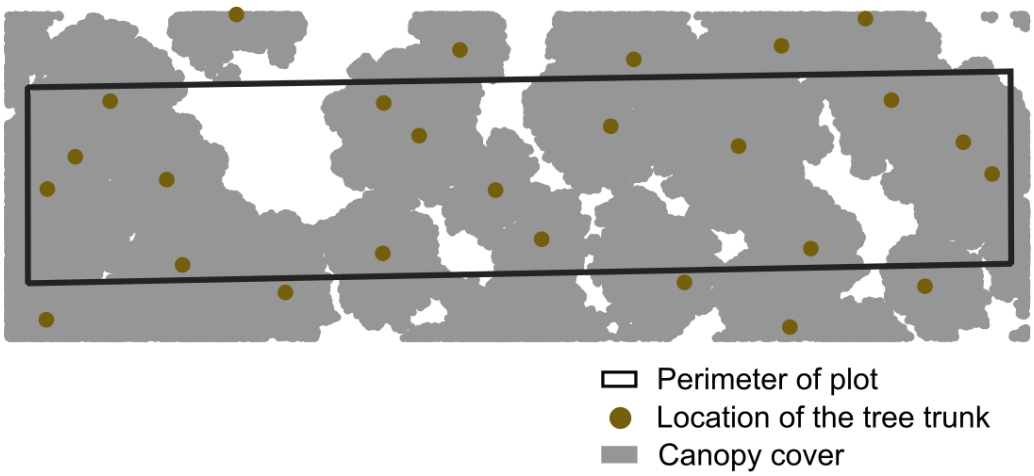

Fig. 17. Canopy cover retrieved from the GeoSLAM point cloud (example from Plot 6). Brown points represent the tree trunks whose canopies (grey area) affect the plot.

To complement the structural characterization of the plots, we calculated the Stand Density Index SDI (Reineke, 1933) and the total basal area (BA). In summer 2020, we measured all tree diameters and heights using a digital calliper and a hypsometer (VERTEX), respectively.

Landsat Data

The Normalised Difference Vegetation Index (NDVI, Rouse et al., (1973)) is the most frequently used spectral index in remote sensing (Huang et al., 2020). Algebraically, it is the ratio-normalised difference of infrared minus red (NIR - Red/NIR + Red) and is interpreted as a measure of the vegetation vigour in a given time (e.g., Mennis, (2001)). When NDVI values are compared between two times, this difference reflects the capacity of vegetation to produce energy, i.e., its primary productivity during the period considered (Vicente-Serrano et al., 2016).

In this work, we calculated NDVI values from Landsat imagery acquired by the Thematic Mapper (TM), Enhanced Thematic Mapper Plus (ETM+), and Operational Land Imager (OLI) sensors from 2012 to 2021. Since the annual primary productivity is represented by the difference between the season maximum and minimum NDVI values (Vicente-Serrano et al., 2016), our target dates for selection of imagery were 14 February (winter) and 15 August (summer), but these dates were flexible to accommodate orbital cycles and cloudiness. Average values of all 30 m pixels intersected by the field plots were retrieved, and the absolute value of the difference between summer and winter NDVI was evaluated and assigned to each plot.

Statistical Analysis

The statistical analysis to predict all mushroom and *Lactarius deliciosus* yields started from a database with eight covariates (Tab. 5). To get some understanding of the relationships between yields and the climatic, structural, and primary productivity predictors, and to select the most explanatory ones, we explored Pearson correlations between each pair of variables (Fig. 18). SDI was highly correlated with basal area (R = 0.86); therefore, only one of them was included in the models to avoid collinearity (Dormann et al., 2013). The correlation between all mushroom yields and *Lactarius deliciosus* yields (R = 0.66) provided confidence in the moderately high contribution of the latter to the complete pool. Furthermore, despite the high values of correlation found between SDI and Canopy (R = -0.78) and between BA and Canopy (R = -0.71), both SDI and BA were candidates in the models as they are evaluated from different data sources.

Unravelling the complex relationship between mushroom yield and its drivers may require powerful statistical tools. Generalised Additive Mixed Models (GAMM) are flexible in modelling complex variables and facilitate identification of the interaction between non-linear factors. Therefore, GAMM models were most suitable to predict mushroom yields with linear and non-linear variables, being more efficient and easier to interpret for all potential users. In addition, GAMMs were used with a random term, which in our case accounts for measuring errors at the plot level. The predictor function for a GAMM (η) has this general formula (Equation (1)):

$$\eta\,(X_{1\,ij},\ldots,X_{q\,ij},K_{1\,ij},\ldots,K_{n\,ij}) = \alpha + \beta_1 \cdot X_{1\,ij} + \ldots + \beta_q \cdot X_{q\,ij} + f_1\,K_{1\,ij} + \ldots + f_n\,K_{n\,ij} + a_j + \varepsilon \sim N(0,\sigma^2) \quad \text{(eq. 1)}$$

where $X_1 \ldots X_q$, $K_1 \ldots K_n$ is a set of n explanatory variables, $\beta_1 \ldots \beta_q$ are regression parameters, $f_1 \ldots f_n$ are nonparametric smoother functions, a_j is the random effect at the plot level, and Ɛ is the error term (Zuur et al., 2009). The indices i and j denote the ith year of yield data and the jth plot of the experiment, respectively.

Prior to the application of GAMM models and to assure its suitability, we tested linear regressions. For each modelling case (overall and *Lactarius deliciosus*), we tested all possible combinations and interactions of variables with the dredge command of the MuMin package in R. Based on the Akaike Information Criterion (AIC) (Akaike, 1998), we selected the best model. Given the poor results obtained by the linear regression tested in a first step (R^2 = 0.3 for all mushroom and R^2 = 0.2 for *Lactarius deliciosus* models), GAMM models were built with *mgcv* package (R Core Team, 2019; Wood, 2017), observing the most explanatory variables that were selected in the previous step. We plotted the relationships among variables for a visual exploration and interpretation of the results, since GAMMs are better interpreted by visual examination than by statistical significance (Biber et al., 2013).

Tab. 5. Description of variables involved in the statistical analysis.

Variable	Description	Max	Min	Mean	Stedv
$Yield_{total}$	Total yield of mushrooms (g)	9504	0	1746	1910.27
$Yield_{Lactarius}$	Total yield of *Lactarius deliciosus* (g)	5706.50	0	67	690.08
$NDVI_{diff}$	Difference between winter and summer NDVI (absolute value)	0.26	0.003	0.10	0.0057
$NDVI_{diffprev}$	Difference between winter and summer NDVI of the previous year (absolute value)	0.26	0.002	0.10	0.0054
Canopy	Canopy cover (%)	79.66	69.96	74.37	2.94
$Volume_{biomass}$	Volume of total aboveground biomass in the plot (m^3 ha^{-1})	301.00	151.50	221.60	49.16
BA	Basal area of the plot (m^2 ha^{-1})	76.40	31.60	54.16	14.08
SDI	Stand Density Index	1414.30	662.18	1034.8	247.79
$Prec_{autumn}$	Accumulated autumn rainfall (mm)	207.40	35.20	126.10	47.12
T_{min}	Average of the autumn months´ minimum temperature (°C)	7.67	5.10	6.11	0.80

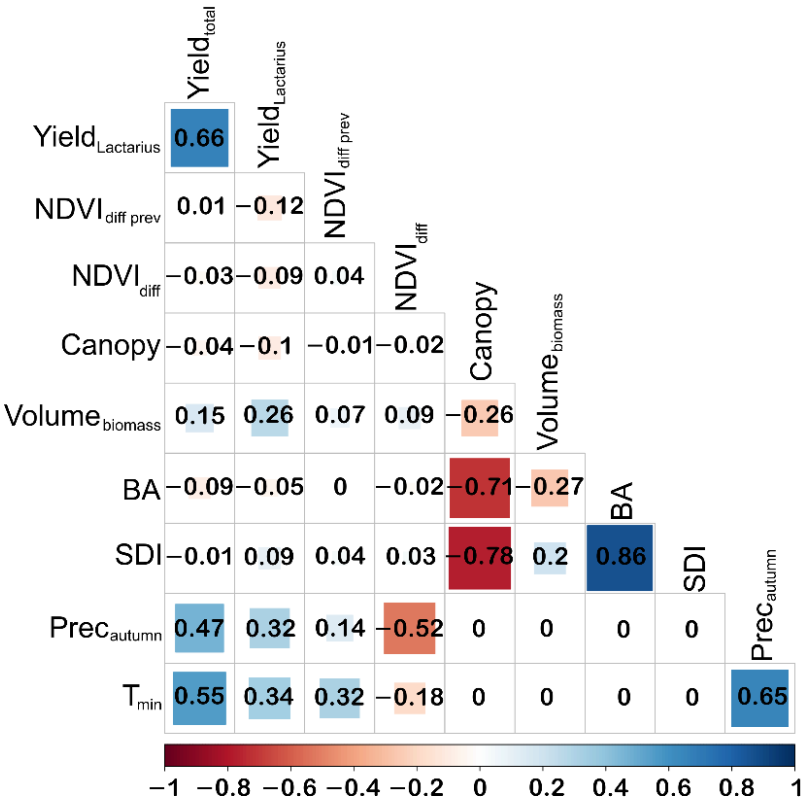

Fig. 18. Pearson correlation between pairs of variables.

RESULTS

Two models, one for the entire mushroom assemblage and one for *Lactarius deliciosus* only, were developed, including climatic and forest structural variables as well as primary productivity as predictors.

In the best model for the entire set of mushrooms, the adjusted coefficient of determination (R^2) was 0.49 and the AIC was 2954.352. The actual model is represented by the following equation (Equation (2)):

$$Yield_{total} = f_1(Prec_{autumn}) + f_2(Volume_{biomass}, NDVI_{diff}) + f_3(SDI) + f_4(Canopy, T_{min}) + random + \varepsilon \quad \text{(eq. 2)}$$

where f_i are the nonparametric smoother functions summarised in table (Tab. 6). The non-linear parameters are represented in figure (Fig. 19) for visual interpretation.

The edf (effective degrees of freedom) values in table (Tab. 6), which provides a measure of the linearity of the relationship between variables (Hunsicker et al., 2016), showed that mushroom yield has a highly non-linear relationship with autumn precipitation and SDI and has a non-linear relationship with the interactions between $Volume_{biomass}$ and $NDVI_{diff}$ and between canopy cover and T_{min}.

Tab. 6. Parameters describing the smoother functions, where the significance codes are for a p-value = 0 '***', p-value = 0.001 '**', p-value = 0.01 '*', p-value = 0.05 '·' and p-value = 0.1 ' '.

	Edf	p-value	Significance
$f_1(Prec_{autumn})$	3.682	<0.0000	***
$f_2(Volume_{biomass}, NDVI_{diff})$	2.000	0.0001	***
$f_3(SDI)$	2.658	0.0112	*
$f_4(Canopy, T_{min})$	2.000	0.0959	·

Increased rainfall during the autumn months ($Prec_{autumn}$ > 150) was associated with an increment in the mushroom yield, but there was no positive effect with $Prec_{autumn}$ below this value (Fig. 19a). There was an optimum relationship between stand density and mushroom production with highest production at SDI values between 1000 and 1200; however, for higher SDI values the mushroom yield decreases (Fig. 19b). The interaction between plot $Volume_{biomass}$ and $NDVI_{diff}$ (Fig. 19c) indicated that mushroom yield increases with increasing $Volume_{biomass}$ and higher primary productivity. The interaction between Canopy and T_{min} (Fig. 19d) indicated that mushroom yield is higher when the minimum temperature in autumn and the canopy cover are both higher.

Visualising the common effect of SDI and $NDVI_{diff}$ on mushroom yield facilitates its interpretation (Fig. 20). For an SDI value of approximately 650, the predicted yield of all mushrooms together is lowest. It increases when stand density is rather high (SDI 950) but decreases again at even denser stands (SDI 1250). Note that the effect of $NDVI_{diff}$ on the mushroom production is even stronger. Between $NDVI_{diff}$ 0.05 and 0.25, mushroom production increases by approx. 800 units.

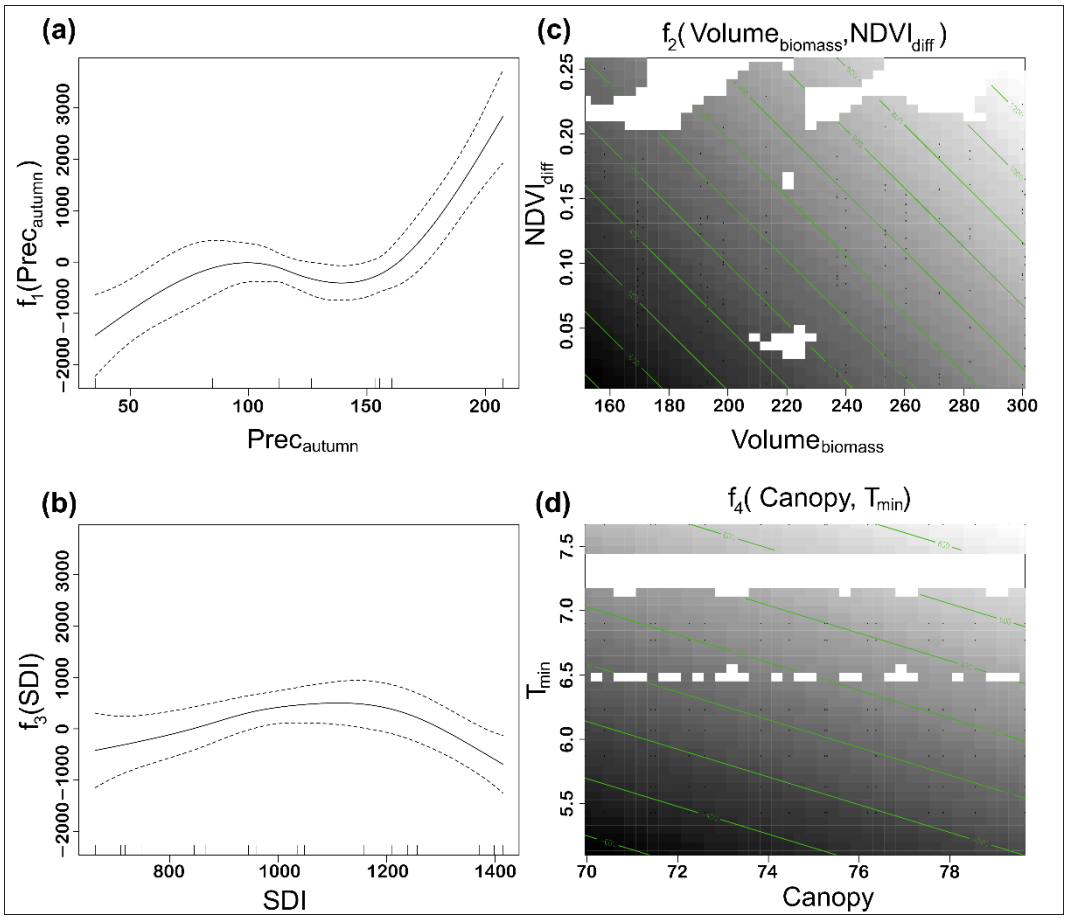

Fig. 19. Non-linear effects of the variables for the model developed for all mushroom species together (Equation (2)). (a) $Prec_{autumn}$; (b) SDI; (c) interaction between $Volume_{biomass}$ and $NDVI_{diff}$; and (d) interaction between Canopy and T_{min}. In two-dimensional plots (c,d), white shows a positive effect and black a negative effect; green contour lines show where the function has a constant value.

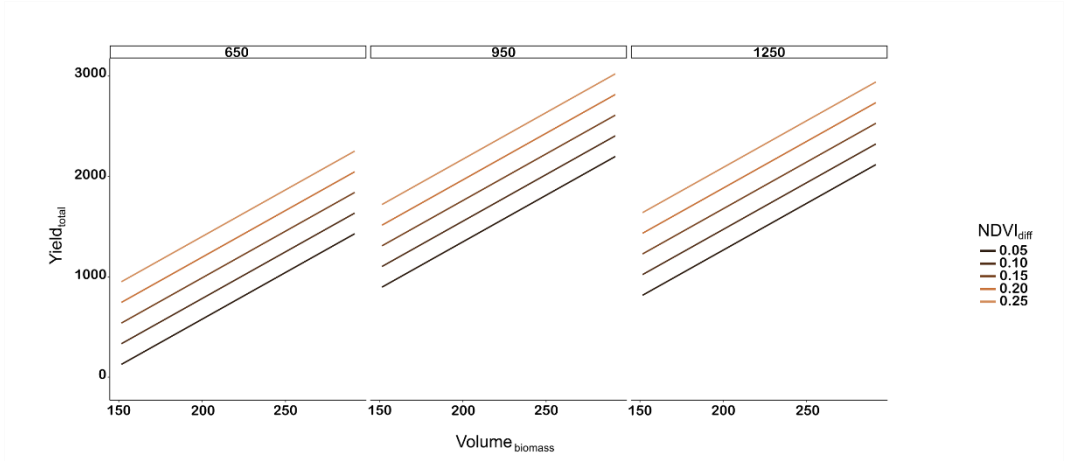

Fig. 20. Model predictions for all mushroom yields. $Yield_{total}$ (Y-axis) versus $Volume_{biomass}$ are shown for five different $NDVI_{diff}$ values and SDI values of 650, 950 and 1250.

The model generated for Lactarius deliciosus (R^2 = 0.3, AIC = 2658.378) is represented in Equation (3), and its parameters are summarised in table (Tab. 7).

$$Yield_{Lactarius} = f_1(Prec_{autumn}) + f_2(Volume_{biomass}, NDVI_{diff}) + f_3(BA) + random + \varepsilon \quad \text{(eq. 3)}$$

where, as before, f_i is a nonparametric smoother function. Similar to the previous case, in figure (Fig.21), the non-linear parameters are displayed for visual interpretation.

Tab. 7. Parameters describing the smoother functions of the model of *Lactarius deliciosus* yield, where the significance codes are for a p-value=0 '***', p-value = 0.001 '**', p-value = 0.01 '*', p-value = 0.05 '·' and p-value = 0.1 ' '.

	Edf	p-value	Significance
$f_1(Prec_{autumn})$	3.318	<0.0000	***
$f_2(Volume_{biomass}, NDVI_{diff})$	3.741	0.0002	***
$f_3(BA)$	2.035	0.0694	·

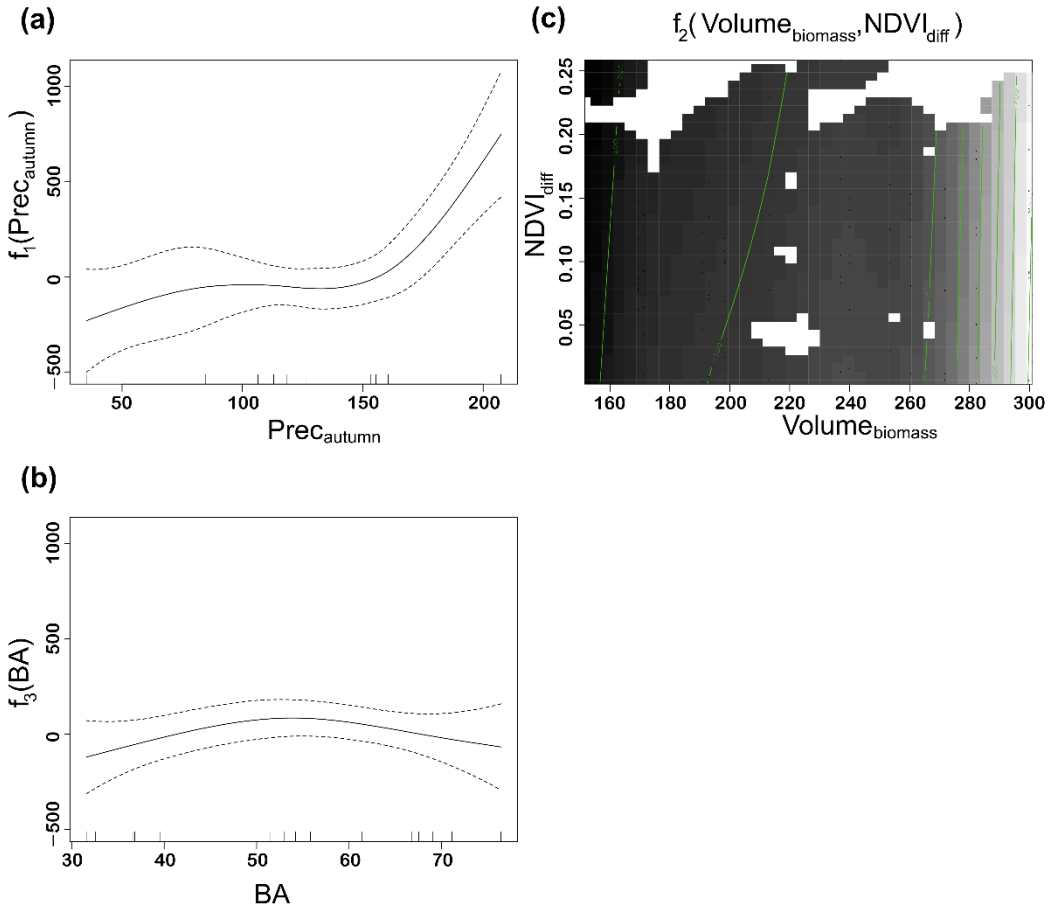

Fig. 21. Non-linear effects of the variables for the model developed for *Lactarius deliciosus* (Equation (3)). (a) $Prec_{autumn}$; (b) BA; and (c) interaction between $Volume_{biomass}$ and $NDVI_{diff}$. In the two-dimensional graph (c), white shows a positive effect and black a negative effect; green contour lines show where the function has a constant value.

In this case, the edf indicates that *Lactarius deliciosus* yields have a highly non-linear relationship with the autumn precipitation and with the interaction between vegetation biomass and primary productivity, and that for basal area the relationship is less pronounced.

For an optimal yield of *Lactarius deliciosus* in Mediterranean dry forests of *P. pinaster*, various circumstances are required: abundant rainfall in the autumn months, high values of the interrelationship between $Volume_{biomass}$ and $NDVI_{diff}$ (primary productivity), and BA not exceeding 55–60 m^2 ha^{-1}. Interestingly, when BA exceeds 60 the *Lactarius deliciosus* yield is lower (Fig.21).

DISCUSSION

Mushroom production is an ecosystem service highly demanded by society in the study area, not only because of the touristic and gastronomic resource that the exploitation of edible species represents but also for its important role in the functioning of ecosystems. According to the latest monitoring report on SDG 15 target in 2022, the risk of species extinction is increasing at a rate unprecedented in history (United Nations, 2022b). Fungi are organisms seriously threatened by global change processes (Ágreda et al., 2015; Morera et al., 2022) and whose life cycles are largely unknown (Van der Heijden and Sanders, 2002). In this sense, the use of remotely sensed data and its processing with advanced mathematical techniques may facilitate our progress in determining the factors that trigger mushroom production and in predicting their yields. Having mushroom yield models will enable the inclusion of mushrooms in sustainable forest management plans in order to maintain the economic activity linked to their exploitation without compromising this resource.

Progress is currently being made in mapping, on a global scale, the distribution of mushrooms by applying artificial intelligence (Anthony et al., 2022; Steidinger et al., 2019). Likewise, the use of remote sensing data is helping advance our knowledge of mushroom biology and the factors that trigger their production (Olano et al., 2020; Thers et al., 2017; Peura et al., 2016), a key step in understanding their life cycle to facilitate its management.

This work presents an approach for assessing the effects of climatic, structural, and primary productivity variables of Mediterranean dry forests of *Pinus pinaster* in Spain on mushroom yields and, in particular, on those of the edible species *Lactarius deliciosus*. Through remotely sensed data that are transformed into derived variables (NDVI from Landsat and canopy cover from TLS) and the application of GAMM models, we found that mushroom fruiting, for the overall pool of species and for *Lactarius deliciosus* specifically, is equally triggered by the cumulative precipitation of autumn ($Prec_{autumn}$ > 150 mm). This finding, firstly demonstrated by the ranking of independent variables in our models, is not novel (Olano et al., 2020), but it is complemented by identifying other influencing factors which result from the interaction between various parameters. In this sense, we noted the strength of the interaction between forest vegetation volume ($Volume_{biomass}$) and primary productivity ($NDVI_{diff}$), both characterised using remotely sensed data, as a second factor. Finally, the other statistically significant variables in both models were structural, in agreement with other authors (e.g., Bonet et al., (2008)). Interestingly, when modelling *Lactarius deliciosus* yields alone, basal area becomes more relevant than SDI, pointing to an optimal range of BA in which *Lactarius deliciosus* fruits. In Miina et al., (2016), it was already demonstrated that there is an optimum BA for mushroom production, which depends on the forest dominant species and is approximately 35–40 m^2 ha^{-1} for *P. pinaster*. In our study area, BA seemed to positively influence *Lactarius deliciosus* yields up to a maximum value of 50 m^2 ha^{-1}. Evapotranspiration in forests of lower densities leads to less water availability, while at higher densities temperature may be reduced; this is linked to lower illumination and directly affects mushroom yields. When modelling the entire pool of wild mushroom species, SDI and the interaction between canopy cover and T_{min} were the most relevant, possibly indicating the minimum conditions necessary to achieve mushroom fruiting. The moderate fit of our models (R^2 ~ 0.49) indicates that

the independent variables explain the dependent variable to some extent but can be further improved, both in terms of sample size and the type and number of parameters.

The role of remotely sensed variables became relevant in estimating yields, through the interaction of vegetation volume ($Volume_{biomass}$) with primary productivity ($NDVI_{diff}$) in both predictive models as well as the interaction of Canopy with minimum temperature (T_{min}) in the overall model. Vegetation primary productivity was historically among the first variables to be estimated with multitemporal RS data (Tucker and Sellers, 1986), and currently it can be routinely evaluated at a range of spatial scales thanks to the regular and frequent data acquired by operational programs of different optical sensors (Song et al., 2013). The structural parameters, readily estimated in our plots with point clouds acquired with a mobile TLS, would have been unreachable otherwise, and certainly places our work as an example of novel application for the employment of TLS data (Åkerblom and Kaitaniemi, 2021).

Vegetation volume interacting with primary productivity in the yield models suggests the potential for including forest growth rate, a measurable structural parameter, in future modelling efforts. In fact, Kuikka et al., (2003) already demonstrated that there is a relationship between maximum mushroom production and the forest stand growth rate and showed the example of the mycorrhizal sporocarps development in relation with the growth and photosynthetic rate of the host trees (Calama et al., 2010). Post-treatment conditions following forest thinning have also been shown to facilitate short-term successional changes in fungal sporocarp assemblage (Collado et al., 2021). Sustainable forest management should ensure good mushroom production when keeping the stand density high but not overstocked.

Climate variables, forest primary productivity and forest structure determine the production of mushrooms in Mediterranean forests. Remotely sensed data, multitemporal optical and TLS point clouds in particular, are presented here as a key source of data with strong potential for development of mushroom yields predictive models. The inclusion of variables related to stand development, such as current growth, may further improve the models, developing simple harvest predictive equations that would enable forest managers to establish guidelines for fungal sustainable harvest.

CONCLUSIONS

A combination of active and passive remotely sensed data was shown to be relevant for assessment of the overall mushroom productivity in Mediterranean dry forests of Pinus *pinaster*, and specifically for *Lactarius deliciosus*. Advanced statistical analysis with Generalized Additive Mixed Models (GAMM) unravelled the complex relationships among forest primary productivity, structural parameters, and climatic variables driving the amount of wild mushroom harvests. The most relevant factors triggering mushroom fruiting were the accumulated precipitation of autumn and the interaction of vegetation volume with primary productivity, the latter two estimated from TLS point clouds and Landsat multitemporal NDVI, respectively. Lastly, whilst primary productivity and the interaction of canopy cover and fall low temperatures are key in the estimation of overall yields, basal area is more relevant for estimation of *Lactarius deliciosus*. The capacity of remote sensing to extend models of mushroom yields at medium to large scale promises relevant opportunities for the inclusion of these non-wood forest products in sustainable management plans and SDGs achievement.

AUTHOR CONTRIBUTIONS

Conceptualization, R.M.-R.; methodology, R.M.-R.; formal analysis, A.T.-C.; data curation, R.M.-R. and L.B.; writing—original draft preparation, R.M.-R., C.G. and B.Á.; writing—review and editing, R.M.-R., A.T.-C., L.B. and E.U.; supervision, C.G. and B.Á. All authors have read and agreed to the published version of the manuscript.

FUNDING

This work was supported by the Spanish Ministry of Science and Innovation, under grant DI-17-9626. This work has received funding from the European Union's Horizon 2020 research and innovation programme under the Marie Skłodowska-Curie grant agreement No. 778322.

DATA AVAILABILITY STATEMENT

Mycological data employed in this work belong to Castilla y León Regional Government (Servicio de Medio Ambiente). We were granted permission to use the dataset for scientific research but are not allowed to share them publicly.

ACKNOWLEDGMENTS

Acknowledgement to Consejería de Medioambiente de la Junta de Castilla y León for maintaining the network of plots and providing the mushroom production data, as well as Valonsadero Forestry Centre and Cesefor Foundation for their work in mushroom data collection. Fredrerico Simoes is thanked for collecting the TLS data.

CONFLICTS OF INTEREST

The authors declare no conflict of interest.

Capítulo 3: Towards prediction of forest wild mushrooms yields with time series of Sentinel-1 interferometric coherence data

Martínez-Rodrigo, R., Águeda, B., López-Sánchez, J. M., Altelarrea, J.M., Alejandro, P., Gómez, C. (2023).

Capítulo 3: Towards prediction of forest wild mushrooms yields with time series of Sentinel-1 interferometric coherence data

Raquel Martínez Rodrigo [1,2], Beatriz Águeda [2], Juan Manuel López-Sánchez [3], José Miguel Altelarrea [4], Pablo Alejandro [5], Cristina Gómez [2,6]

[1] föra forest technologies, Campus Duques de Soria, E-42004 Soria, Spain
[2] iuFOR-EiFAB, Universidad de Valladolid, Campus Duques de Soria, E-42004 Soria, Spain
[3] Institute for Computer Research, University of Alicante, 03080 Alicante, Spain
[4] Fundación Cesefor, Calle C, E-42005 Soria, Spain
[5] Quasar Science Resources, Ctra. La Coruña km 22.3, Las Rozas, 28232 Madrid. Spain
[6] Department of Geography and Environment, School of Geoscience, University of Aberdeen, Aberdeen AB24 3UE, UK

ABSTRACT

Edible wild mushrooms constitute a marketable non-wood forest product with high relevance worldwide, therefore there is growing interest in developing tools for estimation of yields. Remote sensing is a powerful technology for characterization of forest structure and condition, both essential factors in triggering mushroom production. In this work we explore options to apply Synthetic Aperture Radar (SAR) data from C-band Sentinel-1 to characterize, at the plot level, wild mushroom productive forests in the Mediterranean region, which provide saprotroph and ectomycorrhizal mushrooms. Seventeen permanent plots with mushroom yield data collected weekly during the productive season are characterized with dense time series of Sentinel-1 backscatter intensity (VV and VH polarizations) and 6-day interval interferometric VV coherence during period 2018 – 2021. Weekly-regularized series of SAR data are decomposed with a LOESS approach into trend, seasonality, and remainder. Trends are explored with the Theil-Sen test, and periodicity is characterized with the Discrete Fast Fourier transformation. Seasonal patterns of SAR-time series are described and related to mycorrhizal and saprotroph guilds separately. Our results indicate that time series of interferometric coherence show cyclic patterns related with annual mushroom yields and may constitute an indicator of triggering factors in mushroom production, whereas backscatter intensity is strongly correlated with precipitation, making noisy signals without a clear interpretable pattern. Exploring the potential of remotely sensed data for prediction and quantification of mushroom yields contributes to improve our understanding of fungus biological cycles and uses.

INTRODUCTION

Predicting mushroom presence, occurrence and productivity has growing interest (Herrero et al., 2019; Küçüker and Baskent, 2014) as fungi provide a wide range of ecosystem services (Devkota et al., 2023) and contribute to maintain and augment biodiversity of other taxa (Cockle et al., 2012; Müller and Bütler, 2010). The triggering factors in mushroom production are complex (Alday et al., 2017b), being precipitation of paramount importance (Ágreda et al., 2015). Furthermore, mushroom development and productivity are strongly related with forest structure (Tomao et al., 2017), particularly with density and age (Martínez-Rodrigo et al., 2022; Ágreda et al., 2013).

Satellite remote sensing has become a major technology in environmental applications (Beland et al., 2019). Remote sensing is particularly well suited for the assessment of forest resources (White et al., 2016) and changes over time, thanks to its overall perspective and spatial completeness (Li and Roy, 2017). The assessment of forest products, particularly wood (e.g., Eitel et al., 2020) but also non-wood products like pine-nuts (e.g., Blázquez-Casado et al., 2019), cork (e.g., Soares et al., 2022) or mushrooms (e.g., Olano et al., 2020) has been favoured using remote sensing. Although passive sensors from MODIS, Landsat or Sentinel-2 are widely employed, active sensors are gaining ground for a range of applications (e.g., Ballère et al., 2021). For instance, LiDAR is used to characterise forest structure (Dassot et al., 2011), and has shown potential for the estimation of mushroom yields in Mediterranean forests (Martínez-Rodrigo et al., 2022; Pascual and de Miguel, 2022).

Synthetic Aperture Radar (SAR) technology has the ability to work both day and night in all atmospheric conditions (Pulella et al., 2020b), and it is well-suited for characterization of forest structure (Neumann et al., 2010; Gómez et al., 2021). Moreover, the high frequency of data and open access policy of the Copernicus Sentinel-1 program (https://scihub.copernicus.eu/), together with improved image processing, have triggered new opportunities for application of SAR-based approaches in characterization of forests (Dostálová et al., 2018), mapping of above-ground forest biomass (Cartus et al., 2022), and assessment of change (Tanase et al., 2019).

Time series of radiometric data identify intra-annual vegetation patterns (Gómez et al., 2020) and anomalies (Rubio-Cuadrado et al., 2021). Since retrieving good quality time series of optical data, without gaps, becomes difficult in cloud-prone areas (Komisarenko et al., 2022), time series of SAR data are being explored for applications like seasonality and phenological characterization (Dubois et al. 2020; Frison et al., 2018) and detection of anomalies (Schellenberg et al., 2023).

Backscatter intensity is sensitive to vegetation humidity (Ezzahar et al., 2020), a triggering factor of fungi production (Ágreda et al., 2015). Processing easiness and intuitive interpretation make backscatter intensity a preferred technique in SAR-based time series analysis. At C-band, the VH backscatter intensity is more sensitive to volume, making the upper canopy response dominant in this polarization (Brown et al., 2003), whereas VV backscatter is more sensitive to texture and may respond to the vegetation-soil interplay (Veloso et al., 2017).

Interferometric SAR (InSAR) exploits the phase difference between two complex SAR observations of the same area acquired from different sensor positions, and extracts distance information about the Earth's terrain (Gens and Van Genderen, 1996;

Ferreti et al., 2000). Interferometry has been applied for land cover classification (Rizzoli et al., 2022; Jacob et al., 2020) and crop mapping and monitoring (Villarroya-Carpio et al., 2022; Mestre-Quereda et al., 2020). In a forestry context, the interferometric coherence parameter can be related to structure (Pinto et al., 2013) and time series of this parameter have shown useful to detect changes (Mastro et al., 2022). The temporal decorrelation of repeat-pass InSAR is known to hinder some applications (Ahmed et al., 2011), but it may facilitate the identification of triggering punctual phenomena like mushroom production.

Our goal is to explore the capacity of time series of C-band SAR data from Sentinel-1 to characterize mushroom yields at plot level in Mediterranean forests, with a longer-term aim of developing production predictive models. The specific objectives pursued are: (1) to build time series of Sentinel-1 data over mushroom productive pine plots and characterize different temporal patterns; and (2) to explore the relationship between C-band SAR time series patterns and saprotroph and ectomycorrhizal mushrooms weekly yields.

MATERIAL AND METHODS

Study area and experimental design

The study area, centred at coordinates 41.61 N, -2.54 W, encompasses 17,000 ha of pine forests in Soria province, Spain (Fig. 22). These reforestations of Pinus pinaster Ait. also host Quercus pyrenaica Willd. resprouts. The area is relatively flat, with altitude in the range 1000 - 1200 m. The climate is Continental Mediterranean, with cool winters (average January temperature of 2 ºC) and marked summer drought, with annual rainfall between 500 and 700 mm.

Seventeen permanent plots of 150 m2 (5x30 m) have been established in this forest since 1997, with an external fence preventing harvesting and trampling. Plots are stratified to represent different forest structures (Figure 1). Diameter and height of all trees within the plots were measured in 2020 and the volume of biomass was derived from TLS measurements acquired in 2022 (Martínez-Rodrigo et al., 2022). All edible fungi fruiting bodies (sporocarps) are sampled on a weekly basis during the main fruiting period, which corresponds to the autumn months of September-December. Sporocarps are collected, fresh-weighted, and identified to the species level (Ágreda et al., 2015). A database with values of annual mushroom production at the plot level records the yields, indicating species, number of individuals and biomass per species. We used a temporal subset (2018-2021) of this database and split the sample into ectomycorrhizal and saprotroph trophic guilds (Rinaldi et al., 2008) for a more detailed understanding of the relationship between SAR data and mushroom production.

Sentinel-1 and precipitation data

Sentinel-1 is a dual satellite mission of the Copernicus programme developed and managed by the European Space Agency (ESA). Sentinel-1A and -1B satellites hold a C-band (frequency centred at 5.405 GHz equivalent to a wavelength of 5.56 cm) Synthetic Aperture Radar (SAR) sensor with capacity to work in VV + VH dual polarization (ESA-Sentinel-1, 2023). The default acquisition mode over land is Interferometric Wide swath (IW), which provides data worldwide with 5 x 20m spatial resolution and a nominal 6-day temporal resolution if both satellites are considered (Torres et al., 2012).

To work with four complete years of time series data, we downloaded all accessible good quality data acquired over the study area from 5th January 2018 to 21st December 2021, when the power supply system failure in Sentinel-1B precluded further dual acquisitions. Sentinel-1 data were downloaded from the Alaska Satellite Facility (ASF, https://search.asf.alaska.edu/).

Daily precipitation data were retrieved from the Spanish Meteorological Agency (AEMET, http://www.aemet.es) station in Soria.

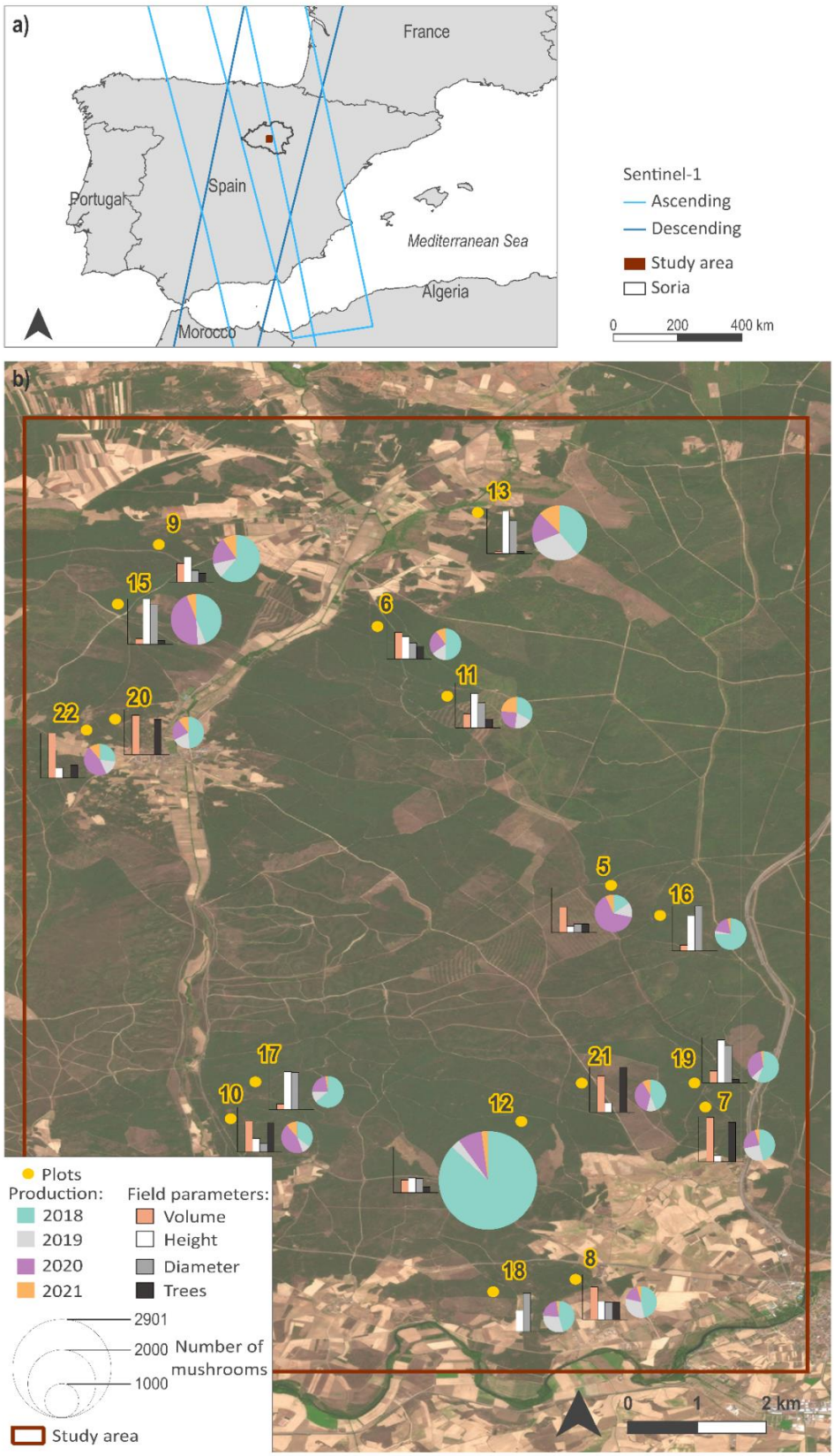

Fig. 22. Study area. a) Location in Spain and Sentinel-1 orbits. b) Arrangement of plots with structural and mushroom productive characterization (2018-2021). Pie charts represent total mushroom production in number and proportion of each year considered. Bar charts show plot structural parameters in a relative scale with values normalized between 0 and 1.

Analysis workflow

The methodology followed in this work includes time series processing of remotely sensed data and field measurements, imputation of data to experimental plots, and statistical analysis of time series data (Fig. 23).

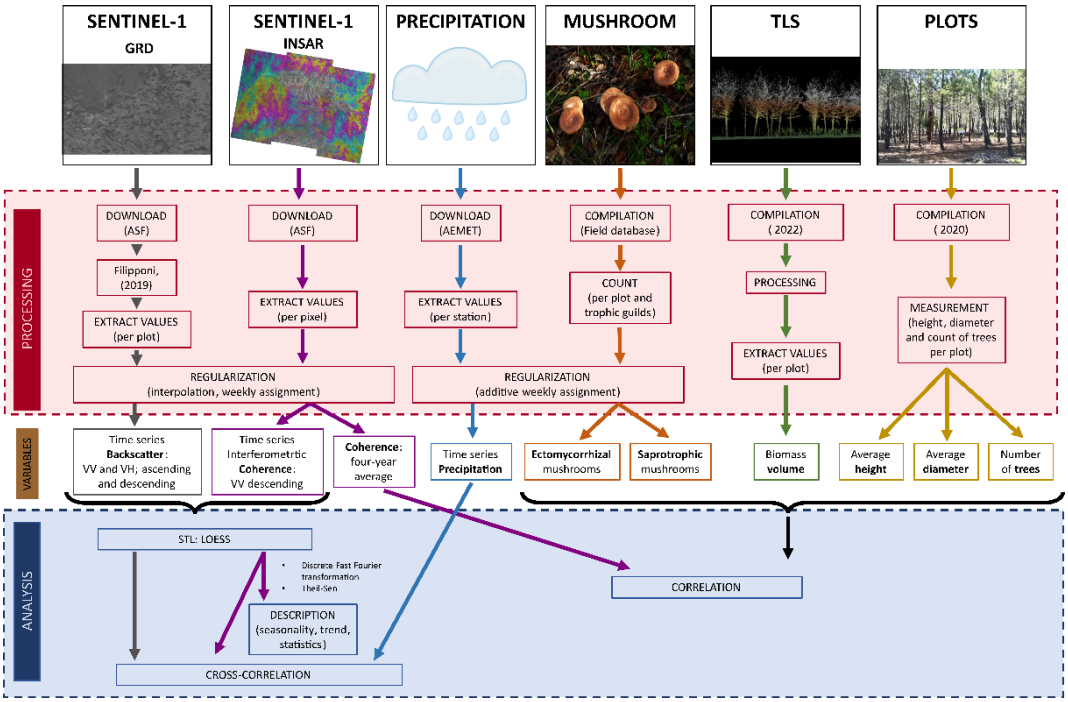

Fig. 23. Schematic workflow of the methods´ main stages for characterization of mushroom productive plots with time series of Sentinel-1 SAR data.

Backscatter intensity datasets

To derive time series of backscatter intensity, 1,076 Sentinel-1 slices from ascending and descending orbits (Tab. 8) were downloaded in Ground Range Detected (GRD) mode. GRD products are multi-looked, projected to ground range with an Earth ellipsoid model (e.g., WGS84), and display square pixels representing the amplitude of the returned SAR pulse. GRD products were further processed with a standard processing workflow (Filipponi, 2019) employing the Sentinel-1 Toolbox in SNAP. Our processing includes apply orbit file, thermal noise removal, calibration to radiometric backscatter, terrain flattening, speckle filter (Boxcar, 5x5), Range Doppler terrain correction, and linear to dB transformation. The outcomes are raster sets of backscatter intensity values corrected by local topography and various sources of noise, at 10x10 m square pixels projected to WGS84 UTM30.

Tab. 8. Summary of Sentinel-1 datasets downloaded and processed, indicating number of dates these images the entire study area.

	2018			2019			2020			2021			TOTAL
Orbit type	Asc	Des	Tot	Asc.	Des	Tot	Asc	Des	Tot	Asc	Des	Tot	
Slices downloaded & processed	128	151	279	114	107	221	151	148	299	152	125	277	1076
Data dates	97	61	158	85	58	143	120	59	179	120	57	177	657

Interferometric coherence datasets

Six-day interval VV-pol interferograms were ordered and downloaded from the ASF Data Search Vertex portal already processed with HyP3 (Hogenson et al., 2020), to generate time series. When selecting InSAR pairs, we chose the number of looks (10 x 2), to obtain 40 m pixel resolution data.

We retrieved interferograms from 235 image pairs in descending orbit, from 5th January 2018 to 21st December 2021, making up a regular series only interrupted three times due to the lack of three Sentinel-1 acquisitions (29/06/2019, 08/12/2020 and 11/08/2021). The same number of interferometric pairs were available in ascending orbit, but due to their incomplete coverage of the study area we discarded their use.

Retrieval of SAR and precipitation time series

Time series of VV and VH backscatter intensity corresponding to the average value of pixels in the mushroom plots, and VV interferometric coherence corresponding to the plots' centroids were retrieved. These time series were regularized to seven-day frequency by averaging weekly values and interpolating missing data with a third-degree polynomial model. A seasonal, trend and remainder decomposition (STL, Seasonal-Trend Decomposition) was applied for denoising, simplifying the data with a LOESS smoother (Cleveland et al., 1990). Precipitation time series were built with weekly accumulated values of rainfall.

Characterization of Sentinel-1 time series

The denoised seasonal plus trend time series of SAR backscatter intensity and interferometric coherence of each plot were analysed, as indicator of variations at intra- and interannual scales. The presence and degree of trend was tested with the Theil-Sen test (Theil, 1950; Sen, 1968) assimilating the linear trend to the series slope (Chervenkov and Slavov, 2019). Seasonality of the interferometric coherence seasonal component was analysed via Fourier decomposition, disaggregating the time series into simple functions (Hsu, 1987) with the Fourier fast transformation (Brigham, 1988). The main frequencies were interpreted as indicators of cyclic patterns.

Statistical relationship between SAR and precipitation time series

To explore the temporal relationship between SAR time series (backscatter intensity and interferometric coherence) with precipitation, the cross correlation between both sets of data were explored at weekly scale. The aim was to determine whether an event in one of the time series (precipitation) triggers the change of values in the other (SAR) or if they are independent (Brockwell and Davis, 2016). In this case the backscatter (VV and VH) and coherence average values of all-plots were considered.

To explore the temporal relationship between interferometric coherence and mushroom yields, the rate and directionality of change of the SAR interferometric coherence series temporal derivative was explored as in Gómez et al. (2011). We were interested in the relationship with the yearly first emergence of mushroom in productive plots.

RESULTS

Characterization of mushroom productive plots

Mushroom harvest was rather variable per year and plot during the period 2018-2021. The average annual production was 233 mushrooms per plot, 105 ectomycorrhizal and 128 saprotrophs. Overall, years 2018 and 2020 were the most productive, although with high variability per plot. Plots 12 and 17 were the most and least productive, respectively.

Tab. 9. Description of structural variables in mushroom productive plots

Variable	Units	Max	Min	Mean	Stedv	Plot (Max)	Plot (Min)
Volume biomass	m^3 ha^{-1}	300.95	151.53	221.60	49.16	22	18
Average height	m	16.91	8.90	12.94	2.57	15	20
Average diameter	cm	42.58	16.23	27.71	9.34	16	21
Trees	Number	50.00	9.00	21.47	13.34	21	18, 17 and 16

Plots are structurally diverse (Tab. 9) with 8.9 - 16.91 m average tree height and 16.23 - 42.58 cm average tree diameter. Plot 21 has the maximum number of trees with minimum average diameter, and plot 16 has the minimum number of trees with largest average diameter. Plot 15 has the tallest trees on average, and plot 20 the shortest. Plot 22 has the most volume biomass, and plot 18 is the least dense and with minimum volume biomass.

Relationship between interferometric coherence and field parameters

There is a strong and negative relationship between the interferometric coherence and the average tree height at the plot level (R = -0.70) and between coherence and average diameter of trees (R = -0.67) in their range of values (8-18 m for tree height and 0.16-0.42 m for tree diameter). The relationship of interferometric coherence with plot volume of biomass per plot and number of trees per plot is strong and positive (R = 0.57 and R = 0.56 respectively) (Fig. 24).

The relationship of interferometric coherence with average production of ectomycorrhizal mushrooms (R = 0.47) is strong and positive, whereas it is low and negative with the average production of saprophytic mushrooms (R = -0.17) (Fig. 25).

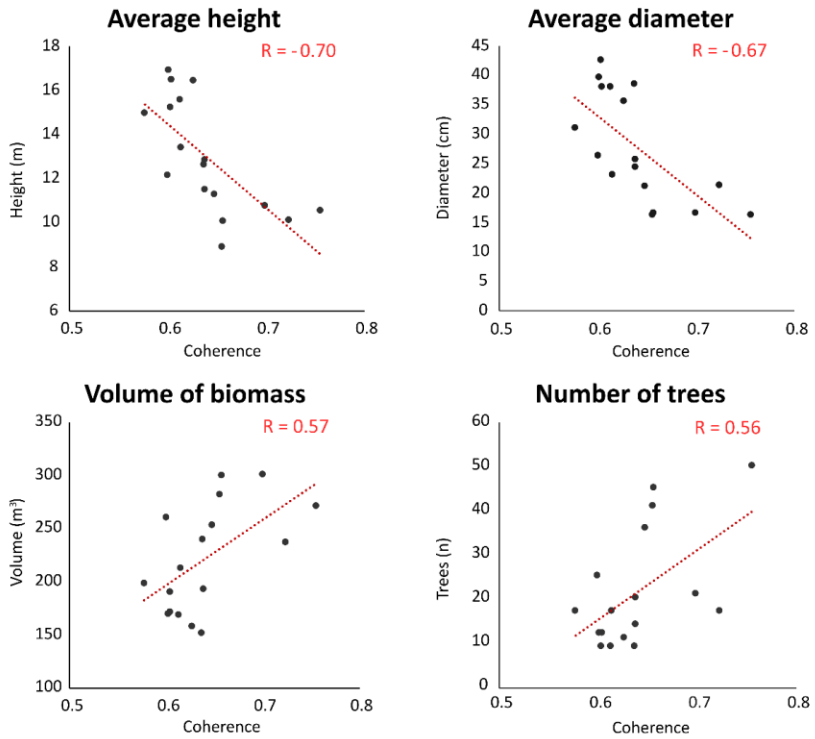

Fig. 24. Statistical relationship between interferometric coherence and forest structural variables

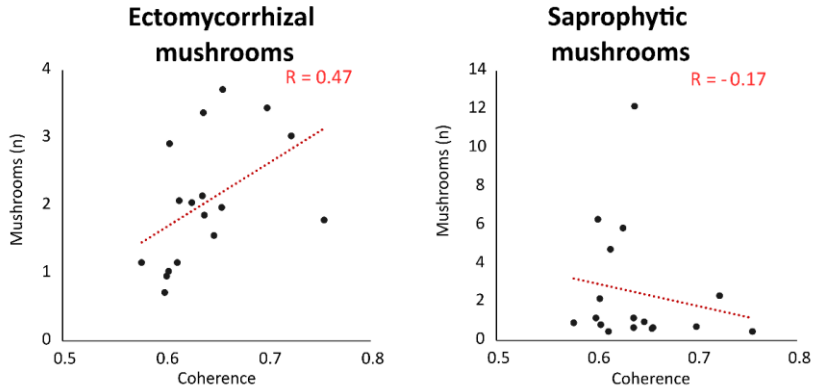

Fig. 25. Statistical relationship between interferometric coherence and mushroom production

Characterization of Sentinel-1 backscatter intensity time series

During the four years of data inspected, Sentinel-1 cross-pol (VV) backscatter intensity corresponding to mushroom plots was higher than co-pol (VH) intensity in both descending (morning) and ascending (evening) orbits (Fig. 26). Averaging values of the entire time series per plot, the lowest intensity, both in VH and VV, corresponded to plot 22 (plot with most biomass volume) in the evening and to plot 21 (plot with most number of trees) in the morning acquisitions; the highest value corresponded to plots 17 and 11 in morning and to plots 8 and 19 in evening orbits. The average dynamic range

of VH and VV backscatter intensity values was 4.1 and 3.9 dB in ascending orbit and 2.9 and 3.4 dB in descending orbit, and the maximum values were 5.9 dB in plots 12 and 22 (ascending) and 3.9, 4.8 dB in plots 7 and 22 (descending).

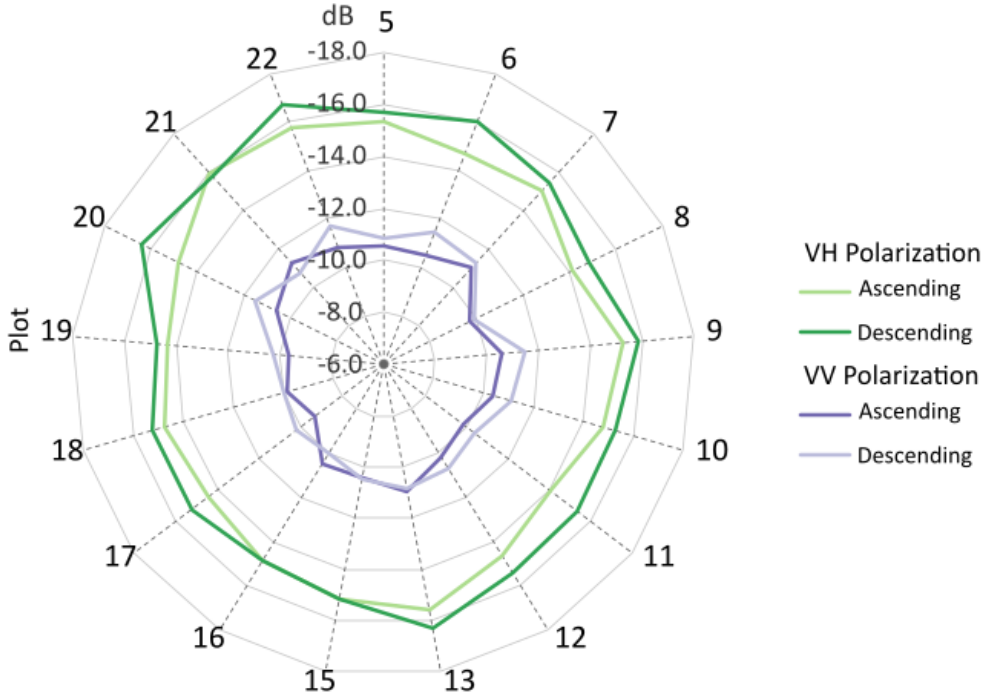

Fig. 26. Average values of intensity per plot during the period considered (2018 – 2021), per polarization and orbit direction.

The evening time series (ascending) show most plots with a decreasing trend over time in both VH and VV polarizations, whereas in the morning time series (descending) most plots show an increasing trend over time. Plots with more pronounced positive trend were 8, 11 and 15 (plot with tallest trees) in morning takes and plots 22, 15, 9 and 7 in evening takes. Plots with more pronounced negative trend were 18, 8, and 7 in ascending orbit and plots 5 and 7 in descending orbit.

SAR intensity time series evaluated by the Theil-Sen slope do not show a marked trend. A statistical summary of trend values in the backscatter coefficient time series in different plots is compiled in Tab 10. Furthermore, the overall patterns of intensity series are irregular and noisy, not showing any cyclic structure over the four-year period considered.

Tab. 10. Statistical summary of Theil-Sen slope values for the time series of the backscatter coefficient.

Orbit	Polarization	Plots		Range			Number of plots according to trend	
		Max Trend	Min Trend	Max	Min	Mean	Positive	Negative
Ascending	VV	22 and 7	16 and 9	12.39	-13.51	-3.05	5	12
	VH	15 and 9	18 and 8	12.62	-16.61	-0.72	8	9
Descending	VV	11 and 8	15 and 6	44.82	-46.59	5.61	11	6
	VH	15 and 11	5 and 13	35.5	-28.19	5.76	8	9

Characterization of Sentinel-1 interferometric coherence time series

Average interferometric coherence in descending orbit and over the entire period ranged between 0.59 (plot 8) and 0.75 (plot 21). All coherence time series had a positive trend and high slope values over time. Calculated with Theil-Sen test these values ranged between 237 (plot 9) and 114.29 (plot 6). The increasing trend of coherence is highest in plots 9, 21, 18 and 7 and lowest in plots 6, 16, 15 and 11.

Coherence time series show a pattern with annual periodicity in all plots, readily identified by visual inspection, complemented with individualized minor traits. Highest values of coherence (0.76 - 0.98) are recorded in September and lowest values (0.16 – 0.35) in January (Figure 6). Fourier analysis demonstrates that, in addition to the annual frequency, most plots have 26-, 17- and 13-week frequency pattern, that is, a cyclicity every six, three and two months. Plots 6 and 18 do not show the 13-week cyclicity and plot 8 lacks the 17-week cyclicity. The amplitude in the Fourier decomposition represents the magnitude of each component function. In our case it shows that the annual periodicity (amplitude 10.72-22.46) is dominant over other less relevant periodicities (Tab. 11). Plot 17, with most number of trees, records the maximum amplitude in the 26-week frequency and plot 22 (maximum volume of biomass) in the 13-week frequency.

Tab. 11. Summary of the Fourier amplitude statistics of coherence time series.

Amplitude				Plot	
Range					
Period	Max	Min	Mean	Max	Min
52	22.46	10.72	17.23	6	21
26	12.35	3.66	7.445	17	13
17	8.27	2.15	4.59	13	11
13	5.11	1.53	2.71	22	9

In most plots mushroom production is triggered when coherence drops drastically (Fig. 27). A majority of plots start producing ectomycorrhizal sporocarps four weeks after a maximum value of coherence change towards lower values (local minimum in the derivative values). Some exceptions are plots 20, 16, and 17 which ectomycorrhizal production starts a few weeks after the maximum change in coherence.

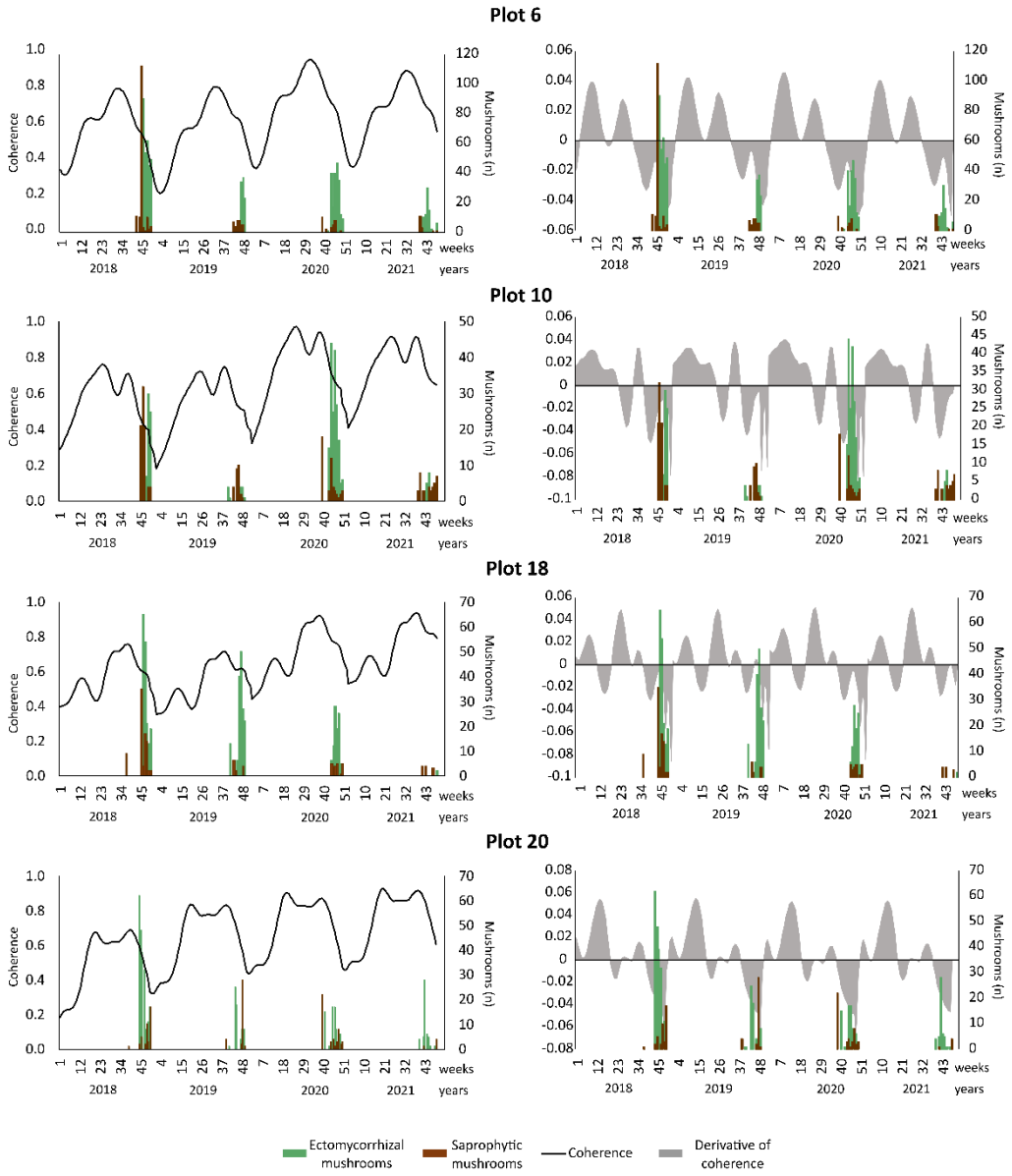

Fig. 27. Examples of time series patterns of coherence in mushroom productive plots and mushroom production. Left: interferometric coherence; right: temporal derivative of interferometric coherence.

Statistical relationship between SAR and precipitation time series

Our analysis of cross correlation between precipitation and SAR features time series shows there is a significant (> 95% confidence interval) relationship between precipitation and backscatter intensity in both VH and VV polarizations, with zero delay in the ascending orbit (Fig. 28a and 28b) and a 2–3-week delay in the descending orbit (Fig. 28c and 28d). Precipitation and interferometric coherence are not immediately cross-correlated in these forests (Fig. 29).

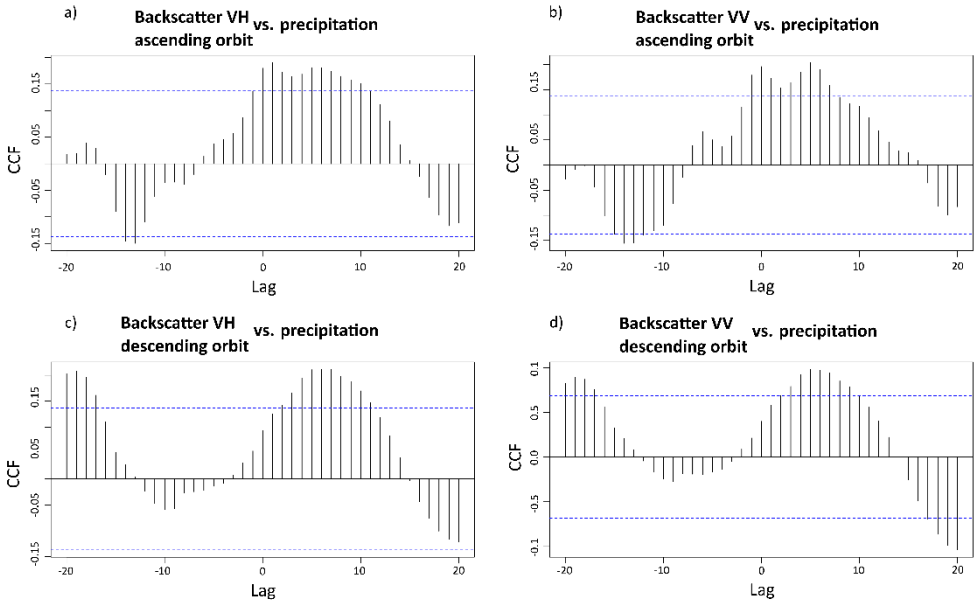

Fig. 28. Cross-correlation between backscatter intensity and precipitation. Weekly lags between both series are represented in the X axis. Y-values represent Pearson coefficients. Blue dotted lines mark the 0.95 confidence interval.

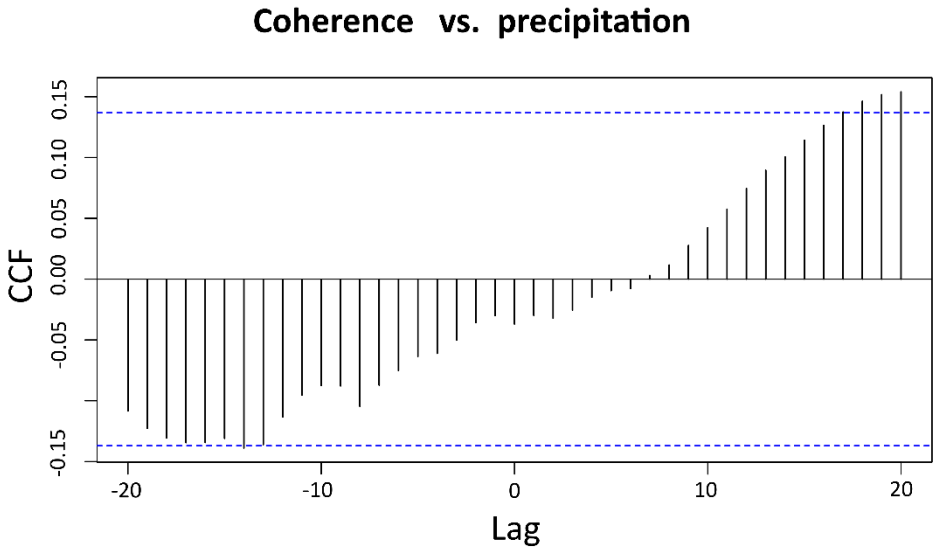

Fig. 29. Cross-correlation between interferometric coherence and precipitation. Weekly lags between both series are represented in the X axis. Y-values represent Pearson coefficients. Blue dotted lines mark the 0.95 confidence interval.

DISCUSSION

Wild mushroom production is directly related with forest structure (Tomao et al., 2017) as well as with climate and terrain characteristics. Of these three factors, only forest structure may be configured with management, by addressing species composition and basal area (Collado et al., 2020). ALS-based forest inventory was recently proposed as part of a tactical forest planning based on clustered silvicultural treatments to promote mushroom yields (Pascual and de-Miguel, 2022). The ALS-based inventory could be further enhanced by remotely sensed data from the ESA's Copernicus programme, increasing the spatial resolution and the revisit time of inventories.

SAR data may be used alone for characterization of forest structure at the stand level (e.g., Gómez et al., 2021), but it may produce synergies with optical data (e.g., Li et al., 2022), and even be advantageous under persistently cloudy circumstances. Although backscatter intensity is more frequently employed, interferometric approaches provide further opportunities, by exploiting the phase difference and the scene coherence between various data acquisitions. Therefore, Sentinel-1 interferometric coherence is increasingly being explored for a range of purposes (e.g., Abdel-Hamid et al., 2021 for monitoring grasslands, Ohki et al., 2020 for landslide detection) leveraged by the accessibility to data. The short temporal-pass enabled by Sentinel-1 constellation has been identified as a key factor for improving estimations of forest biomass and volume (Cartus et al., 2022), and for monitoring change and deforestation (Mastro et al., 2022) when using time series of Sentinel-1 coherence. The advantage of short temporal-pass in time series of coherence has been also highlighted by Seppi et al., (2022) working with L-band SAOCOM-1 in Argentinian forests. Our work with 6-day pass of Sentinel-1 time series contributes to this novel body of research with an effort to describe wild mushroom productive plots and with a further aim to enable modelling of production.

In this work, four years of weekly time series from Sentinel-1 were retrieved from areas corresponding with mushroom naturally productive plots in dry pines of Spain. Time series of backscatter intensity in both VH and VV polarizations, as well as VV interferometric coherence were built to characterize seasonal patterns of variation and to relate those patterns with weekly wild mushroom harvests from field surveys. The SAR time-series features triggering autumn mushroom productivity in different plots were described.

Our results indicate that the intensity of backscatter is highly influenced by the variability of precipitation. Since precipitation triggers the mushroom production (Ágreda et al., 2015), backscatter intensity, and VH polarization values in particular, would seem useful for the assessment of this non-wood forest resource. However, in sparse and short forests like ours in Spain, the C-band radar signal reaches the ground, strongly influencing the backscatter intensity. Therefore, the backscatter time series become noisy and lose power to be considered as a predictor of mushroom yields.

High correlations were found between time-averaged values of coherence and mean plot height (R = 0.70), mean tree diameter (R = 0.67), plot volume (R = 0.57) and number of trees (R = 0.56) confirming that coherence is a good descriptor of forest stand structure. The relationship between interferometric coherence and mushroom

production is stronger for ectomycorrhizal than for saprotrophic mushrooms (R = 0.47 versus R = -0.17). In mycorrhizal species, the production of sporocarps (mushrooms) rely mostly on resources from carbon supplied by the host tree (Büntgen et al., 2011), whereas saprotrophic species acquire carbon from processes of decomposition closely linked to soil moisture and temperature (Rousk and Bååth, 2011). By being more connected to the condition of the forest stand, mycorrhizal species production can more effectively be assessed with SAR data than saprotrophic ones.

Time series of interferometric coherence measured with a 6-day interval in this forest scene are relatively stable, not influenced by punctual rainfall and only varying with more persistent changes in the local conditions. Therefore, coherence time-series could be a potential indicator of triggering drivers in mushroom production. The dynamic range over time of coherence values become key to exploit the predicting capacity of the time series. A larger range of coherence indicates that there are more transitional variations in the stand, produced by environmental factors like frost, persistent wind and accumulated rainfall, that change forest condition. These types of disturbances would also change forest NDVI driving the annual spectrophenological patterns (Gómez et al., 2020). In this sense, Bai et al., (2020) demonstrated the correlation between coherence amplitude and NDVI time series in monsoon forests of China, and Villarroya-Carpio et al., (2022) in agricultural crops of Spain. In our study area, mushroom production is directly linked with forest primary productivity as portrayed by NDVI temporal curves (Olano et al., 2020). The relationship between NDVI and interferometric coherence time series locally should be explored in future work to get further insights of the potential and synergies of both parameters as indicators of the time when fungal fruiting is triggered. Through a simple exercise relating the temporal derivative of coherence time series and time of mushroom start of season, we observed that when changes occur in the forest stand, whether due to autumn instability by rainfall or wind, the strongest decrease in coherence anticipates mushroom production, which occurs 4-6 weeks later.

The accessibility to Analysis Ready Format data facilitates complex analysis (Zhu, 2019) for countless applications. We accessed interferometric coherence from ASF, releasing the complexity of SAR data processing, but at the same time precluding analysis of non-standardly processed VV coherence. Other sources of interferometric coherence evaluated globally (Kellndorfer et al., 2022) enable the potential characterization of forest structure for further applications. Furthermore, self-processing of data provides flexibility in the parametrization and preparation of the data, opening options to explore combinations of indices (e.g., Villaroya-Carpio et al., 2023) that may be complementary in the explanation of vegetation temporal behaviour. The overall availability and free access to remotely sensed data of high spatial and temporal resolution make it of utmost interest to contribute to the characterisation of ecosystems. There is opportunity to contribute to the sustainable, efficient, and effective management of ecosystem functions, like predicting and quantifying wild mushroom yields.

CONCLUSIONS

SAR data open a beneficial avenue for the estimation and prediction of mushroom production in Mediterranean forests. Although time series of backscatter intensity is strongly correlated with precipitation and make noisy signals difficult to interpret, time series of interference coherence may constitute an indicator of triggering factors in mushroom production. It is desirable to incorporate more field data and different forest conditions, as well as alternative SAR-based techniques in future works to get further insights and develop efficient tools for the sustainable management of these non-wood forest products.

Conclusiones

Conclusiones

En este apartado se enumeran las conclusiones que derivan de cada uno de los capítulos que se han desarrollado en esta tesis doctoral:

1. La combinación de datos procedentes de sensores remotos con datos meteo-climáticos mejora la capacidad para modelizar la predicción de la producción de setas silvestres en los bosques mediterráneos.

2. La combinación de datos procedentes de sensores activos y de sensores pasivos es relevante para la evaluación de la productividad de setas en los bosques mediterráneos de Pinus pinaster.

3. El análisis estadístico avanzado con modelos mixtos aditivos generalizados (GAMM) refleja las complejas relaciones entre la productividad primaria forestal (calculada mediante series NDVI de Landsat), los parámetros estructurales de la masa (calculados a partir de datos de TLS) y las variables meteo-climáticas para la producción de setas silvestres en bosques mediterráneos.

4. Los factores más relevantes que desencadenan la producción de setas silvestres en bosques mediterráneos son la precipitación acumulada de otoño y la interacción entre el volumen de biomasa (estructura) con la productividad primaria (vigor).

5. Las series temporales de datos SAR muestran patrones de cambio relacionados con el momento de fructificación de las setas silvestres. Las series temporales de coherencia interferométrica son elementos útiles para construir indicadores de los factores desencadenantes de la producción de setas silvestres.

6. Incorporar el análisis de datos incluyendo las imágenes SAR en futuros trabajos será clave para obtener más información y desarrollar mejores y más eficientes herramientas que apoyen la gestión de las setas silvestres en los bosques mediterráneos.

7. La combinación de datos procedentes de la teledetección con datos meteo-climáticos abre el camino para enfrentar el desafío de predecir las cosechas de setas silvestres, y, por lo tanto, los rendimientos de este recurso con alta resolución espacial y temporal.

8. La capacidad de la teledetección para mejorar los modelos de producción de setas silvestres ofrece oportunidades relevantes para la inclusión de estos PFNM en los planes de gestión sostenible de los bosques.

Referencias

Referencias

Abdel-Hamid, A., Dubovyk, O., and Greve, K. 2021. The potential of sentinel-1 InSAR coherence for grasslands monitoring in Eastern Cape, South Africa. *International Journal of Applied Earth Observation and Geoinformation*, 98, 102306. https://doi.org/10.1016/j.jag.2021.102306

Abou-Shaara, H.F., Eid, K.S.A., 2019. Increasing the profitability of propolis production in honeybee colonies by utilizing remote sensing techniques to spot locations of trees as potential sources of resin. *Remote Sensing* Letters 10, 922–927. https://doi.org/10.1080/2150704X.2019.1633488

Ágreda, T., Águeda, B., Fernández-Toirán, M., Vicente-Serrano, S.M. and Òlano, J.M., 2016. Long-term monitoring reveals a highly structured interspecific variability in climatic control of sporocarp production. *Agricultural and Forest Meteorology* 223, 39–47. https://doi.org/10.1016/j.agrformet.2016.03.015

Ágreda, T., Águeda, B., Olano, J.M., Vicente-Serrano, S.M. and Fernández-Toirán, M., 2015. Increased evapotranspiration demand in a Mediterranean climate might cause a decline in fungal yields under global warming. *Global Change Biology* 21. https://doi.org/10.1111/gcb.12960

Ágreda, T., Cisneros, Ó., Águeda, B., and Fernández-Toirán, L. M, 2013. Age class influence on the yield of edible fungi in a managed Mediterranean forest. *Mycorrhiza*. https://doi.org/10.1007/s00572-013-0522-y

Águeda, B., Parladé, J., de Miguel, A.M. and Martínez-Peña, F., 2006. Characterization and identification of field ectomycorrhizae of Boletus edulis and Cistus ladanifer. *Mycologia* 98, 23–30. https://doi.org/10.1080/15572536.2006.11832709

Aho, K., Derryberry, D. and Peterson, T., 2014. Model selection for ecologists: the worldviews of AIC and BIC. *Ecology*. https://doi.org/10.1890/13-1452.1.

Ahmed, R., Siqueira, P., Hensley, S., Chapman, B., Bergen, K., 2011. A survey of temporal decorrelation from spaceborne L-Band repeat-pass InSAR. *Remote Sensing of Environment* 115, 2887–2896. https://doi.org/10.1016/j.rse.2010.03.017

Akaike, H. 1998. Information Theory and an Extension of the Maximum Likelihood Principle. In E. Parzen, K. Tanabe, and G. Kitagawa (Eds.), *Selected Papers of Hirotugu Akaike* (pp. 199–213). Springer New York. https://doi.org/10.1007/978-1-4612-1694-0_15

Åkerblom, M., and Kaitaniemi, P. 2021. Terrestrial laser scanning: A new standard of forest measuring and modelling ? *Annals of Botany*, 128, 653–661.

Alcamo, J., Ash, N.J., Butler, C.D., Callicott, J.B., Capistrano, D., Carpenter, S.R., Castilla, J.C., Chambers, R., Chopra, K., Cropper, A., Daily, G.C., Dasgupta, P., de Groot, R., Dietz, T., Duraiappah, A.K., Gadgil, M., Hamilton, K., Bennett, E.M., Hassan, R., Lambin, E.F., Lebel, L., Leemans, R., Jiyuan, L., Malingreau, J.-P., May, R.M., McCalla, A.F., Reid, W.V., Sarukhán, J., Whyte, A., Gallopin, G., Kasperson, R., Munasinghe, M., Olivé, L., Padoch, C., Romm, J.,y Vessuri, H., 2003. Ecosistemas y Bienestar Humano: Marco para la Evaluación. Informe del Grupo de Trabajo sobre Marco Conceptual de la Evaluación de Ecosistemas del Milenio. *World Resources Institute*.

Alday, J.G., Bonet, J.A., Oria-de-Rueda, J.A., Martínez-de-Aragón, J., Aldea, J., Martín-Pinto, P., de-Miguel, S., Hernández-Rodríguez, M., and Martínez-Peña, F., 2017a. Record breaking mushroom yields in Spain. *Fungal Ecology* 26, 144–146. https://doi.org/10.1016/j.funeco.2017.01.004

Alday, J.G., Martínez De Aragón, J., De-Miguel, S., and Bonet, J.A., 2017b. Mushroom biomass and diversity are driven by different spatio-Temporal scales along Mediterranean elevation gradients. *Scientific Reports* 7. https://doi.org/10.1038/srep45824

Al-hamed, T., Shiyab, S.M., and Al-Bakri, J., 2022. Morpho-physiological Effects of Drought on Medicinal Plants and the Potential Use of Remote Sensing - A Review. *Jordan Journal of Earth and Environmental Sciences* 13 (2), 105-113

Allen, M., 1991. The Ecology of Mycorrhizae. *Cambrigde University Press*.

Alonso Ponce, R., Águeda, B., Ágreda, T., Modrego, M. P., Aldea, J., Fernández-toirán, L. M., and Martínez-peña, F. 2011. Rockroses and Boletus edulis ectomycorrhizal association: Realized niche and climatic suitability in Spain. *Fungal Ecology*, 4(3), 224–232. https://doi.org/10.1016/j.funeco.2010.10.002

Álvarez-Martínez, J.M., Jiménez-Alfaro, B., Barquín, J., Ondiviela, B., Recio, M., Silió-Calzada, A., and Juanes, J.A., 2017. Modelling the area of occupancy of habitat types with remote sensing. *Methods in Ecology and Evolution* 9, 580–593. https://doi.org/10.1111/2041-210X.12925

Altelarrea, J. M., Blázquez-Casado, A., Gómez, C., Martínez, D., y Tejero, J. 2022. Smartbasket: Ciencia ciudadana para la evaluación del recurso micológico en España. *8CFE*, Lleida, Cataluña, España.

Andrew, C., Heegaard, E., Høiland, K., Senn-Irlet, B., Kuyper, T.W., Krisai-Greilhuber, I., Kirk, P.M., Heilmann-Clausen, J., Gange, A.C., Egli, S., Bässler, C., Büntgen, U., Boddy, L., and Kauserud, H., 2018. Explaining European fungal fruiting phenology with climate variability. *Ecology* 99, 1306–1315. https://doi.org/10.1002/ecy.2237.

Andrew, C., Büntgen, U., Egli, S., Senn-Irlet, B., Grytnes, J.A., Heilmann-Clausen, J., Boddy, L., Bässler, C., Gange, A.C., Heegaard, E., Høiland, K., Kirk, P.M., KrisaiGreilhüber, I., Kuyper, T.W., and Kauserud, H., 2019. Open- source data reveal how collections- based fungal diversity is sensitive to global change. *Appl. Plant Sci.* 7, e1227. https://doi.org/10.1002/aps3.1227.

Anthony, M. A., Crowther, T. W., van der Linde, S., Suz, L. M., Bidartondo, M. I., Cox, F., Schaub, M., Rautio, P., Ferretti, M., Vesterdal, L., De Vos, B., Dettwiler, M., Eickenscheidt, N., Schmitz, A., Meesenburg, H., Andreae, H., Jacob, F., Dietrich, H.-P., Waldner, P., … Averill, C. (2022). Forest tree growth is linked to mycorrhizal fungal composition and function across Europe. *The ISME Journal*, 16(5), 1327–1336. https://doi.org/10.1038/s41396-021-01159-7

Arzac, A., Babushkina, E.A., Fonti, P., Slobodchikova, V., Sviderskaya, I.V., and Vaganov, E.A., 2018a. Evidences of wider latewood in Pinus sylvestris from a forest-steppe of Southern Siberia. *Dendrochronologia* 49, 1–8. https://doi.org/10.1016/j.dendro. 2018.02.007.

Arzac, A., Rozas, V., Rozenberg, P., and Olano, J.M., 2018b. Water availability controls Pinus pinaster xylem growth and density: a multi-proxy approach along its environmental range. *Agric. For. Meteorol.* 250–251, 171–180. https://doi.org/10.1016/j.agrformet.2017.12.257.

Assal, T.J., Steen, V.A., Caltrider, T., Cundy, T., Stewart, C., Manning, N., and Anderson, P.J., 2021. Monitoring long-term riparian vegetation trends to inform local habitat management in a mountainous environment. *Ecological Indicators* 127, 107807. https://doi.org/10.1016/j.ecolind.2021.107807

Aubard, V., Paulo, J.A., and Silva, J.M.N., 2019. Long-Term Monitoring of Cork and Holm Oak Stands Productivity in Portugal with Landsat Imagery. *Remote Sensing* 11, 525. https://doi.org/10.3390/rs11050525

Bai, Z., Fang, S., Gao, J., Zhang, Y., Jin, G., Wang, S., Zhu, Y., and Xu, J. 2020. Could Vegetation Index be Derive from Synthetic Aperture Radar? – The Linear Relationship between Interferometric Coherence and NDVI. *Scientific Reports*, 10(1), 6749. https://doi.org/10.1038/s41598-020-63560-0

Ballère, M., Bouvet, A., Mermoz, S., Toan, T. L., Koleck, T., Bedeau, C., André, M., Forestier, E., Frison, P.-L., and Lardeux, C. 2021. SAR data for tropical forest disturbance alerts in French Guiana: Benefit over optical imagery. *Remote Sensing of Environment*, 252, 112159. https://doi.org/10.1016/j.rse.2020.112159

Barrett, F., McRoberts, R.E., Tomppo, E., Cienciala, E., and Waser, L.T., 2016. A questionnaire-based review of the operational use of remotely sensed data by national forest inventories. *Remote Sens. Environ*. https://doi.org/10.1016/j.rse.2015.08. 029.

Barrett, B.W., Dwyer, E., and Whelan, P., 2009. Soil moisture retrieval from active spaceborne microwave observations: An evaluation of current techniques. *Remote Sensing* 1, 210–242. https://doi.org/10.3390/rs1030210

Banskota, A., Kayastha, N., Falkowski, M. J., Wulder, M. A., Froese, R. E., and White, J. C. 2014. Forest Monitoring Using Landsat Time Series Data: A Review. *Canadian Journal of Remote Sensing*, 40(5), 362–384. https://doi.org/10.1080/07038992.2014.987376

Barton, K., 2009. Mu-MIn: multi-model inference. R Package Version 0.12.2/r18.

Beland, M., Sparrow, B., Harding, D., Chasmer, L., Phinn, S., Antonarakis, A., and Strahler, A. 2019. On promoting the use of lidar systems in forest ecosystem research. *Forest Ecology and Management* 450 https://doi.org/10.1016/j.foreco.2019.117484

Bengoa, J.L., Blanco Medina, V., and Nafría García, D.A., 2017. Clasificación semiautomática de cubiertas naturales arboladas en Castilla y León. Presented at the *7o Congreso Forestal* Español., Plasencia, Cáceres, España.

Biber, P., Seifert, S., Zaplata, M. K., Schaaf, W., Pretzsch, H., and Fischer, A. 2013. Relationships between substrate, surface characteristics, and vegetation in an initial ecosystem. *Biogeosciences*, 10(12), 8283–8303. https://doi.org/10.5194/bg-10-8283-2013

Birky, A.K., 2001. NDVI and a simple model of deciduous forest seasonal dynamics. *Ecol. Modell.* 143, 43–58. https://doi.org/10.1016/S0304-3800(01)00354-4.

Bhagat, V., 2017. Space-borne Active Microwave Remote Sensing of Soil Moisture: A Review. *Remote Sensing of Land* 1, 53–86. https://doi.org/10.21523/gcj1.17010104

Blaschke, T., Hay, G.J., Weng, Q., and Resch, B., 2011. Collective Sensing: Integrating Geospatial Technologies to Understand Urban Systems—An Overview. *Remote Sensing* 3, 1743–1776. https://doi.org/10.3390/rs3081743

Blázquez-Casado, Á., Calama, R., Valbuena, M., Vergarechea, M., and Rodríguez, F., 2019. Combining low-density LiDAR and satellite images to discriminate species in mixed Mediterranean forest. *Annals of Forest Science* 76, 57. https://doi.org/10.1007/s13595-019-0835-x

Boa, E.R., 2004. Wild edible fungi: a global overview of their use and importance to people, Non-wood forest products. *Food and Agriculture Organization of the United Nations*, Rome.

Bonet, J. A., de-Miguel, S., Martínez de Aragón, J., Pukkala, T., and Palahí, M. 2012. Immediate effect of thinning on the yield of Lactarius group deliciosus in Pinus pinaster forests in Northeastern Spain. *Forest Ecology and Management*, 265, 211–217. https://doi.org/10.1016/j.foreco.2011.10.039

Bonet, J.A., Palahí, M., Colinas, C., Pukkala, T., Fischer, C.R., Miina, J., and Martínez de Aragón, J., 2010. Modelling the production and species richness of wild mushrooms in pine forests of the Central Pyrenees in northeastern Spain. *Canadian Journal of Forest Research* 40, 347–356. https://doi.org/10.1139/X09-198

Bonet, J.A., Pukkala, T., Fischer, C.R., Palahí, M., Aragón, J.M.D., and Colinas, C., 2008. Empirical models for predicting the production of wild mushrooms in Scots pine (Pinus sylvestris L.) forests in the Central Pyrenees. *Annals of Forest Science* 65. https://doi.org/10.1051/forest:2007089

Borlaf-Mena, I., Badea, O., and Tanase, M. A. 2021. Assessing the Utility of Sentinel-1 Coherence Time Series for Temperate and Tropical Forest Mapping. *Remote Sensing*, 13(23), 4814. https://doi.org/10.3390/rs13234814

Bouslihim, Y., Kharrou, M.H., Miftah, A., Attou, T., Bouchaou, L., and Chehbouni, A., 2022. Comparing Pan-sharpened Landsat-9 and Sentinel-2 for Land-Use Classification Using Machine Learning Classifiers. *J geovis spat anal* 6, 35. https://doi.org/10.1007/s41651-022-00130-0

Brigham, E. O. (1988). The fast Fourier transform and its applications. Prentice Hall.

Brenko, A., Buršić, D., Zgrablić, Ž., and Martinez de Arano, I., 2018. A Road Map for innovating NWFPs value chains for the Mushrooms and Truffles iNet. *Conclusions issued from the Scoping seminar – 19 and 20 June 2018 of the Innovation Networks of Cork*, Resins and Edibles in the Mediterranean basin project. Incredible.

Brockwell, P. J., and Davis, R. A. 2016. Introduction to Time Series and Forecasting. *Springer International Publishing*. https://doi.org/10.1007/978-3-319-29854-2

Brown, S. C. M., Quegan, S., Morrison, K., Bennett, J. C., and Cookmartin, G. 2003. High-resolution measurements of scattering in wheat canopies-implications for crop parameter retrieval. *IEEE Transactions on Geoscience and Remote Sensing*, 41(7), 1602–1610. https://doi.org/10.1109/TGRS.2003.814132

Büntgen, U., Kauserud, H., and Egli, S., 2012. Linking climate variability to mushroom productivity and phenology. *Front. Ecol. Environ*. 10, 14–19. https://doi.org/10.1890/ 110064.

Büntgen, U., Tegel, W., Egli, S., Stobbe, U., Sproll, L., & Stenseth, N. C., 2011. Truffles and climate change. *Frontiers in Ecology and the Environment*, 9(3), 150–151. https://doi.org/10.1890/11.WB.004

Cabo, C., Ordóñez, C., López-Sánchez, C.A., and Armesto, J., 2018. Automatic dendrometry: Tree detection, tree height and diameter estimation using terrestrial laser scanning. *International Journal of Applied Earth Observation and Geoinformation* 69, 164–174. https://doi.org/10.1016/j.jag.2018.01.011

Calama, R., Tomé, M., Sánchez-González, M., Miina, J., Spanos, K., and Palahí, M. 2010. Modelling Non-Wood Forest Products in Europe: A review Introduction: Importance. *Forest Systems*, 19, 69–85. https://doi.org/10.5424/fs/201019S-9324

Campbell, J.B., and Wynne, R.H., 2011. Introduction to Remote Sensing. *The guilford Press*, New York, NY - London.

Cartus, O. and Santoro, M., 2019. Exploring combinations of multi-temporal and multi-frequency radar backscatter observations to estimate above-ground biomass of tropical forest. *Remote Sensing of Environment* 232, 111313. https://doi.org/10.1016/j.rse.2019.111313

Cartus, O., Santoro, M., Wegmuller, U., Labriere, N. and Chave, J., 2022. Sentinel-1 Coherence for Mapping Above-Ground Biomass in Semiarid Forest Areas. *IEEE Geosci. Remote Sensing Lett*. 19, 1–5. https://doi.org/10.1109/LGRS.2021.3071949

Caudullo, G., Welk, E., and San-Miguel-Ayanz, J. 2017. Chorological maps for the main European woody species. *Data in Brief*, 12, 662–666. https://doi.org/10.1016/J.DIB.2017.05.007

Chaudhary, V., and Kumar, S., 2020. Marine oil slicks detection using spaceborne and airborne SAR data. *Advances in Space Research* 66, 854–872. https://doi.org/10.1016/j.asr.2020.05.003

Cheek, M., Nic Lughadha, E., Kirk, P., Lindon, H., Carretero, J., Looney, B., Douglas, B., Haelewaters, D., Gaya, E., Llewellyn, T., Ainsworth, A.M., Gafforov, Y., Hyde, K., Crous, P., Hughes, M., Walker, B.E., Campostrini Forzza, R., Wong, K.M., and Niskanen, T., 2020. New scientific discoveries: Plants and fungi. *Plants People Planet* 2, 371–388. https://doi.org/10.1002/ppp3.10148

Chervenkov, H., and Slavov, K. 2019. Theil–Sen Estimator vs. Ordinary Least Squares—Trend Analysis for Selected ETCCDI Climate Indices. 'Prof. Marin Drinov' *Publishing House of Bulgarian Academy of Sciences*. https://doi.org/10.7546/CRABS.2019.01.06

Chuvieco, E., 2010. Teledetección ambiental: La observación de la Tierra desde el espacio. *Ariel Ciencia*.

Cisneros-Araujo, P., Goicolea, T., Mateo-Sánchez, M.C., García-Viñás, J.I., Marchamalo, M., Mercier, A., and Gastón, A., 2021. The Role of Remote Sensing Data in Habitat Suitability and Connectivity Modeling: Insights from the Cantabrian Brown Bear. *Remote Sensing* 13, 1138. https://doi.org/10.3390/rs13061138

Cleveland, R. B., Cleveland, W. S., McRae, J. E., and Terpenning, I. 1990. STL: A Seasonal-Trend decomposition procedure based on loess. *Official Statistics*, 6(1), 3–73.

Cockle, K. L., Martin, K., and Robledo, G. 2012. Linking fungi, trees, and hole-using birds in a Neotropical tree-cavity network: Pathways of cavity production and implications for conservation. *Forest Ecology and Management*, 264, 210–219. https://doi.org/10.1016/J.FORECO.2011.10.015

Cohen, W.B., and Goward, S.N., 2004. Landsat's Role in Ecological Applications of Remote Sensing. *BioScience* 54, 535. https://doi.org/10.1641/0006-3568(2004)054[0535:LRIEAO]2.0.CO;2

Collado, E., Bonet, J.A., Camarero, J.J., Egli, S., Peter, M., Salo, K., Martínez-Peña, F., Ohenoja, E., Martín-Pinto, P., Primicia, I., Büntgen, U., Kurttila, M., Oria-de-Rueda, J.A., Martínez-de-Aragón, J., Miina, J., and de-Miguel, S., 2019. Mushroom productivity trends in relation to tree growth and climate across different European forest biomes. *Sci. Total Environ*. 689, 602–615. https://doi.org/10.1016/j.scitotenv.2019.06.471.

Collado, E., Bonet, J. A., Alday, J. G., Martínez de Aragón, J., and de-Miguel, S. 2021. Impact of forest thinning on aboveground macrofungal community composition and diversity in Mediterranean pine stands. *Ecological Indicators*, 133, 108340. https://doi.org/10.1016/J.ECOLIND.2021.108340

Collado, E., Castaño, C., Bonet, J. A., Hagenbo, A., Martínez de Aragón, J., and de-Miguel, S. 2020. Divergent above- and below-ground responses of fungal functional groups to forest thinning. *Soil Biology and Biochemistry*, 150, 108010. https://doi.org/10.1016/j.soilbio.2020.108010

Correction: Stop neglecting fungi, 2017. *Nat Microbiol* 2, 17123. https://doi.org/10.1038/nmicrobiol.2017.123

Costanza, R., d'Arge, R., de Groot, R., Farber, S., Grasso, M., Hannon, B., Limburg, K., Naeem, S., O'Neill, R.V., Paruelo, J., Raskin, R.G., Sutton, P., and van den Belt, M., 1997. The value of the world's ecosystem services and natural capital. *Nature* 387, 253–260. https://doi.org/10.1038/387253a0

CREAF, 2016. ¿Qué son los servicios ecosistémicos? - Blog CREAF. URL https://blog.creaf.cat/es/conocimiento/que-son-los-servicios-ecosistemicos/

Croitoru, L. 2007. Valuing the non-timber forest products in the Mediterranean region. *Ecological Economics*, 63(4), 768–775. https://doi.org/10.1016/J.ECOLECON.2007.01.014

Daily, G.C. (ed.), 1997. Nature's services. Societal dependence on natural ecosystems. *Island Press*, Washington, DC.

Dasari, K., Anjaneyulu, L., and Nadimikeri, J., 2022. Application of C-band sentinel-1A SAR data as proxies for detecting oil spills of Chennai, East Coast of India. *Marine Pollution Bulletin* 174, 113182. https://doi.org/10.1016/j.marpolbul.2021.113182

Dassot, M., Constant, T., and Fournier, M. 2011. The use of terrestrial LiDAR technology in forest science: Application fields, benefits and challenges. *Annals of Forest Science*, 68(5), 959–974. https://doi.org/10.1007/s13595-011-0102-2

de-Miguel, S., Bonet, J.A., Pukkala, T., and Martínez de Aragón, J., 2014. Impact of forest management intensity on landscape-level mushroom productivity: A regional model-based scenario analysis. *Forest Ecology and Management* 330, 218–227. https://doi.org/10.1016/j.foreco.2014.07.014

Devkota, S., Fang, W., Arunachalam, K., Phyo, K.M.M., and Shakya, B., 2023. Systematic review of fungi, their diversity and role in ecosystem services from the Far Eastern Himalayan Landscape (FHL). *Heliyon* 9, e12756. https://doi.org/10.1016/j.heliyon.2022.e12756

Disney, M., Burt, A., Calders, K., Schaaf, C., and Stovall, A., 2019. Innovations in Ground and Airborne Technologies as Reference and for Training and Validation: Terrestrial Laser Scanning (TLS). *Surv Geophys* 40, 937–958. https://doi.org/10.1007/s10712-019-09527-x

Domingo, D., Montealegre, A.L., Lamelas, M.T., García-Martín, A., de la Riva, J., Rodríguez, F., and Alonso, R., 2019. Quantifying forest residual biomass in Pinus halepensis Miller stands using Airborne Laser Scanning data. *GIScience and Remote Sensing* 56, 1210–1232. https://doi.org/10.1080/15481603.2019.1641653

Dorigo, W., Wagner, W., Albergel, C., Albrecht, F., Balsamo, G., Brocca, L., Chung, D., Ertl, M., Forkel, M., Gruber, A., Haas, E., Hamer, P., Hirschi, M., Ikonen, J., de Jeu, R., Kidd, R., and Lahoz, W., 2017. ESA CCI Soil Moisture for improved Earth system understanding: state-of-the art and future directions. *Remote Sensing of Environment*, submitted. https://doi.org/10.1016/j.rse.2017.07.001

Dorigo, W.A., Xaver, A., Vreugdenhil, M., Gruber, A., Hegyiová, A., Sanchis-Dufau, A.D., Zamojski, D., Cordes, C., Wagner, W., and Drusch, M., 2013. Global automated quality control of in situ soil moisture data from the International Soil Moisture Network. *Vadose Zone* J. 12. https://doi.org/10.2136/vzj2012.0097.

Dormann, C. F., Elith, J., Bacher, S., Buchmann, C., Carl, G., Carr, G., Garc, J. R., Gruber, B., Lafourcade, B., Leit, P. J., Tamara, M., Mcclean, C., Osborne, P. E., Der, B. S., Skidmore, A. K., Zurell, D., and Lautenbach, S. 2013. Collinearity: A review of methods to deal with it and a simulation study evaluating their performance. *Ecography*, 36, 27–46. https://doi.org/10.1111/j.1600-0587.2012.07348.x

Dostálová, A., Wagner, W., Milenković, M., and Hollaus, M., 2018. Annual seasonality in Sentinel-1 signal for forest mapping and forest type classification. *International Journal of Remote Sensing* 39, 7738–7760. https://doi.org/10.1080/01431161.2018.1479788

Dubayah, R.O., and Drake, J.B., 2000. Lidar Remote Sensing for Forestry Applications. *Journal of Forestry* 98, 44–46.

Dubois, C., Mueller, M. M., Pathe, C., Jagdhuber, T., Cremer, F., Thiel, C., and Schmullius, C. 2020. Characterization of land cover seasonality in Sentinel-1 time series data. ISPRS Annals of the Photogrammetry, *Remote Sensing and Spatial Information Sciences*, V-3–2020, 97–104. https://doi.org/10.5194/isprs-annals-V-3-2020-97-2020

Egli, S., 2011. Mycorrhizal mushroom diversity and productivity—an indicator of forest health? *Annals of Forest Science* 68, 81–88. https://doi.org/10.1007/s13595-010-0009-3

Egli, S., Peter, M., Buser, C., Stahel, W., and Ayer, F., 2006. Mushroom picking does not impair future harvests - results of a long-term study in Switzerland. *Biol. Conserv*. 129, 271–276. https://doi.org/10.1016/j.biocon.2005.10.042.

Ehrlich, P.R., and Ehrlich, A.H., 1981. Extinction: the causes and consequences of the disappearance of species. *Random House*, New York.

Eitel, J. U. H., Griffin, K. L., Boelman, N. T., Maguire, A. J., Meddens, A. J. H., Jensen, J., Vierling, L. A., Schmiege, S. C., and Jennewein, J. S. 2020. Remote sensing tracks daily radial wood growth of evergreen needleleaf trees. *Global Change Biology*, 26(7), 4068–4078. https://doi.org/10.1111/gcb.15112

Entekhabi, D., Rodriguez-Iturbe, I., and Castelli, F., 1996. Mutual interaction of soil moisture state and atmospheric processes. *J. Hydrol.* 184, 3–17. https://doi.org/10.1016/ 0022-1694(95)02965-6.

Erlandsson, R., Arneberg, M. K., Tømmervik, H., Finne, E. A., Nilsen, L., and Bjerke, J. W. 2023. Feasibility of active handheld NDVI sensors for monitoring lichen ground cover. *Fungal Ecology*, 63, 101233. https://doi.org/10.1016/j.funeco.2023.101233

ESA - Copernicus, 2014. Copernicus Open Acess Hub [https://scihub.copernicus.eu/].

ESA, 2023. El programa Copérnico [WWW Document]. URL https://www.esa.int/Space_in_Member_States/Spain/El_programa_Copernico

ESA-SENTINEL-1, 2023. Sentinel-1 - Missions - Sentinel Online - Sentinel Online [WWW Document]. URL https://sentinels.copernicus.eu/web/sentinel/missions/sentinel-1

ESA-SENTINEL-2, 2023. Sentinel-2 - Missions - Sentinel Online - Sentinel Online [WWW Document]. URL https://sentinels.copernicus.eu/web/sentinel/missions/sentinel-2

ESA-SENTINEL-3, 2023. Sentinel-3 - Sentinel Online [WWW Document]. URL https://sentinels.copernicus.eu/web/sentinel/missions/sentinel-3

ESA-SENTINEL-4, 2023. Sentinel-4 - Missions - Sentinel Online - Sentinel Online [WWW Document]. URL https://sentinels.copernicus.eu/web/sentinel/missions/sentinel-4

ESA-SENTINEL-5, 2023. Sentinel-5 - Missions - Sentinel Online - Sentinel Online [WWW Document]. URL https://sentinels.copernicus.eu/web/sentinel/missions/sentinel-5

ESA-SENTINEL-5P, 2023. Sentinel-5P - Missions - Sentinel Online - Sentinel Online [WWW Document]. URL https://sentinels.copernicus.eu/web/sentinel/missions/sentinel-5p

ESA-SENTINEL-6, 2023. Sentinel-6 - Sentinel Online [WWW Document]. URL https://sentinels.copernicus.eu/web/sentinel/missions/sentinel-6

Esteban, J., Fernández-Landa, A., Tomé, J.L., Gómez, C., and Marchamalo, M., 2021. Identification of Silvicultural Practices in Mediterranean Forests Integrating Landsat Time Series and a Single Coverage of ALS Data. *Remote Sensing* 13, 3611. https://doi.org/10.3390/rs13183611

Ezzahar, J., Ouaadi, N., Zribi, M., Elfarkh, J., Aouade, G., Khabba, S., Er-Raki, S., Chehbouni, A., and Jarlan, L., 2019. Evaluation of Backscattering Models and Support Vector Machine for the Retrieval of Bare Soil Moisture from Sentinel-1 Data. *Remote Sensing*, 12(1), 72. https://doi.org/10.3390/rs12010072

Fadeev, N.B., Skrypitsyna, T.N., Kurkov, V.M., and Sidelnikov, N.I., 2019. Use of Remote Sensing Data and GIS Technologies for Monitoring Stocks of Medicinal Plants: Problems and Prospects, in: Bychkov, I., Voronin, V. (Eds.), Information Technologies in the Research of Biodiversity. *Springer International Publishing*, Cham, pp. 14–21.

FAO, 2022. El estado de los bosques del mundo 2022. *FAO*, Roma. https://doi.org/10.4060/cb9360es

FAO, 2021. Evaluación de los recursos forestales mundiales 2020. *FAO*. https://doi.org/10.4060/ca9825es

FAO, 1999. Hacia una definición uniforme de los productos forestales no madereros. *Unasylva*.

FAO and Plan Bleu, 2018. State of Mediterranean Forests 2018. *Food and Agriculture Organization of the United Nations*, Rome and Plan Bleu, Marseille.

Fernández-Toirán, L.M., Ágreda, T., and Olano, J.M., 2006. Stand age and sampling year effect on the fungal fruit body community in Pinus pinaster forests in central Spain. *Can. J. Bot*. 84, 1249–1258. https://doi.org/10.1139/B06-087.

Ferretti, A., Prati, C., and Rocca, F., 2000. Nonlinear subsidence rate estimation using permanent scatterers in differential SAR interferometry. *IEEE Transactions on Geoscience and Remote Sensing*, 38(5), 2202–2212. https://doi.org/10.1109/36.868878

Ferro-Famil, L., and Pottier, E., 2016. 1 - Synthetic Aperture Radar Imaging, in: Baghdadi, N., Zribi, M. (Eds.), Microwave *Remote Sensing of Land Surface. Elsevier*, pp. 1–65. https://doi.org/10.1016/B978-1-78548-159-8.50001-3

Filipponi, F., 2019. Sentinel-1 GRD Preprocessing Workflow. 3rd International Electronic Conference on *Remote Sensing*, 11. https://doi.org/10.3390/ECRS-3-06201

Flores-Anderson, A.I., Herndon, K.E., Thapa, R.B., and Cherrington, E (Eds.)., 2019. The SAR Handbook: Comprehensive Methodologies for Forest Monitoring and Biomass Estimation. *NASA*.

Forest Europe, 2015. State of Europe's forests 2015, *Spanish Ministry of Agriculture, Food and the Environment*. ed. Madrid.

Frison, P.-L., Fruneau, B., Kmiha, S., Soudani, K., Dufrêne, E., Toan, T. L., Koleck, T., Villard, L., Mougin, E., and Rudant, J.-P., 2018. Potential of Sentinel-1 Data for Monitoring Temperate Mixed Forest Phenology. *Remote Sensing*, 10(12), 2049. https://doi.org/10.3390/rs10122049

Gates, D.M., Keegan, H.J., Schleter, J.C., and Weidner, V.R., 1965. Spectral Properties of Plants. *Appl. Opt*. 4, 11. https://doi.org/10.1364/AO.4.000011

Gens, R., and Genderen, J. L. V., 1996. Review Article SAR interferometry—Issues, techniques, applications. *International Journal of Remote Sensing*, 17(10), 1803–1835. https://doi.org/10.1080/01431169608948741

Ghizoni Santos, E., Henrique Nunes, M., Jackson, T., and Eiji Maeda, E., 2022. Quantifying tropical forest disturbances using canopy structural traits derived from terrestrial laser scanning. *Forest Ecology and Management* 524, 120546. https://doi.org/10.1016/j.foreco.2022.120546

Ghosh, S.M., and Behera, M.D., 2021. Aboveground biomass estimates of tropical mangrove forest using Sentinel-1 SAR coherence data - The superiority of deep learning over a semi-empirical model. *Computers and Geosciences* 150, 104737. https://doi.org/10.1016/j.cageo.2021.104737

Gómez, C., Alejandro, P., Hermosilla, T., Montes, F., Pascual, C., and Ruiz, L.Á., 2019. Remote sensing for the Spanish forests in the 21 st century : a review of advances , needs , and opportunities. *Forest systems*, 28, 1–33. https://doi.org/10.5424/fs/2019281-14221

Gómez, C., Alejandro, P., and Montes, F., 2020. Phenological characterization of Fagus sylvatica L. in Mediterranean populations of the Spanish Central Range with Landsat OLI/ETM+ and Sentinel-2A/B. *Revista de Teledetección*, 55, 71. https://doi.org/10.4995/raet.2020.13561

Gómez, C., Caiza Morales, L., Sangüesa-Barreda, G., Olano, J.M., y Domingo, D., 2022. Desarrollo de herramientas de detección temprana de defoliación por procesionaria del pino mediante teledetección y aprendizaje computacional. *Presented at the 8CFE*, Lleida, Cataluña, España.

Gómez, C., Lopez-Sanchez, J. M., Romero-Puig, N., Zhu, J., Fu, H., He, W., Xie, Y., and Xie, Q. 2021. Canopy Height Estimation in Mediterranean Forests of Spain With TanDEM-X Data. *IEEE Journal of Selected Topics in Applied Earth Observations and Remote Sensing*, 14, 2956–2970. https://doi.org/10.1109/JSTARS.2021.3060691

Gómez, C., White, J.C., and Wulder, M.A., 2011. Characterizing the state and processes of change in a dynamic forest environment using hierarchical spatio-temporal segmentation. *Remote Sensing of Environment* 115, 1665–1679. https://doi.org/10.1016/j.rse.2011.02.025

Gómez, C., White, J. C., and Wulder, M. A. 2016. Optical remotely sensed time series data for land cover classification: A review. *ISPRS Journal of Photogrammetry and Remote Sensing*, 116, 55–72. https://doi.org/10.1016/j.isprsjprs.2016.03.008

González-Zamora, Á., García-Barreda, S., Martínez-Fernández, J., Almendra-Martín, L., Gaona, J., and Benito-Verdugo, P., 2022. Soil Moisture and Black Truffle Production Variability in the Iberian Peninsula. *Forests* 13, 819. https://doi.org/10.3390/f13060819

Graf, R.F., Mathys, L., and Bollmann, K., 2009. Habitat assessment for forest dwelling species using LiDAR remote sensing: Capercaillie in the Alps. *Forest Ecology and Management* 257, 160–167. https://doi.org/10.1016/j.foreco.2008.08.021

Gruber, A., Scanlon, T., Van Der Schalie, R., Wagner, W., and Dorigo, W., 2019. Evolution of the ESA CCI soil moisture climate data records and their underlying merging methodology. *Earth Syst. Sci. Data* 11, 717–739. https://doi.org/10.5194/essd-11-717- 2019.

Guillen-Climent, M.L., Mas, H., Fernández-Landa, A., Algeet-Abarquero, N., y Tomé, J.L., 2020. Uso de imágenes hiperespectrales para la predicción del marchitamiento de Pinus halepensis (Mill.) en el bosque mediterráneo. *Rev. Teledetec*. 59. https://doi.org/10.4995/raet.2020.13289

Hagenbo, A., Alday, J.G., Martínez, J., Carles, D.A., Sergio, C., and Bonet, J.A., 2022. Variations in biomass of fungal guilds are primarily driven by factors related to soil conditions in Mediterranean Pinus pinaster forests. *Biology and Fertility of Soils* 487–501. https://doi.org/10.1007/s00374-022-01621-4

Haneda, L.E., Brancalion, P.H.S., Molin, P.G., Ferreira, M.P., Silva, C.A., Almeida, C.T. de, Resende, A.F., Santoro, G.B., Rosa, M., Guillemot, J., Maire, G.L., Feret, J.-B., and de Almeida, D.R.A., 2023. Forest landscape restoration: Spectral behavior and diversity of tropical tree cover classes. *Remote Sensing Applications: Society and Environment* 29, 100882. https://doi.org/10.1016/j.rsase.2022.100882

Hao, T., Guillera-Arroita, G., May, T.W., Lahoz-Monfort, J.J., and Elith, J., 2020. Using Species Distribution Models For Fungi. *Fungal Biology Reviews* 34, 74–88. https://doi.org/10.1016/j.fbr.2020.01.002

Hansen, M. C., Potapov, P. V., Moore, R., Hancher, M., Turubanova, S. A., and Tyukavina, A. 2013. High-Resolution Global Maps of 21st- Century Forest cover Change. *Science* 134 (November), 850–854.

Hawksworth, D.L., and Lücking, R., 2017. Fungal Diversity Revisited: 2.2 to 3.8 Million Species. *Microbiol Spectr* 5. https://doi.org/10.1128/microbiolspec.FUNK-0052-2016

Herrero, C., Berraondo, I., Bravo, F., Pando, V., Ordóñez, C., Olaizola, J., Martín-Pinto, P., and Oria de Rueda, J.A., 2019. Predicting mushroom productivity from long-term fielddata series in mediterranean Pinus pinaster ait. forests in the context of climate change. *Forests* 10, 206. https://doi.org/10.3390/f10030206.

Hogenson, K., Kristenson, H., Kennedy, J., Johnston, A., Rine, J., Logan, T., Zhu, J., Williams, F., Herrmann, J., Smale, J., and Meyer, F., 2020. Hybrid Pluggable Processing Pipeline (HyP3): A cloud-native infrastructure for generic processing of SAR data [Computer software]. https://doi.org/10.5281/zenodo.4646138

Hsu, H. P (1987). Análisis de Fourier. *Addison-Wesley Iberoamericana*.

Huang, P. and Pretzsch, H., 2010. Using terrestrial laser scanner for estimating leaf areas of individual trees in a conifer forest. *Trees* 24, 609–619. https://doi.org/10.1007/s00468-010-0431-z

Huang, S., Tang, L., Hupy, J. P., Wang, Y., and Shao, G. 2020. A commentary review on the use of normalized difference vegetation index (NDVI) in the era of popular remote sensing. *Journal of Forestry Research*, 32(1), 1–6. https://doi.org/10.1007/s11676-020-01155-1

Hunsicker, M. E., KAppel, C. V., Selkoe, K. A., Halpern, B. S., Scarborough, C., Mease, L., and Amrhein, A. 2016. Characterizing driver–response relationships in marine pelagic ecosystems for improved ocean management. *Ecological Applications*, 26(3), 651–663.

Hutchison, L.J., 1999. Lactarius, in: Cairney, J.W.G., and Chambers, S.M. (Eds.), Ectomycorrhizal Fungi Key Genera in Profile. *Springer Berlin Heidelberg*, pp. 269–285. https://doi.org/10.1007/978-3-662-06827-4_11

Jacob, A. W., Vicente-Guijalba, F., Lopez-Martinez, C., Lopez-Sanchez, J. M., Litzinger, M., Kristen, H., Mestre-Quereda, A., Ziolkowski, D., Lavalle, M., Notarnicola, C., Suresh, G., Antropov, O., Ge, S., Praks, J., Ban, Y., Pottier, E., Mallorqui Franquet, J. J., Duro, J., and Engdahl, M. E., 2020. Sentinel-1 InSAR Coherence for Land Cover Mapping: A Comparison of Multiple Feature-Based Classifiers. *IEEE Journal of Selected Topics in Applied Earth Observations and Remote Sensing*, 13, 535–552. https://doi.org/10.1109/JSTARS.2019.2958847

Jacobs, M., Hilmers, T., Leroy, B.M.L., Lemme, H., Kienlein, S., Müller, J., Weisser, W.W., and Pretzsch, H., 2022. Assessment of defoliation and subsequent growth losses caused by Lymantria dispar using terrestrial laser scanning (TLS). *Trees* 36, 819–834. https://doi.org/10.1007/s00468-021-02255-z

Jacobs, M., Rais, A., and Pretzsch, H., 2021. How drought stress becomes visible upon detecting tree shape using terrestrial laser scanning (TLS). *Forest Ecology and Management* 489, 118975. https://doi.org/10.1016/j.foreco.2021.118975

Jensen, J.R., 2005. Introductory digital image processing. A reomote sensing perspective., 3rd ed. *Prentice-Hall*, NJ, USA.

Ji, Z., Pan, Y., Zhu, X., Wang, J., and Li, Q. 2021. Prediction of Crop Yield Using Phenological Information Extracted from Remote Sensing Vegetation Index. *Sensors*, 21(4), 1406. https://doi.org/10.3390/s21041406

Jönsson, P., and Eklundh, L., 2004. TIMESAT—a program for analyzing time-series of satellite sensor data. *Computers and Geosciences* 30, 833–845. https://doi.org/10.1016/j.cageo.2004.05.006

Karavani, A., De Cáceres, M., Martínez de Aragón, J., Bonet, J.A., and de-Miguel, S., 2018. Effect of climatic and soil moisture conditions on mushroom productivity and related ecosystem services in Mediterranean pine stands facing climate change. *Agricultural and Forest Meteorology* 248, 432–440. https://doi.org/10.1016/j.agrformet.2017.10.024

Kauserud, H., Stige, L.C., Vik, J.O., Økland, R.H., Høiland, K., Stenseth, and N.Chr., 2008. Mushroom fruiting and climate change. *Proc. Natl. Acad. Sci. U.S.A.* 105, 3811–3814. https://doi.org/10.1073/pnas.0709037105

Kellndorfer, J., Cartus, O., Lavalle, M., Magnard, C., Milillo, P., Oveisgharan, S., Osmanoglu, B., Rosen, P. A., and Wegmüller, U., 2022. Global seasonal Sentinel-1 interferometric coherence and backscatter data set. *Scientific Data*, 9(1), 73. https://doi.org/10.1038/s41597-022-01189-6

Kennedy, R. E., Andréfouët, S., Cohen, W. B., Gómez, C., Griffiths, P., Hais, M., Healey, S. P., Helmer, E. H., Hostert, P., Lyons, M. B., Meigs, G. W., Pflugmacher, D., Phinn, S. R., Powell, S. L., Scarth, P., Sen, S., Schroeder, T. A., Schneider, A., Sonnenschein, R. and Zhu, Z. 2014. Bringing an ecological view of change to Landsat-based remote sensing. *Frontiers in Ecology and the Environment*, 12(6), 339–346. https://doi.org/10.1890/130066

Koide, R. T., Fernandez, C., and Petprakob, K. 2011. General principles in the community ecology of ectomycorrhizal fungi. *Annals of Forest Science*, 68(1), 45–55. https://doi.org/10.1007/s13595-010-0006-6

Komisarenko, V., Voormansik, K., Elshawi, R., and Sakr, S. 2022. Exploiting time series of Sentinel-1 and Sentinel-2 to detect grassland mowing events using deep learning with reject region. *Scientific Reports*, 12(1), 983. https://doi.org/10.1038/s41598-022-04932-6

Kositsyn, V.N., 1999. Air potos in mapping wild forest berry reources. *Mapping Sciences and Remote Sensing* 36, 133–136. https://doi.org/10.1080/07493878.1999.10642114

Küçüker, D.M. and Başkent, E.Z., 2017a. Sustaining the joint production of timber and Lactarius mushroom: A case study of a forest management planning unit in Northwestern Turkey. *Sustainability* (Switzerland) 9, 1–14. https://doi.org/10.3390/su9010092

Küçüker, D.M. and Başkent, E.Z., 2017b. Impact of forest management intensity on mushroom occurrence and yield with a simulation-based decision support system. *Forest Ecology and Management* 389, 240–248. https://doi.org/10.1016/j.foreco.2016.12.035

Küçüker, D.M. and Başkent, E.Z., 2014. Spatial prediction of Lactarius deliciosus and Lactarius salmonicolor mushroom distribution with logistic regression models in the Kızılcasu Planning Unit, Turkey. *Mycorrhiza* 25, 1–11. https://doi.org/10.1007/s00572-014-0583-6

Kuikka, K., Härmä, E., Markkola, A., Rautio, P., Roitto, M., Saikkonen, K., Ahonen-Jonnarth, U., Finlay, R., and Tuomi, J. 2003. Severe defoliation of scots pine reduces reproductive investment by ectomycorrhizal symbionts. *Ecology*, 84(8), 2051–2061. https://doi.org/10.1890/02-0359

Lauber, C.L., Strickland, M.S., Bradford, M.A. and Fierer, N., 2008. The influence of soil properties on the structure of bacterial and fungal communities across land-use types. *Soil Biology and Biochemistry* 40, 2407–2415. https://doi.org/10.1016/j.soilbio.2008.05.021

Lechner, A. M., Foody, G. M., and Boyd, D. S. 2020. Applications in Remote Sensing to Forest *Ecology and Management*. *One Earth*, 2(5), 405–412. https://doi.org/10.1016/j.oneear.2020.05.001

Lecigne, B., Delagrange, S., and Messier, C. 2018. Exploring trees in three dimensions: VoxR, a novel voxel-based R package dedicated to analysing the complex arrangement of tree crowns. *Annals of Botany*, 121, 589–601. https://doi.org/10.1093/aob/mcx095

Lefsky, M.A., Cohen, W.B., Parker, G.G. and Harding, D.J., 2002. Lidar Remote Sensing for Ecosystem Studies. *Sciences-New York* 52, 19–30. https://doi.org/10.1641/0006-3568(2002)052

Leutner, B.F., Reineking, B., Müller, J., Bachmann, M., Beierkuhnlein, C., Dech, S. and Wegmann, M., 2012. Modelling forest α-diversity and floristic composition - on the added value of LiDAR plus hyperspectral remote sensing. *Remote Sensing* 4, 2818–2845. https://doi.org/10.3390/rs4092818

Li, J., and Roy, D. P. 2017. A global analysis of Sentinel-2a, Sentinel-2b and Landsat-8 data revisit intervals and implications for terrestrial monitoring. *Remote Sensing*, 9(9). https://doi.org/10.3390/rs9090902

Li, X., Ye, Z., Long, J., Zheng, H. and Lin, H., 2022. Inversion of Coniferous Forest Stock Volume Based on Backscatter and InSAR Coherence Factors of Sentinel-1 Hyper-Temporal Images and Spectral Variables of Landsat 8 OLI. *Remote Sensing* 14, 2754. https://doi.org/10.3390/rs14122754

Li, Y., Hess, C., von Wehrden, H., Härdtle, W. and von Oheimb, G., 2014. Assessing tree dendrometrics in young regenerating plantations using terrestrial laser scanning. *Annals of Forest Science* 71, 453–462. https://doi.org/10.1007/s13595-014-0358-4

Li, Y., Wang, X., Chen, Y., Gong, X., Yao, C., Cao, W., and Lian, J. 2023. Application of predictor variables to support regression kriging for the spatial distribution of soil organic carbon stocks in native temperate grasslands. *Journal of Soils and Sediments*, 23(2), 700–717. https://doi.org/10.1007/s11368-022-03370-1

Liu, Y.Y., Dorigo, W.A., Parinussa, R.M., De Jeu, R.A.M., Wagner, W., McCabe, M.F., Evans, J.P., and Van Dijk A.I.J.M., 2012. Trend-preserving blending of passive and active microwave soil moisture retrievals. *Remote Sens. Environ*. 123, 280–297. https://doi.org/10.1016/j.rse.2012.03.014.

Liang, L., Hawbaker, T.J., Zhu, Z., Li, X. and Gong, P., 2016. Forest disturbance interactions and successional pathways in the Southern Rocky Mountains. *Forest Ecology and Management* 375, 35–45. https://doi.org/10.1016/j.foreco.2016.05.010

Lim, K., Treitz, P., Wulder, M., St-Onge, B., and Flood, M., 2003. LiDAR remote sensing of forest structure. *Progress in Physical Geography: Earth and Environment* 27, 88–106. https://doi.org/10.1191/0309133303pp360ra

Loveland, T.R., Anderson, M.C., Huntington, J.L., Irons, J.R., Johnson, D.M., Rocchio, L.E.P., Woodcock, C.E., and Wulder, M.A., 2022. Seeing Our Planet Anew: Fifty Years of Landsat. photogramm eng remote sensing 88, 429–436. https://doi.org/10.14358/PERS.88.7.429

Lovrić, M., Da Re, R., Vidale, E., Prokofieva, I., Wong, J., Pettenella, D., Verkerk, P.J., and Mavsar, R., 2021. Collection and consumption of non-wood forest products in Europe. Forestry: An International *Journal of Forest Research* 94, 757–770. https://doi.org/10.1093/forestry/cpab018

MacDicken, K.G., 2015. Global Forest Resources Assessment 2015: What, why and how? *Forest Ecology and Management* 352, 3–8. https://doi.org/10.1016/j.foreco.2015.02.006

Marchionni, D.S., y Cavayas, F., 2014. La teledetección por radar como fuente de información litológica y estructural: Análisis espacial de imágenes SAR de RADARSAT-1. *Geoacta* 39, 62–89.

Martínez de Arano, I., Maltoni, S., Picardo, A., Mutke, S., Amaral Paulo, J., Baraket, M., Baudriller-Cacaud, H., Bec, R., Bonet, J.A., Brenko, A., Buršić, D., Chapelet, B., Correia, A., Cristobal, R., Ducos, G., Fernandez, L., Galinat, F., Hamrouni, L., Husson, H., Khalfaoui, M., Libbrecht, S., Markos, N., Muir, G., Pasalodos, M., Marois, O., Andrighetto, N., Giacomon, J., Rodriguez, A., Rubio, R., Santos Silva, C., Sorrenti, S., Stara, K., Soares, P., Taghouti, I., Tome, M., Vidale, E., y Walter, S., 2021. Productos forestales no madereros para la conservación de la naturaleza, la economía verde y el bienestar humano. Recomendaciones para la acción política en Europa. Un libro blanco basado en las lecciones aprendidas alrededor del Mediterráneo.

Martínez-Peña, F., Ágreda, T., Águeda, B., Ortega-Martínez, P., and Fernández-Toirán, L.M., 2012. Edible sporocarp production by age class in a Scots pine stand in Northern Spain. *Mycorrhiza*. https://doi.org/10.1007/s00572-011-0389-8

Martínez-Peña, F., Oria-de-Rueda, J.A., y Ágreda, T., 2011. Manual para la gestión del recurso micológico forestal en Castilla y león.

Martínez-Rodrigo, R., Gómez, C., Toraño-Caicoya, A., Bohnhorst, L., Uhl, E., and Águeda, B., 2022. Stand Structural Characteristics Derived from Combined TLS and Landsat Data Support Predictions of Mushroom Yields in Mediterranean Forest. *Remote Sensing* 14, 5025. https://doi.org/10.3390/rs14195025

Masek, J. G., Goward, S. N., Kennedy, R. E., Cohen, W. B., Moisen, G. G., Schleeweis, K., and Huang, C. 2013. United States Forest Disturbance Trends Observed Using Landsat Time Series. *Ecosystems*, 16(6), 1087–1104. https://doi.org/10.1007/s10021-013-9669-9

Mastro, P., Masiello, G., Serio, C., and Pepe, A., 2022. Change Detection Techniques with Synthetic Aperture Radar Images: Experiments with Random Forests and Sentinel-1 Observations. *Remote Sensing*, 14(14), 3323. https://doi.org/10.3390/rs14143323

Mazzia, V., Khaliq, A., and Chiaberge, M., 2019. Improvement in Land Cover and Crop Classification based on Temporal Features Learning from Sentinel-2 Data Using Recurrent-Convolutional Neural Network (R-CNN). *Applied Sciences* 10, 238. https://doi.org/10.3390/app10010238

Mediavilla, O., Olaizola, J., Santos-del-Blanco, L., Oria-de-Rueda, J.A., and Martín-Pinto, P., 2016. Mycorrhization between Cistus ladanifer L. and Boletus edulis Bull is enhanced by the mycorrhiza helper bacteria Pseudomonas fluorescens Migula. *Mycorrhiza* 26, 161–168. https://doi.org/10.1007/s00572-015-0657-0

Mennis, J. 2001. Exploring relationships between ENSO and vegetation vigour in the South- east USA using AVHRR data. *Remote Sensing*, 22(16), 3077–3092. https://doi.org/10.1080/01431160152558251

Mestre-Quereda, A., Lopez-Sanchez, J.M., Vicente-Guijalba, F., Jacob, A.W., and Engdahl, M.E., 2020. Time-Series of Sentinel-1 Interferometric Coherence and Backscatter for Crop-Type Mapping. *IEEE J. Sel. Top. Appl. Earth Observations Remote Sensing* 13, 4070–4084. https://doi.org/10.1109/JSTARS.2020.3008096

M'Hirit, O., 1999. El bosque mediterráneo: espacio ecológico, riqueza económica y bien social. *Unasylva*, Los Bosques del Mediterráneos 50.

Miina, J., Bonet, J. A., Miguel, S. D., Aragón, J. M. D., Kurttila, M., Salo, K., and Tahvanainen, V. 2016. Promoting wild mushroom yields by forest management. https://doi.org/10.13140/RG.2.2.23328.38403

MITECO, 2023. Bosques españoles y su evolución [WWW Document]. URL https://www.miteco.gob.es/es/biodiversidad/temas/inventarios-nacionales/inventario-forestal-nacional/index.aspx

MITECO-Copernicus, 2023. Copernicus [WWW Document]. URL https://www.miteco.gob.es/es/calidad-y-evaluacion-ambiental/temas/agencia-europea-medio-ambiente-informacion-ambiental/copernicus/default.aspx

MITECO-IFN, 2023. Descargas del área de actividad de Biodiversidad y Bosques [WWW Document]. URL https://www.miteco.gob.es/es/biodiversidad/servicios/banco-datos-naturaleza/informacion-disponible/cartografia_informacion_disp.aspx

Moeslund, J.E., Zlinszky, A., Ejrnæs, R., Brunbjerg, A.K., Bøcher, P.K., Svenning, J.C., and Normand, S., 2019. Light detection and ranging explains diversity of plants, fungi, lichens, and bryophytes across multiple habitats and large geographic extent. *Ecol. Appl.* 29, e01907. https://doi.org/10.1002/eap.1907.

Montealegre, A.L., Lamelas, M.T., de la Riva, J., García-Martín, A., and Escribano, F., 2016. Use of low point density ALS data to estimate stand-level structural variables in Mediterranean Aleppo pine forest. *Forestry* 89, 373–382. https://doi.org/10.1093/forestry/cpw008

Montero, G., y Cañellas, I., 1999. Gestión sostenible del bosque mediterráneo en España. *Unasylva,* Los Bosques del Mediterráneos 50.

Montes, C., Santos, F., Martín-López, B., González, J., Aguado, M., López-Santiago, C., Benayas, J., y Gómez Sal, A., 2012. La Evaluación de los Ecosistemas del Milenio en España. Del equilibrio entre la conservación y el desarrollo a la conservación para el bienestar humano., in: *Evaluación de Los Ecosistemas Del Milenio En España. Ambienta*.

Moran, M.S., Hymer, D.C., Qi, J., and Sano, E.E., 2000. Soil moisture evaluation using multi-temporal synthetic aperture radar (SAR) in semiarid rangeland. *Agric. For. Meteorol.* 105, 69–80. https://doi.org/10.1016/S0168-1923(00)00189-1.

Morera, A., Martínez de Aragón, J., De Cáceres, M., Bonet, J.A., and de-Miguel, S., 2022. Historical and future spatially-explicit climate change impacts on mycorrhizal and saprotrophic macrofungal productivity in Mediterranean pine forests. *Agricultural and Forest Meteorology* 319, 108918. https://doi.org/10.1016/J.AGRFORMET.2022.108918

Müller, J., and Bütler, R. 2010. A review of habitat thresholds for dead wood: A baseline for management recommendations in European forests. *European Journal of Forest Research*, 129(6), 981–992. https://doi.org/10.1007/s10342-010-0400-5

NASA, 2021. Landsat Next | Landsat Science [WWW Document]. URL https://landsat.gsfc.nasa.gov/satellites/landsat-next/

Nasiri, V., Le Bris, A., Darvishsefat, A.A., and Moradi, F., 2022. Integration of radar and optical sentinel images for land use mapping in a complex landscape (case study: Arasbaran Protected Area). *Arab J Geosci* 15, 1759. https://doi.org/10.1007/s12517-022-11035-z

Neumann, M., Ferro-Famil, L., and Reigber, A., 2010. Estimation of Forest Structure, Ground, and Canopy Layer Characteristics From Multibaseline Polarimetric Interferometric SAR Data. *IEEE Transactions on Geoscience and Remote Sensing*, 48(3), 1086–1104. https://doi.org/10.1109/TGRS.2009.2031101

Newnham, G.J., Armston, J.D., Calders, K., Disney, M.I., Lovell, J.L., Schaaf, C.B., Strahler, A.H., and Danson, F.M., 2015. Terrestrial Laser Scanning for Plot-Scale Forest Measurement. *Curr Forestry Rep* 1, 239–251. https://doi.org/10.1007/s40725-015-0025-5

Niego, A.G.T., Rapior, S., Thongklang, N., Raspé, O., Hyde, K.D., and Mortimer, P., 2023. Reviewing the contributions of macrofungi to forest ecosystem processes and services. *Fungal Biology Reviews* 44, 100294. https://doi.org/10.1016/j.fbr.2022.11.002

Nikaein, T., Iannini, L., Molijn, R.A., and Lopez-Dekker, P., 2021. On the Value of Sentinel-1 InSAR Coherence Time-Series for Vegetation Classification. *Remote Sensing* 13, 3300. https://doi.org/10.3390/rs13163300

Ohki, M., Abe, T., Tadono, T., and Shimada, M., 2020. Landslide detection in mountainous forest areas using polarimetry and interferometric coherence. *Earth, Planets and Space*, 72(1), 67. https://doi.org/10.1186/s40623-020-01191-5

Olano, J.M., Martínez-Rodrigo, R., Altelarrea, J.M., Ágreda, T., Fernández-Toirán, M., García-Cervigón, A.I., Rodríguez-Puerta, F., and Águeda, B., 2020. Primary productivity and climate control mushroom yields in Mediterranean pine forests. *Agricultural and Forest Meteorology*. https://doi.org/10.1016/j.agrformet.2020.108015

Olesk, A., Praks, J., Antropov, O., Zalite, K., Arumäe, T., and Voormansik, K., 2016. Interferometric SAR Coherence Models for Characterization of Hemiboreal Forests Using TanDEM-X Data. *Remote Sensing*, 8(9), 700. https://doi.org/10.3390/rs8090700

Oria-de-Rueda, J. A., Hernández-Rodríguez, M., Martín-Pinto, P., Pando, V., and Olaizola, J. 2010. Could artificial reforestations provide as much production and diversity of fungal species as natural forest stands in marginal Mediterranean areas? *Forest Ecology and Management*, 260(2), 171–180. https://doi.org/10.1016/J.FORECO.2010.04.009

Oria de Rueda, J.A., de la Parra, B., Olaizola, J., Martín-Pinto, P., Martínez de Azagra, A. y Álvarez, A., 2008. Selvicultura micológica. Compendio de Selvicultura aplicada en España.

Othmani, A., Lew Yan Voon, L.F.C., Stolz, C., and Piboule, A., 2013. Single tree species classification from Terrestrial Laser Scanning data for forest inventory. *Pattern Recognition Letters* 34, 2144–2150. https://doi.org/10.1016/j.patrec.2013.08.004

Pace, G., Gutiérrez-Cánovas, C., Henriques, R., Carvalho-Santos, C., Cássio, F., and Pascoal, C., 2022. Remote sensing indicators to assess riparian vegetation and river ecosystem health. *Ecological Indicators* 144, 109519. https://doi.org/10.1016/j.ecolind.2022.109519

Paloscia, S., Pettinato, S., Santi, E., Notarnicola, C., Pasolli, L., and Reppucci, A., 2013. Soil moisture mapping using Sentinel-1 images: Algorithm and preliminary validation. *Remote Sensing of Environment* 134, 234–248. https://doi.org/10.1016/j.rse.2013.02.027

Pascu, I.-S., Dobre, A.-C., Badea, O., and Tănase, M.A., 2019. Estimating forest stand structure attributes from terrestrial laser scans. *Science of The Total Environment* 691, 205–215. https://doi.org/10.1016/j.scitotenv.2019.06.536

Pascual, A., and de-Miguel, S., 2022. Evaluation of mushroom production potential by combining spatial optimization and LiDAR-based forest mapping data. *Science of The Total Environment* 850, 157980. https://doi.org/10.1016/j.scitotenv.2022.157980

Peñuelas, J., and Sardans, J., 2021. Global Change and Forest Disturbances in the Mediterranean Basin: Breakthroughs, Knowledge Gaps, and Recommendations. *Forests* 12, 603. https://doi.org/10.3390/f12050603

Pérez-Cabello, F., Montorio, R., and Alves, D.B., 2021. Remote sensing techniques to assess post-fire vegetation recovery. *Current Opinion in Environmental Science and Health* 21, 100251. https://doi.org/10.1016/j.coesh.2021.100251

Peura, M., Silveyra Gonzalez, R., Müller, J., Heurich, M., Vierling, L.A., Mönkkönen, M., and Bässler, C., 2016. Mapping a 'cryptic kingdom': Performance of lidar derived environmental variables in modelling the occurrence of forest fungi. *Remote Sensing of Environment* 186, 428–438. https://doi.org/10.1016/J.RSE.2016.09.003

Pinto, N., Simard, M., and Dubayah, R., 2013. Using InSAR Coherence to Map Stand Age in a Boreal Forest. *Remote Sensing* 5, 42–56. https://doi.org/10.3390/rs5010042

Prăvălie, R., Sîrodoev, I., Nita, I.-A., Patriche, C., Dumitraşcu, M., Roşca, B., Tişcovschi, A., Bandoc, G., Săvulescu, I., Mănoiu, V., and Birsan, M.-V. 2022. NDVI-based ecological dynamics of forest vegetation and its relationship to climate change in Romania during 1987–2018. *Ecological Indicators*, 136, 108629. https://doi.org/10.1016/j.ecolind.2022.108629

Primicia, I., Camarero, J.J., Martínez de Aragón, J., de-Miguel, S., and Bonet, J.A., 2016. Linkages between climate, seasonal wood formation and mycorrhizal mushroom yields. Agric. For. Meteorol. 228–229, 339–348. https://doi.org/10.1016/j. agrformet.2016.07.013.

Pulella, A., Sica, F., and Rizzoli, P., 2020a. Monthly Deforestation Monitoring with Sentinel-1 Multi-temporal Signatures and InSAR Coherences. Rev. *Teledetec.* 1. https://doi.org/10.4995/raet.2020.14308

Pulella, A., Aragão Santos, R., Sica, F., Posovszky, P., and Rizzoli, P., 2020b. Multi-Temporal Sentinel-1 Backscatter and Coherence for Rainforest Mapping. *Remote Sensing* 12, 847. https://doi.org/10.3390/rs12050847

R Core Team, 2019. R: A Language and Environment For Statistical Computing. R Foundation for Statistical Computing. Austria. https://www.R-project.org.

Regos, A., Gonçalves, J., Arenas-Castro, S., Alcaraz-Segura, D., Guisan, A., and Honrado, J.P., 2022. Mainstreaming remotely sensed ecosystem functioning in ecological niche models. *Remote Sens Ecol Conserv* 8, 431–447. https://doi.org/10.1002/rse2.255

Reineke, L. H. 1933. Perfecting a stand-density index for even-aged forest. *Journal of Agricultural Research* 46, 627–638.

Rinaldi, A. C., Comandini, O., and Kuyper, T. W., 2008. Ectomycorrhizal fungal diversity: Seperating the wheat from the chaff. *Fungal Diversity*, 33, 1–45.

Rizzoli, P., Dell'Amore, L., Bueso-Bello, J.-L., Gollin, N., Carcereri, D., and Martone, M., 2022. On the Derivation of Volume Decorrelation From TanDEM-X Bistatic Coherence. *IEEE Journal of Selected Topics in Applied Earth Observations and Remote Sensing*, 15, 3504–3518. https://doi.org/10.1109/JSTARS.2022.3170076

Rodríguez-Puerta, F., Alonso Ponce, R., Pérez-Rodríguez, F., Águeda, B., Martín-García, S., Martínez-Rodrigo, R., and Lizarralde, I., 2020. Comparison of Machine Learning Algorithms for Wildland-Urban Interface Fuelbreak Planning Integrating ALS and UAV-Borne LiDAR Data and Multispectral Images. *Drones* 4, 21. https://doi.org/10.3390/drones4020021

Robock, A., 2014. Hydrology, Floods and droughts: soil moisture. *Encyclopedia of Atmospheric Sciences:* Second Edition. Elsevier Inc, pp. 232–239. https://doi.org/10. 1016/B978-0-12-382225-3.00169-9.

Rodell, M., Houser, P.R., Jambor, U., Gottschalck, J., Mitchell, K., Meng, C.J., Arsenault, K., Cosgrove, B., Radakovich, J., Bosilovich, M., Entin, J.K., Walker, J.P., Lohmann, D., and Toll, D., 2004. The global land data assimilation system. Bull. Am. *Meteorol. Soc*. 85, 381–394. https://doi.org/10.1175/BAMS-85-3-381.

Rouse, J.W., Haas, R.H., and Deering, D.W., 1973. Monitoring vegetation systems in the great plains with ERTS-1. NASA, editor. *Third ERTS Symposium*. 309–317.

Rousk, J., and Bååth, E., 2011. Growth of saprotrophic fungi and bacteria in soil: Growth of saprotrophic fungi and bacteria in soil. FEMS *Microbiology Ecology*, 78(1), 17–30. https://doi.org/10.1111/j.1574-6941.2011.01106.x

Rubio-Cuadrado, Á., Camarero, J. J., Rodríguez-Calcerrada, J., Perea, R., Gómez, C., Montes, F., and Gil, L., 2021. Impact of successive spring frosts on leaf phenology and radial growth in three deciduous tree species with contrasting climate requirements in central Spain. *Tree Physiology*, 41(12), 2279–2292. https://doi.org/10.1093/treephys/tpab076

Rühling, Å., and Tyler, G. 1990. Soil Factors Influencing the Distribution of Macrofungi in Oak Forests of Southern Sweden. *Holarctic Ecology*, 13(1), 11–18.

Sabaté, S., Gracia, C.A., and Sánchez, A., 2002. Likely effects of climate change on growth of Quercus ilex, Pinus halepensis, Pinus pinaster, Pinus sylvestris and Fagus sylvatica forests in the Mediterranean region. *Forest Ecology and Management* 162, 23–37. https://doi.org/10.1016/S0378-1127(02)00048-8

Sahel, Y., Dellahi, Y., and Chahhou, D., 2022. Mapping the Site of Biological and Ecological Interest of Rganat-Bouchkal (Tsili) Argan forest (Moroccan Central Plateau) using remote sensing. IOP Conf. *Ser.: Earth Environ. Sci*. 1090, 012001. https://doi.org/10.1088/1755-1315/1090/1/012001

Sánchez-González, M., Calama, R., y Bonet, J.A., 2020. Los productos forestales no madereros en España: Del monte a la industria. *Instituto Nacional de Investigación y Tecnología Agraria y Alimentaria*, Madrid.

Sánchez-González, M., de-Miguel, S., Martin-Pinto, P., Martínez-Peña, F., Pasalodos-Tato, M., Oria-de-Rueda, J.A., Martínez de Aragón, J., Cañellas, I., and Bonet, J.A., 2019. Yield models for predicting aboveground ectomycorrhizal fungal productivity in Pinus sylvestris and Pinus pinaster stands of northern Spain. *For. Ecosyst*. 6, 52. https://doi.org/10.1186/s40663-019-0211-1

Sánchez-González, M., Pasalodos-Tato, M., and Cañellas, I. (Editors), 2015. Description of the improvements in the models for multipurpose trees (MPT) and non-wood forest products (NWFP). D2.2 of the StarTree project FP7 project no. 311919 KBBE.2012.1.2-06. *European Commission* 69.

Sangüesa-Barreda, G., Camarero, J.J., García-Martín, A., Hernández, R., and de la Riva, J., 2014. Remote-sensing and tree-ring based characterization of forest defoliation and growth loss due to the Mediterranean pine processionary moth. *Forest Ecology and Management* 320, 171–181. https://doi.org/10.1016/j.foreco.2014.03.008

Sato, H., Morimoto, S., and Hattori, T., 2012. A thirty-year survey reveals that ecosystem function of fungi predicts phenology of mushroom fruiting. *PLoS ONE* 7, e49777. https://doi.org/10.1371/journal.pone.0049777.

Schellenberg, K., Jagdhuber, T., Zehner, M., Hese, S., Urban, M., Urbazaev, M., Hartmann, H., Schmullius, C., and Dubois, C., 2023. Potential of Sentinel-1 SAR to Assess Damage in Drought-Affected Temperate Deciduous Broadleaf Forests. *Remote Sensing*, 15(4), 1004. https://doi.org/10.3390/rs15041004

Schlesinger, W.H., 1997. Biogeochemistry: An Analysis of Global Change, second ed. *Academic Press*.

Schloss, A.L., Kicklighter, D.W., Kaduk, J., and Wittenberg, U., 1999. Comparing global models of terrestrial net primary productivity (NPP): comparison of NPP to climate and the normalized difference vegetation index (NDVI). *Glob. Chang. Biol.* 5, 25–34. https://doi.org/10.1046/j.1365-2486.1999.00004.x.

Seo, B., Lee, J., Lee, K.-D., Hong, S., and Kang, S. 2019. Improving remotely-sensed crop monitoring by NDVI-based crop phenology estimators for corn and soybeans in Iowa and Illinois, USA. *Field Crops Research*, 238, 113–128. https://doi.org/10.1016/j.fcr.2019.03.015

Sen, P. K., 1968. Estimates of the Regression Coefficient Based on Kendall's Tau. *Journal of the American Statistical Association*, 63(324), 1379–1389. https://doi.org/10.1080/01621459.1968.10480934

Seppi, S. A., López-Martinez, C., and Joseau, M. J., 2022. Assessment of L-Band SAOCOM InSAR Coherence and Its Comparison with C-Band: A Case Study Over Managed Forests in Argentina. *Remote Sensing*, 14(22), 5652. https://doi.org/10.3390/rs14225652

Song, C., Dannenberg, M. P., and Hwang, T. 2013. Optical remote sensing of terrestrial ecosystem primary productivity. *Progress in Physical Geography*, 37(6), 834–854. https://doi.org/10.1177/0309133313507944

Soares, C., Silva, J.M.N., Boavida-Portugal, J., and Cerasoli, S., 2022. Spectral-Based Monitoring of Climate Effects on the Inter-Annual Variability of Different Plant Functional Types in Mediterranean Cork Oak Woodlands. *Remote Sensing* 14, 711. https://doi.org/10.3390/rs14030711

Steidinger, B. S., Crowther, T. W., Liang, J., Van Nuland, M. E., Werner, G. D. A., Reich, P. B., Nabuurs, G. J., de-Miguel, S., Zhou, M., Picard, N., Herault, B., Zhao, X., Zhang, C., Routh, D., Peay, K. G., Abegg, M., Adou Yao, C. Y., Alberti, G., Almeyda Zambrano, A., … consortium, G. 2019. Climatic controls of decomposition drive the global biogeography of forest-tree symbioses. *Nature*, 569(7756), 404–408. https://doi.org/10.1038/s41586-019-1128-0

Straatsma, G., Ayer, F., and Egli, S. 2001. Species richness, abundance, and phenology of fungal fruit bodies over 21 years in a Swiss forest plot. *Mycological Research*, 105(5), 515–523. https://doi.org/10.1017/S0953756201004154

Tahvanainen, V., 2014. Expert model for Boletus edulis yields in northern Karelian spruce forests. *University of Eastern Finland*, Finland.

Tahvanainen, V., Miina, J., Kurttila, M., and Salo, K., 2016. Modelling the yields of marketed mushrooms in Picea abies stands in eastern Finland. *Forest Ecology and Management* 362, 79–88. https://doi.org/10.1016/j.foreco.2015.11.040

Tanase, M. A., Villard, L., Pitar, D., Apostol, B., Petrila, M., Chivulescu, S., Leca, S., Borlaf-Mena, I., Pascu, I.-S., Dobre, A.-C., Pitar, D., Guiman, G., Lorent, A., Anghelus, C., Ciceu, A., Nedea, G., Stanculeanu, R., Popescu, F., Aponte, C., and Badea, O. 2019. Synthetic aperture radar sensitivity to forest changes: A simulations-based study for the Romanian forests. *Science of The Total Environment*, 689, 1104–1114. https://doi.org/10.1016/j.scitotenv.2019.06.494

Taye, Z.M., Martínez-Peña, F., Bonet, J.A., Martínez de Aragón, J., and de-Miguel, S., 2016. Meteorological conditions and site characteristics driving edible mushroom production in Pinus pinaster forests of Central Spain. *Fungal Ecology* 23, 30–41. https://doi.org/10.1016/j.funeco.2016.05.008

Theil, H., 1950. A Rank-Invariant Method of Linear and Polynomial Regression Analysis, 1-2; Confidence regions for the parameters of linear regression equations in two, three and more variables. *Indagationes Mathematicae*, 1(2).

Thers, H., Brunbjerg, A.K., Læssøe, T., Ejrnæs, R., Bøcher, P.K., and Svenning, J.C., 2017. Lidar-derived variables as a proxy for fungal species richness and composition in temperate Northern Europe. *Remote Sensing of Environment* 200, 102–113. https://doi.org/10.1016/j.rse.2017.08.011

Tomao, A., Bonet, J.A., Martínez de Aragón, J., and de-Miguel, S., 2017. Is silviculture able to enhance wild forest mushroom resources? Current knowledge and future perspectives. *Forest Ecology and Management* 402, 102–114. https://doi.org/10.1016/j.foreco.2017.07.039

Torres, P., Rodes-Blanco, M., Viana-Soto, A., Nieto, H., and García, M., 2021. The Role of Remote Sensing for the Assessment and Monitoring of Forest Health: A Systematic Evidence Synthesis. *Forests* 12, 1134. https://doi.org/10.3390/f12081134

Torres, R., Snoeij, P., Geudtner, D., Bibby, D., Davidson, M., Attema, E., Potin, P., Rommen, B., Floury, N., Brown, M., Traver, I. N., Deghaye, P., Duesmann, B., Rosich, B., Miranda, N., Bruno, C., L'Abbate, M., Croci, R., Pietropaolo, A., … Rostan, F. 2012. GMES Sentinel-1 mission. *Remote Sensing of Environment*, 120, 9–24. https://doi.org/10.1016/j.rse.2011.05.028

Tsokas, A., Rysz, M., Pardalos, P.M., and Dipple, K., 2022. SAR data applications in earth observation: An overview. *Expert Systems with Applications* 205, 117342. https://doi.org/10.1016/j.eswa.2022.117342

Tucker, C. J., and Sellers, P. J. 1986. Satellite remote sensing of primary production. *International Journal of Remote Sensing*, 7(11), 1395–1416. https://doi.org/10.1080/01431168608948944

United Nations. 2022a. THE 17 GOALS | Sustainable Development. https://sdgs.un.org/es/goals

United Nations. 2022b. Indicators ODS. https://unstats.un.org/sdgs/report/2022/Goal-15/

Ulaby, F., Long, D., Blackwell, W., Elachi, C., Fung, A., Ruf, C., Sarabandini, K., Zyl, J., and Zebker, H., 2014. Microwave Radar and Radiometric Remote Sensing. *University of Michigan Press*. https://doi.org/10.3998/0472119356

Unión Europea, 2021. Comunicación de la Comisión al Parlamento Europeo, al Consejo, al Comité Económico y social Europeo y al Comité de las Regiones. Nueva Estrategia de la UE en favor de los Bosques para 2030. COM (2021) 572 final. *Comisión Europea*, Bruselas.

USGS, 2023. Landsat Missions [WWW Document]. URL https://www.usgs.gov/landsat-missions/landsat-satellite-missions

Valladares, F. 2020. Si no sanamos el clima, volveremos a enfermar. The Conversation. http://theconversation.com/si-no-sanamos-el-clima-volveremos-a-enfermar-135091

Van der Heijden, M. G. A., and Sanders, I. R. 2002. *Mycorrhizal Ecology*. Springer.

Vásquez Gassibe, P., Oria-de-Rueda, J. A., y Martín-Pinto, P. 2015. P. pinaster under extreme ecological conditions provides high fungal production and diversity. *Forest Ecology and Management*, 337, 161–173. https://doi.org/10.1016/J.FORECO.2014.11.013

Veloso, A., Mermoz, S., Bouvet, A., Le Toan, T., Planells, M., Dejoux, J.-F., & Ceschia, E., 2017. Understanding the temporal behavior of crops using Sentinel-1 and Sentinel-2-like data for agricultural applications. *Remote Sensing of Environment*, 199, 415–426. https://doi.org/10.1016/j.rse.2017.07.015

Vicente-Serrano, S.M., Camarero, J.J., Olano, J.M., Martín-Hernández, N., Peña-Gallardo, M., Tomás-Burguera, M., Gazol, A., Azorin-Molina, C., Bhuyan, U. and El Kenawy, A., 2016. Diverse relationships between forest growth and the normalized difference vegetation Index at a global scale. *Remote Sens. Environ*. 187, 14–29. https://doi.org/10.1016/j.rse.2016.10.001.

Villarroya-Carpio, A., Lopez-Sanchez, J. M., and Engdahl, M. E., 2022. Sentinel-1 interferometric coherence as a vegetation index for agriculture. *Remote Sensing of Environment*, 280, 113208. https://doi.org/10.1016/j.rse.2022.113208

Villarroya-Carpio, A. and Lopez-Sanchez J. M., 2023. Multi-Annual Evaluation of Time Series of Sentinel-1 Interferometric Coherence as a Tool for Crop Monitoring. *Sensors*, 23(4), 1833. https://doi.org/10.3390/s23041833

von Arx, G., Arzac, A., Fonti, P., Frank, D., Zweifel, R., Rigling, A., Galiano, L., Gessler, A. and Olano, J.M., 2017. Responses of sapwood ray parenchyma and non-structural carbohydrates of Pinus sylvestris to drought and long-term irrigation. *Funct. Ecol*. 31, 1371–1382. https://doi.org/10.1111/1365-2435.12860.

Wang, C., Qi, J., Moran, S., and Marsett, R. 2004a. Soil moisture estimation in a semiarid rangeland using ERS-2 and TM imagery. *Remote Sensing of Environment*, 90(2), 178–189. https://doi.org/10.1016/j.rse.2003.12.001

Wang, J., Rich, P.M., Price, K.P. and Kettle W.D., 2004b. Relations between NDVI and tree productivity in the central Great Plains. Int. J. *Remote Sens*. 25, 3127–3138.

Wang, Q., Tenhunen, J., Dinh, N.Q., Reichstein, M., Vesala, T. and Keronen, P., 2004c. Similarities in ground- and satellite-based NDVI time series and their relationship to physiological activity of a Scots pine forest in Finland. *Remote Sens. Environ*. 93, 225–237. https://doi.org/10.1016/j.rse.2004.07.006.

White, J. C., Coops, N. C., Wulder, M. A., Vastaranta, M., Hilker, T., and Tompalski, P. 2016. Remote Sensing Technologies for Enhancing Forest Inventories: A Review. *Canadian Journal of Remote Sensing*, 42(5), 619–641. https://doi.org/10.1080/07038992.2016.1207484

Wood, S. N. 2017. Generalized Additive Models: An Introduction with R. *Chapman and Hall/CRC*. https://doi.org/10.1201/9781315370279

Woodcock, C. E., Loveland, T. R., Herold, M., and Bauer, M. E. 2020. Transitioning from change detection to monitoring with remote sensing: A paradigm shift. *Remote Sensing of Environment*, 238, 111558. https://doi.org/10.1016/j.rse.2019.111558

Wong, M.S., Zhu, X., Abbas, S., Kwok, C.Y.T. and Wang, M., 2021. Optical Remote Sensing, in: Shi, W., Goodchild, M.F., Batty, M., Kwan, M.-P., Zhang, A. (Eds.), Urban Informatics, The Urban Book Series. *Springer* Singapore, pp. 315–344. https://doi.org/10.1007/978-981-15-8983-6_20

Wu, Z., Snyder, G., Vadnais, C., Arora, R., Babcock, M., Stensaas, G., Doucette, P. and Newman, T., 2019. User needs for future Landsat missions. *Remote Sensing of Environment* 231, 111214. https://doi.org/10.1016/j.rse.2019.111214

Wulder, M. A., Coops, N. C., Roy, D. P., White, J. C., and Hermosilla, T. 2018. Land cover 2.0. International Journal of *Remote Sensing*, 39(12), 4254–4284. https://doi.org/10.1080/01431161.2018.1452075

Wulder, M.A., Loveland, T.R., Roy, D.P., Crawford, C.J., Masek, J.G., Woodcock, C.E., Allen, R.G., Anderson, M.C., Belward, A.S., Cohen, W.B., Dwyer, J., Erb, A., Gao, F., Griffiths, P., Helder, D., Hermosilla, T., Hipple, J.D., Hostert, P., Hughes, M.J., Huntington, J., Johnson, D.M., Kennedy, R., Kilic, A., Li, Z., Lymburner, L., McCorkel, J., Pahlevan, N., Scambos, T.A., Schaaf, C., Schott, J.R., Sheng, Y., Storey, J., Vermote, E., Vogelmann, J., White, J.C., Wynne, R.H. and Zhu, Z., 2019. Current status of Landsat program, science, and applications. *Remote Sensing of Environment* 225, 127–147. https://doi.org/10.1016/j.rse.2019.02.015

Wulder, M.A., Roy, D.P., Radeloff, V.C., Loveland, T.R., Anderson, M.C., Johnson, D.M., Healey, S., Zhu, Z., Scambos, T.A., Pahlevan, N., Hansen, M., Gorelick, N., Crawford, C.J., Masek, J.G., Hermosilla, T., White, J.C., Belward, A.S., Schaaf, C., Woodcock, C.E., Huntington, J.L., Lymburner, L., Hostert, P., Gao, F., Lyapustin, A., Pekel, J.-F., Strobl, P. and Cook, B.D., 2022. Fifty years of Landsat science and impacts. *Remote Sensing of Environment* 280, 113195. https://doi.org/10.1016/j.rse.2022.113195

Ygorra, B., Frappart, F., Wigneron, J.P., Moisy, C., Catry, T., Baup, F., Hamunyela, E. and Riazanoff, S., 2021. Monitoring loss of tropical forest cover from Sentinel-1 time-series: A CuSum-based approach. *International Journal of Applied Earth Observation and Geoinformation* 103, 102532. https://doi.org/10.1016/j.jag.2021.102532

Zambonelli, A., Bonito, G.M., 2012. Edible Ectomycorrhizal Mushrooms: Current Knowledge and Future Prospects. *Springer*.

Zhang, S., Tsuruta, M., Li, C., Vaario, L.-M., Xia, Y., Matsushita, N., Kurokochi, H., Xu, R., Li, J. and Lian, C., 2022. Estimation of the most suitable nitrogen concentration for sporocarp formation in Laccaria japonica colonizing Pinus densiflora seedlings through in vitro mycelial culture. *Mycorrhiza* 32, 451–464. https://doi.org/10.1007/s00572-022-01085-2

Zhu, X., and Liu, D. 2015. Improving forest aboveground biomass estimation using seasonal Landsat NDVI time-series. *ISPRS Journal of Photogrammetry and Remote Sensing*, 102, 222–231. https://doi.org/10.1016/j.isprsjprs.2014.08.014

Zhu, Z. (2019). Science of Landsat Analysis Ready Data. *Remote sensing* 11(18) 2166. https://doi.org/10.3390/rs11182166

Zhu, Z., Zhang, J., Yang, Z., Aljaddani, A. H., Cohen, W. B., Qiu, S., and Zhou, C. 2020. Continuous monitoring of land disturbance based on Landsat time series. *Remote Sensing of Environment*, 238, 111116. https://doi.org/10.1016/j.rse.2019.03.009

Zuur, A. F., Ieno, E. N., Walker, N. J., Saveliev, A. A., and Smith, G. M. 2009. Mixed Effects Models and Extensions in Ecology with R. *Springer*.

Agradecimientos

GRACIAS

Sabía que llegaría este momento y sois tantas las personas que me habéis ayudado durante este proceso y a las que os tengo que agradecer. Pero primero, quiero agradecer a Paco e Iñigo por haberme dado la oportunidad de hacer las practicas del máster en föra y poder continuar con mis estudios y carrera profesional, hace ya casi 6 años de esto. Durante este periodo en föra han pasado compañer@s, cada uno de vosotr@s habéis aportado y me habéis acompañado durante este trabajo, gracias. Pero sí quiero mencionar a Andrea C, Juanma, Almudena, Alejandro, Diego F y Diego A. por más "jueves de tortilla", Rafa, Fernando, Liber, Carlos, Aitor, Juan y Borja por los "BarFriday" y toda vuestra ayuda, Saray tu misma lo dijiste… compañera de batallas y Andrea R., amiga, gracias por las risas y sobre todo por aguantarme.

En segundo lugar, quiero agradecer a mis directoras. Bea, gracias por apaciguar los problemas y se vean más pequeños. Cristina porque en los momentos difíciles supiste tirar de mí. Gracias a las dos por todo lo que me habéis enseñado y sobre todo por vuestro tiempo y vuestra paciencia conmigo. Txemi, no me olvido de ti, empezaste esta aventura, no la acabaste, pero sé que la has seguido muy de cerca y por eso y por todo lo que me has enseñado desde que fuiste mi profesor, te estoy muy agradecida.

Quiero agradecer también al Prof. Dr. Hans Pretzsch por acogerme en la Universidad Técnica de Múnich, a Astor, Enno y Luke por su ayuda y paciencia conmigo y a todo el equipo por hacer sentirme como en casa.

Mis agradecimientos también al grupo de investigación Cambium, por vuestro apoyo y vuestros "¿Qué tal vas?". Ha sido muy gratificante contar con vuestras muestras de ánimo. Miguel, empezamos juntos y acabaste antes, gracias por compartir estos momentos y por resolverme todas las dudas y crisis que me han ido surgiendo ahora al final.

Gracias a los amigos, los que habéis llegado hasta aquí y a los que os habéis incorporado durante el camino. J., has sido clave estos últimos meses, y has estado ayudándome hasta el final, millones de gracias. A las unicornios y los del tornillo porque habéis estado ahí en todo momento, incluso muchas veces os habéis alegrado más que yo por todos los progresos.

Javi, gracias por tus ánimos, por tu apoyo incondicional y sobre todo por soportarme, este trabajo no habría sido posible sin ti, muchas gracias.

Por último, gracias a mi familia. A mi madre y hermano, sin vosotros llegar hasta aquí habría sido imposible, sois mis dos pilares fundamentales en esta vida.

Ya han pasado cuatro años desde que empecé y habéis pasado mucha gente y de todas las formas posibles me habéis ayudado en este camino, ¡gracias a todas y todos!